U.S. Department of Transportation

United States Coast Guard

Report of the International Ice Patrol in the North Atlantic

International Ice Patrol

1985 Season
Bulletin No. 71

CG-188-40

U.S. Department of Transportation
United States Coast Guard

Commandant
United States Coast Guard

MAILING ADDRESS G-OIO
U. S. COAST GUARD
WASHINGTON, D.C. 20593-0001
(202) 267-1458

17 MAR 1987

Bulletin No. 71

REPORT OF THE INTERNATIONAL ICE PATROL SERVICES IN THE NORTH ATLANTIC OCEAN

Season of 1985

CG-188-40

FOREWORD

Forwarded herewith is bulletin No. 71 of the International Ice Patrol describing the Patrol's services, ice observations and conditions during the 1985 season.

CLYDE E. ROBBINS
Chief, Office of Operations

DISTRIBUTION - SDL No. 124

	a	b	c	d	e	f	g	h	i	j	k	l	m	n	o	p	q	r	s	t	u	v	w	x	y	z
A	1*	1*		1	1	1*	1	1*																		
B		1*	1		10					2				2	5		1									
C	1*																1*									
D																							60			
E																										
F																										
G																										
H																										

* NON-STANDARD DISTRIBUTION:
*A;abfgh LANTAREA only
*B;b LANTAREA (5); B;b PACAREA (1)
*C:aq LANTAREA only
SML CG-4

International Ice Patrol 1985 Annual Report

Contents

Introduction

This is the 71st annual report of the International Ice Patrol Service in the North Atlantic. It contains information on ice conditions and Ice Patrol operations for 1985. The U.S. Coast Guard conducts the International Ice Patrol Service in the North Atlantic under the provisions of Title 46, U.S. Code, Sections 738, 738a through 738d; and the International Convention for the Safety of Life at Sea (SOLAS), 1974 regulations 5-8. This service was initiated shortly after the sinking of the RMS TITANIC on April 15, 1912.

Commander, International Ice Patrol under Commander, Coast Guard Atlantic Area, directed the International Ice Patrol from offices located at Groton, Connecticut. The unit analyzes ice and environmental data, prepares the daily ice bulletins and facsimile charts, and replies to any requests for special ice information. It also controls the aerial Ice Reconnaisance Detachment and any surface patrol cutters when assigned, both of which patrol the southeastern, southern, and southwestern limits of the Grand Banks of Newfoundland for icebergs. The International Ice Patrol makes twice-daily radio broadcasts to warn mariners of the limits of iceberg distribution.

During the 1985 season, International Ice Patrol reconnaissance was conducted by U. S. Coast Guard HC-130 aircraft equipped with Side-Looking Airborne Radar (SLAR), operating from Gander, Newfoundland. No U. S. Coast Guard cutters were deployed as surface patrol vessels this year. There were 1,063 icebergs estimated south of 48°N this year, the traditional measure of the severity of an IIP season.

Vice Admiral P.A. Yost was Commander, Atlantic Area from the start of the 1985 season, 14 March until its end on 29 August 1985. Commander Norman C. Edwards, Jr., U.S. Coast Guard, was Commander, International Ice Patrol during the Ice Patrol season.

Summary of Operations, 1985

From 14 March to 29 August 1985, the International Ice Patrol (IIP), a unit of the U.S. Coast Guard, conducted the International Ice Patrol Service, which has been provided annually since the sinking of the RMS TITANIC on April 15, 1912. During past years, Coast Guard ships and/or aircraft have patrolled the shipping lanes off Newfoundland within the area delineated by 40°N - 52°N, 39°W - 57°W, detecting icebergs and warning mariners of these hazards. During the 1985 Ice Patrol season, Coast Guard HC-130 aircraft flew 72 ice reconnaissance sorties, logging over 507 flight hours. The AN/APS-135 Side-Looking Airborne Radar (SLAR), which was introduced into Ice Patrol duty during the 1983 season, again proved to be an excellent all-weather tool for the detection of both icebergs and sea ice as demonstrated during the BergSearch '84 experiment (Rossiter, *et al.*, 1984). On IIP reconnaissance flights alone, the SLAR provided 53 percent of the 1985 sightings.

A deployment was made from 20-25 February to determine the pre-season iceberg distribution. Based on this trip, regular deployments started on 12 March with the 1985 season opening on 14 March. From that date until 29 August 1985, an aerial Iceberg Reconnaissance Detachment (ICERECDET) operated from Gander, Newfoundland one week out of every two. The season officially closed on 29 August 1985.

During the 1985 season, an estimated 1,063 icebergs drifted south of 48°N latitude. Table 1 shows monthly estimates of the number of icebergs that crossed 48°N.

No U. S. Coast Guard cutters were deployed to act as surface patrol vessels this year. The USCGC EVERGREEN and USCGC NORTHWIND were deployed to conduct oceanographic research for the Ice Patrol during the periods 10 April - 10 May and 1-9 August. On board EVERGREEN, the IIP iceberg drift and deterioration models were evaluated (See Appendices C and D), hydrographic equipment was evaluated, and a joint IIP/USCG Research and Development Center study of surface craft and iceberg target detection performance by the AN/APS-135 SLAR was conducted (Robe, *et al.*, 1985). The NORTHWIND hydrographic cruise was cancelled because of main diesel engine problems on board NORTHWIND.

Other research conducted at IIP during 1985 included an analysis of eddy formation in the vicinity of the Grand Banks (Appendix E), an evaluation of iceberg/ship SLAR target discrimination (Appendix B), and a comparison of ocean fronts detected on National Weather Service satellite imagery and IIP SLAR imagery (Appendix F).

Table 1. Icebergs South of 48°North

	Avg 1900-85	Total 1900-85	Avg 1946-85	Total 1946-85	1985
OCT	1	112	0	5	3
NOV	1	121	0	15	11
DEC	1	100	1	20	7
JAN	2	196	2	76	2
FEB	11	945	12	494	57
MAR	42	3628	38	1526	129
APR	110	9476	116	4631	208
MAY	131	11230	104	4147	205
JUN	70	6025	63	2507	247
JUL	26	2219	26	1023	123
AUG	7	625	6	236	39
SEP	3	297	1	51	32
Annual Total	405	34974	368	14631	1063

As explained in the 1984 Ice Patrol Bulletin (Thayer, 1984), the methodology and technology of iceberg reconnaissance and data analysis have changed significantly over the past 40 years. A change is evident in the source distribution of iceberg sightings in that SLAR accounted for 78% of the USCG iceberg sightings in 1984 (49% of sightings from all sources) but only accounted for 53% of USCG sightings in 1985 (13% of all sightings) (Table 2). (An increased emphasis on icebergs by Canadian Atmospheric and Environmental Service flights and an increased contribution by the commercial shipping community account for other changes in the overall figures.) With icebergs more widely dispersed than normal during much of the 1985 IIP season, it was frequently necessary to search the eastern part of the IIP area. To conserve fuel during these long searches, high altitude legs were flown to and from the search areas. Although SLAR was not operated during these high altitude legs, icebergs could still be sighted in large numbers during good weather. These high-altitude flights were much more frequent during 1985 than 1984. The large number of USCG visual sightings on these flights, together with the changes in reconnaissance procedures described below, greatly decreased the percentage of USCG iceberg sightings that were SLAR-only during 1985.

Further evaluation of SLAR's capability confirms its usefulness in detecting icebergs (Robe, *et al.*, 1985) and the necessity for specific SLAR iceberg reconnaissance procedures to assist with iceberg/ship target discrimination (Appendix B). Specific changes in SLAR reconnaissance procedures were made to maximize visual confirmation of SLAR targets and aid target identification during 1985. These changes consisted of selecting daily search areas for optimal visibility, subjecting SLAR films to more post-flight analysis and making more use of supporting data from other sources.

Table 3 — Aircraft Deployments from 10/1/84 to 9/30/85

Ice Reconnaissance Detachment Deployments	No. of Hours Flown
Pre-season	29.6
In-season	631.0
Post-season	11.3
Total	671.9

Note: In-season ICERECDET flights include transit and logistics flights to and from Gander during the Ice Patrol season. A significantly large number of logistic flights, 14 sorties and 86.1 hours were conducted. There were 72 sorties dedicated solely to ice reconnaissance with a total of 507.8 flight hours. They are summarized as follows:

Month	Number of Sorties	Flight Hours
FEB	4	23.6
MAR	5	38.7
APR	12	85.8
MAY	15	107.5
JUN	13	87.3
JUL	11	83.9
AUG	11	75.7
SEP	1	5.3
TOTAL	72	507.8

Table 2 — Sources of IIP Iceberg Reports by Size

Sighting Source	Growler	Small	Med.	Large	Radar Target	Total	% of Total
Coast Guard SLAR	65	194	182	113	10	564	13.3
Coast Guard Visual	60	155	177	107	0	499	11.8
Canadian SLAR	17	56	115	21	229	438	10.3
Canadian Visual	19	239	187	65	4	514	12.1
Commercial Radar	7	30	114	33	124	308	7.3
Commercial Visual	122	300	808	279	15	1524	36.0
Mobil Oil Canada, LTD	12	81	98	18	18	227	5.4
Lighthouse/Shore	0	2	13	9	0	24	0.6
Other	4	52	47	28	5	136	3.2
Total	306	1109	1741	673	405	4234	100

Iceberg Reconnaissance and Communications

During the 1985 Ice Patrol year (from 1 October 1984 through 30 September 1985), 98 aircraft sorties were flown in support of the International Ice Patrol. These included pre-season flights, ice observation and logistics flights during the season, and post-season flights. Pre-season flights determined iceberg concentrations north of 48°N, necessary to estimate the time when icebergs would threaten the North Atlantic shipping lanes in the vicinity of the Grand Banks of Newfoundland. During the active season, ice observation flights located the southwestern, southern, and southeastern limits of icebergs. Logistics flights were necessary due to aircraft maintenance problems. Post-season flights were made to retrieve parts and equipment from Gander and to close out all business transactions from the season.

U.S. Coast Guard aircraft, deployed from Coast Guard Air Station Elizabeth City, North Carolina, conducted all the aircraft missions. SLAR-equipped HC-130 aircraft were utilized exclusively for aerial ice reconnaissance, and HC-130 and HU-25A aircraft were used on logistics flights. Table 3 (left) shows aircraft utilization during the 1985 season.

During the 1984 season, only 5% of the deployed days were spent on the ground in Gander. In 1985, this figure climbed to 14%. After an aircraft mishap in Groton in March, IIP relied on a single SLAR-equipped HC-130 for much of the 1985 season. The increased use of this one aircraft and its SLAR resulted in an increased number of maintenance problems.

U.S. Coast Guard Communications Station Boston, Massachusetts, NMF/NIK, was the primary radio station used for the dissemination of the daily ice bulletins and facsimile charts after preparation by the Ice Patrol office in Groton. Other transmitting stations for the 0000Z and 1200Z ice bulletins included Canadian Coast Guard Radio Station St. John's/VON, Canadian Forces Radio Station Mill Cove/CFH, and U.S. Navy LCMP Broadcast Stations Norfolk/NAM; Thurso, Scotland; and Keflavik, Iceland.

Canadian Forces Station Mill Cove/CFH as well as AM Radio Station Bracknell/GFE, United Kingdom are radiofacsimile broadcasting stations which used Ice Patrol limits in their broadcasts. Canadian Coast Guard Radio Station St. John's/ VON provided special broadcasts.

The International Ice Patrol requested that all ships transitting the area of the Grand Banks report ice sightings, weather, and sea surface temperatures via U.S. Coast Guard Communications Station Boston, NMF/NIK. Response to this request is shown in Table 4, and Appendix A lists all contributors. Commander, International Ice Patrol extends a sincere thank you to all stations and ships which contributed.

Table 4. Iceberg and SST Reports

Number of ships furnishing Sea Surface Temperature (SST) reports	103
Number of SST reports received	505
Number of ships furnishing ice reports	497
Number of ice reports received	673
First Ice Bulletin	140000Z MAR 85
Last Ice Bulletin	291200Z AUG 85
Number of facsimile charts transmitted	169

Environmental Conditions 1985 Season

Weather in Labrador and East Newfoundland during the 1985 International Ice Patrol season tended to be colder and dryer than normal during the winter and warmer and wetter than normal during the summer (Table 5). The weather stations listed in Table 5 were selected to give a cross-section of weather conditions throughout the province. The colder than normal months of December 1984 through March 1985 caused an early accumulation of sea ice which expanded south of 43°N and persisted longer than normal. This sea ice forced oil drilling rigs off the Grand Banks and protected the icebergs moving into the region.

January: With the Iceland Low southwest of its normal position and deeper than normal (Figure 1), the maritimes experienced a strong northerly flow that brought lower than normal temperatures.

February: The Iceland Low was deeper than normal (Figure 2), causing northwest winds to bring in cold continental air, resulting in below normal temperatures and precipitation in Newfoundland and Labrador (Table 5).

March: During March, the Iceland Low was southwest of its normal position (Figure 3), bringing more continental air than normal into the maritimes and lowering temperatures (Table 5).

April: Surface pressure was near normal during April (Figure 4). With a westerly flow returning to Newfoundland, temperatures and precipitation were normal (Table 5).

May: The Iceland Low was farther west and deeper than normal during May (Figure 5), bringing more marine air into St. John's and greater than normal precipitation (Table 5).

June: Flow, normally southwesterly over Newfoundland, was southerly in June (Figure 6), bringing greater than normal precipitation to Gander (Table 5).

July: Direction of surface winds was normal in July, but the stronger than normal pressure gradient (Figure 7) caused greater southerly flow, bringing above normal precipitation.

August: August temperatures and precipitation were above normal (Table 5). The shape of the isobars in Figure 8 were near normal, but the pressure gradient between a deeper Iceland Low and the Bermuda High caused increased southwest flow bringing in more warm, moist air than normal (Table 5).

September: With the Iceland Low deeper than normal (Figure 9), a westerly flow dominated, bringing warmer, drier air over the maritimes resulting in above normal temperatures (Table 5).

Table 5. Environmental Conditions for 1985 International Ice Patrol Season

	Station	Temp°C Monthly Mean	Temp°C Diff. from Norm.	Total Precipitation (mm)	% of Normal Precipitation	% of Normal Snowfall
OCT 1984	Nain	0.8	1.6	74.2	118.2%	217.9%
	Goose	2.1	0.6	38.7	50.5%	62.8%
	Gander	3.8	2.2	59.4	56.7%	141.0%
	St. John's	5.0	1.9	80.7	55.5%	59.1%
NOV	Nain	-4.6	-1.4	141.1	245.8%	263.3%
	Goose	-3.8	0.0	117.0	155.6%	206.8%
	Gander	1.0	0.8	73.6	68.6%	118.9%
	St. John's	2.8	0.6	100.6	61.9%	50.5%
DEC	Nain	-17.2	-6.5	67.8	119.6%	111.3%
	Goose	-17.2	-4.2	112.5	154.7%	194.6%
	Gander	-4.3	-0.5	68.2	63.0%	80.4%
	St. John's	-2.0	-0.5	109.2	67.7%	52.7%
JAN 1985	Nain	-12.6	-3.2	210.7	338.7%	291.0%
	Goose	-15.6	-0.8	134.0	180.1%	293.9%
	Gander	-7.4	-1.7	96.0	88.0%	122.5%
	St. John's	-5.9	-1.3	111.6	71.6%	102.6%
FEB	Nain	-16.2	-1.1	124.3	248.1%	189.9%
	Goose	-14.5	0.0	25.1	41.4%	66.7%
	Gander	-7.4	-0.6	91.4	91.7%	108.9%
	St. John's	-5.9	-1.4	96.3	68.7%	97.5%
MAR	Nain	-12.0	-1.5	124.3	224.4%	193.3%
	Goose	-9.3	-1.1	56.5	78.3%	146.6%
	Gander	-5.8	-2.7	51.0	46.3%	57.3%
	St. John's	-5.1	-3.2	102.3	77.6%	78.6%
APR	Nain	-8.1	-3.2	119.6	257.2%	253.6%
	Goose	-3.2	-1.5	52.8	86.3%	101.2%
	Gander	-0.6	0.3	86.6	92.9%	112.1%
	St. John's	-0.1	1.1	96.2	83.2%	125.4%
MAY	Nain	-1.0	0.4	52.2	103.0%	42.6%
	Goose	2.8	-2.6	66.5	104.2%	100.0%
	Gander	5.7	0.5	37.2	53.1%	88.5%
	St. John's	4.4	1.0	168.6	165.6%	81.1%
JUN	Nain	6.9	0.5	22.4	35.1%	58.1%
	Goose	11.0	0.3	85.8	92.2%	91.9%
	Gander	11.8	0.0	124.2	154.7%	0.0%
	St. John's	10.4	0.5	88.9	103.9%	0.0%
JUL	Nain	10.8	0.3	89.6	106.0%	0.0%
	Goose	15.5	0.3	235.3	223.9%	*
	Gander	17.7	1.2	107.8	156.2%	*
	St. John's	17.5	2.0	108.8	130.9%	*
AUG	Nain	10.2		46.0		*
	Goose	14.6	4.7	153.3	148.5%	*
	Gander	14.9	0.7	110.0	113.1%	*
	St. John's	13.9	1.4	100.9	83.0%	*
SEP	Nain	8.0		60.5		*
	Goose	9.9	0.8	81.6	96.6%	*
	Gander	11.0	4.6	75.6	93.1%	*
	St. John's	11.0	4.9	54.2	48.4%	*

* No snowfall recorded during this month

Figure 1.

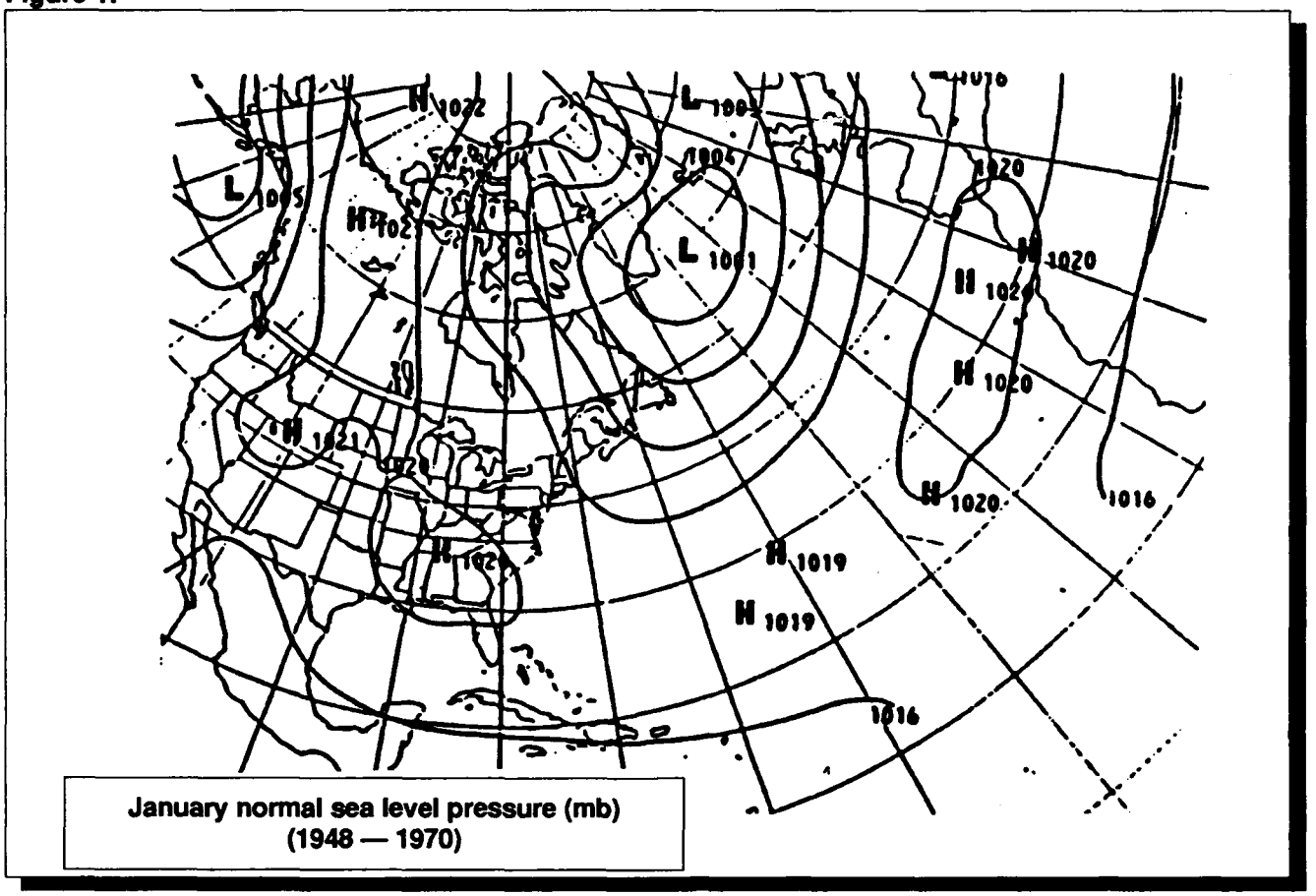

January normal sea level pressure (mb)
(1948 — 1970)

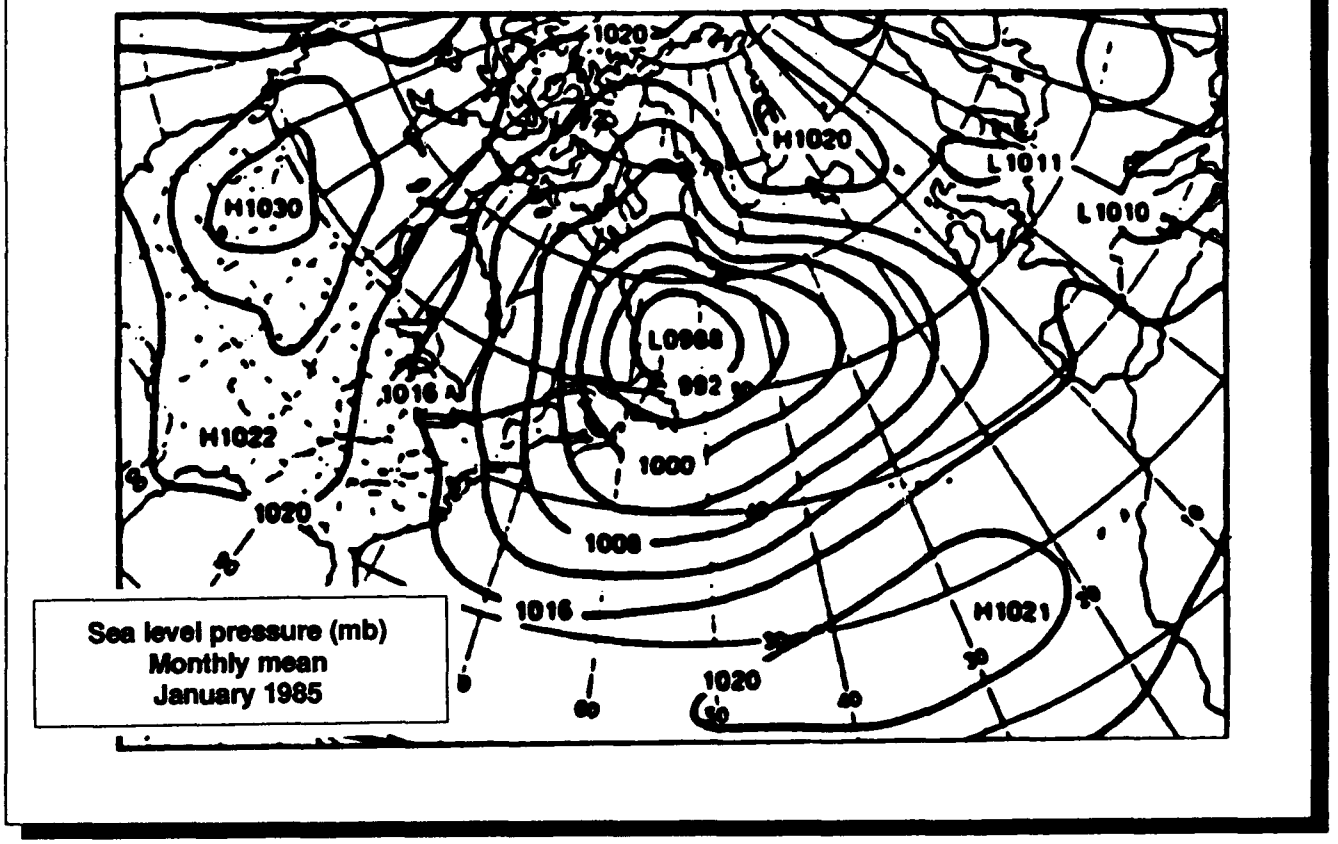

Sea level pressure (mb)
Monthly mean
January 1985

Figure 2.

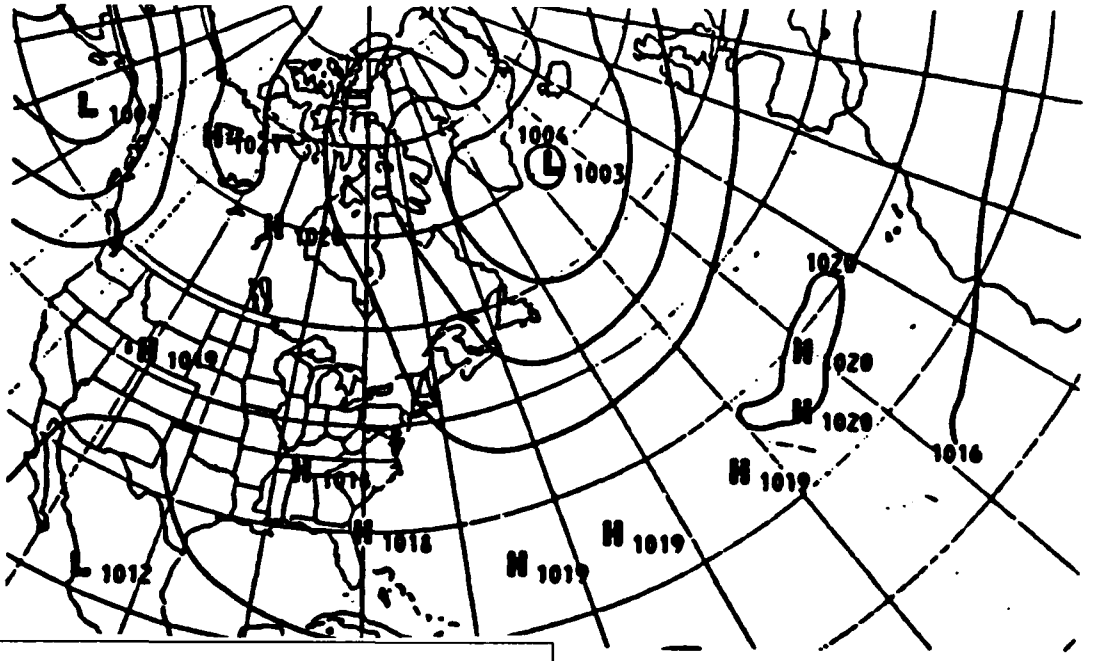

February normal sea level pressure (mb)
(1948 — 1970)

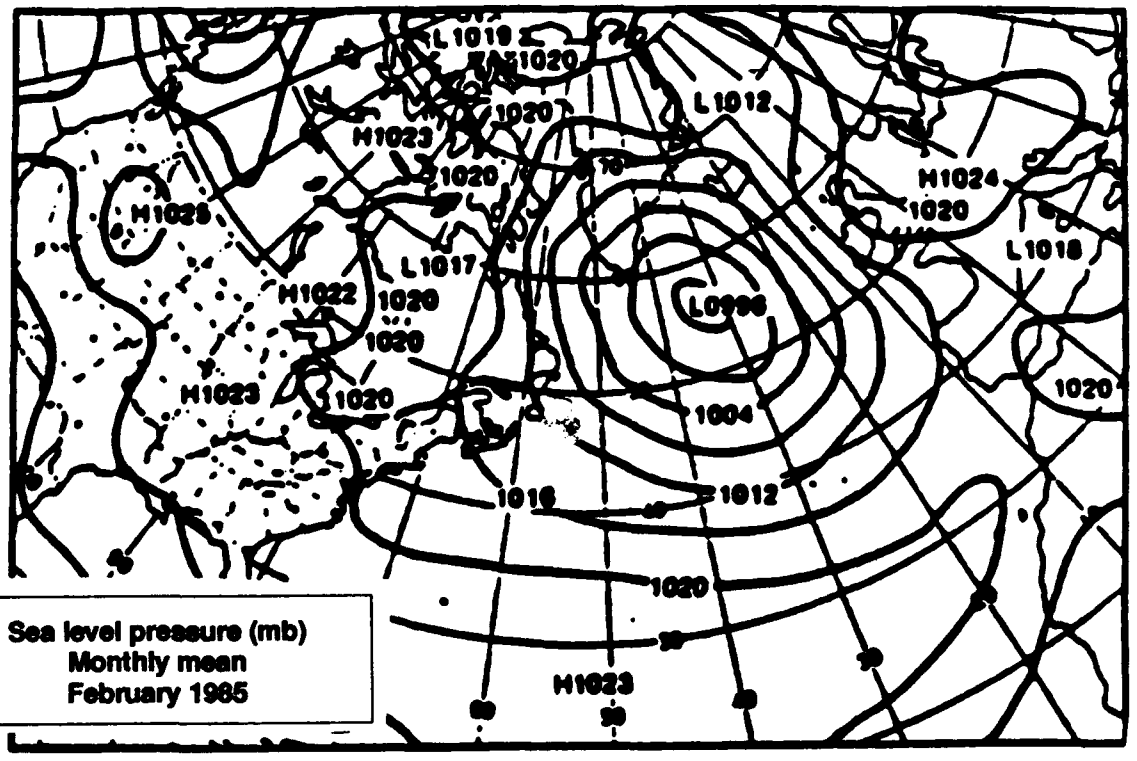

Sea level pressure (mb)
Monthly mean
February 1985

Figure 3.

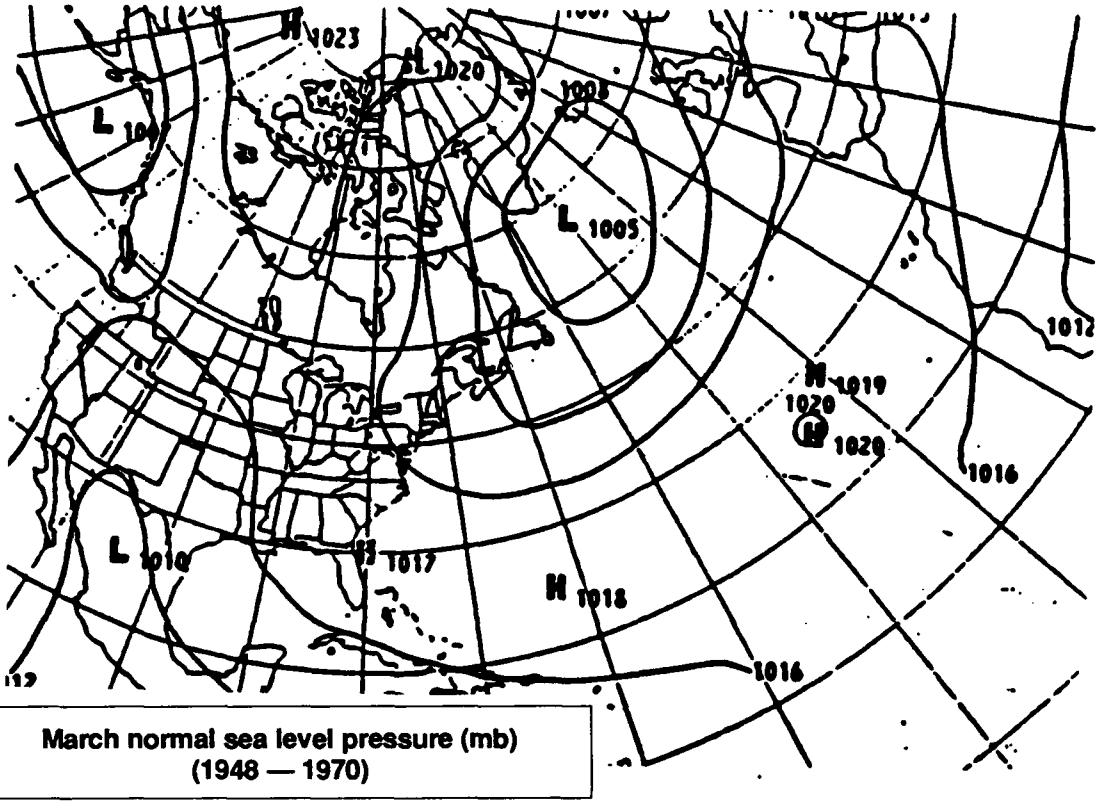

March normal sea level pressure (mb)
(1948 — 1970)

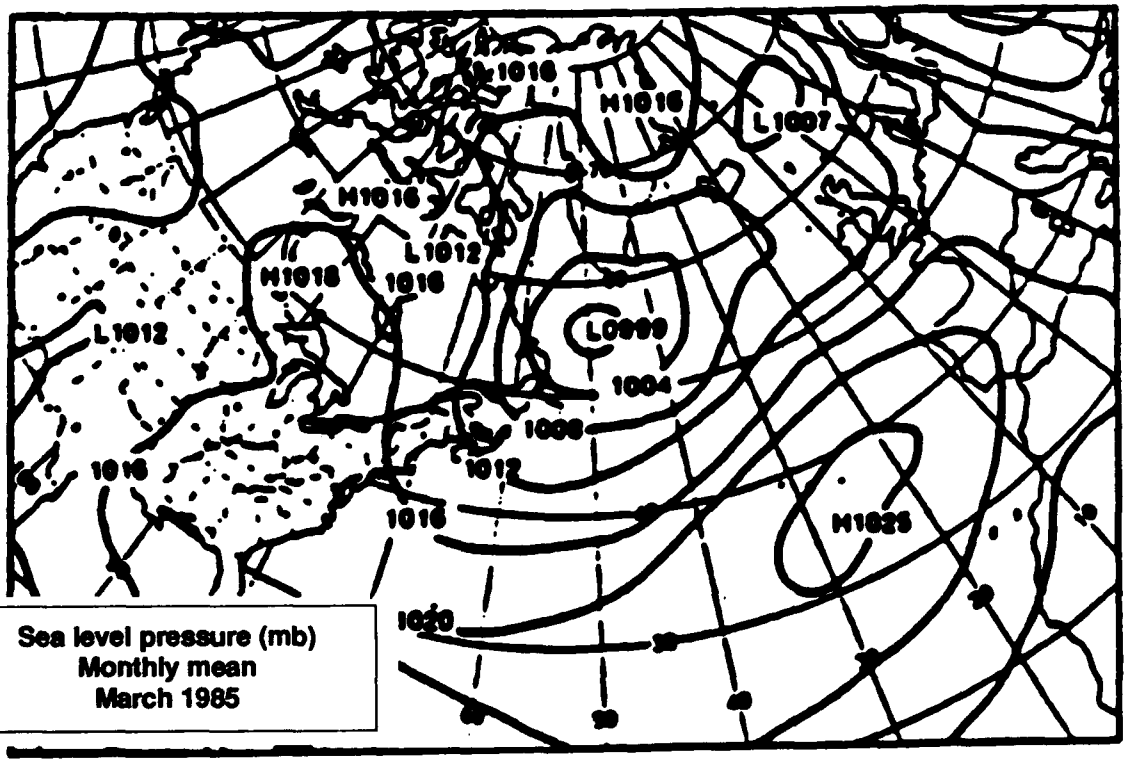

Sea level pressure (mb)
Monthly mean
March 1985

Figure 4.

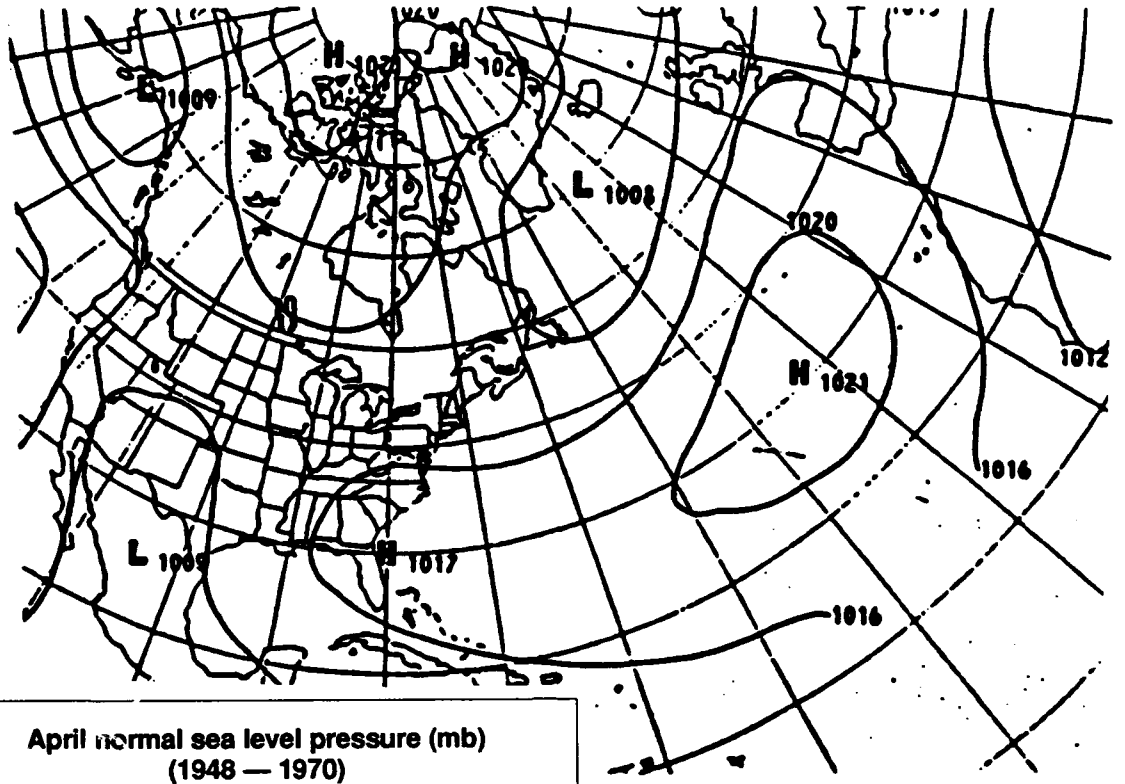

April normal sea level pressure (mb)
(1948 — 1970)

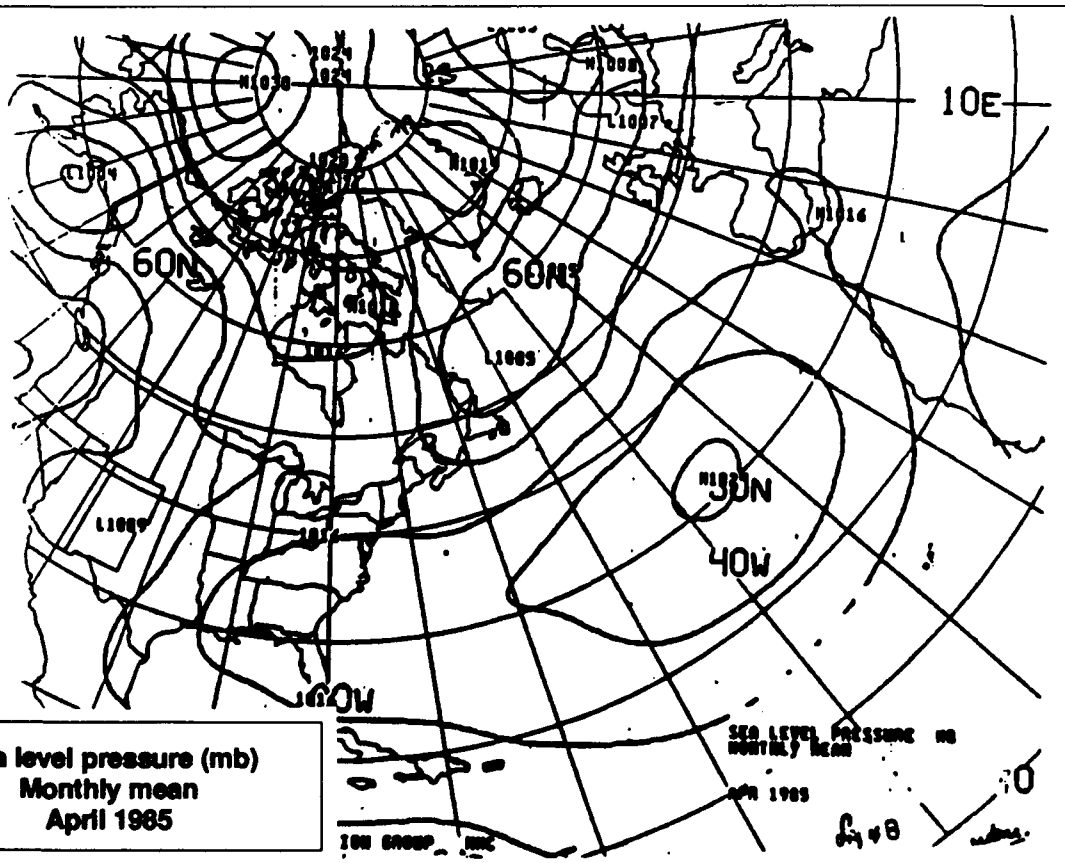

Sea level pressure (mb)
Monthly mean
April 1965

Figure 5.

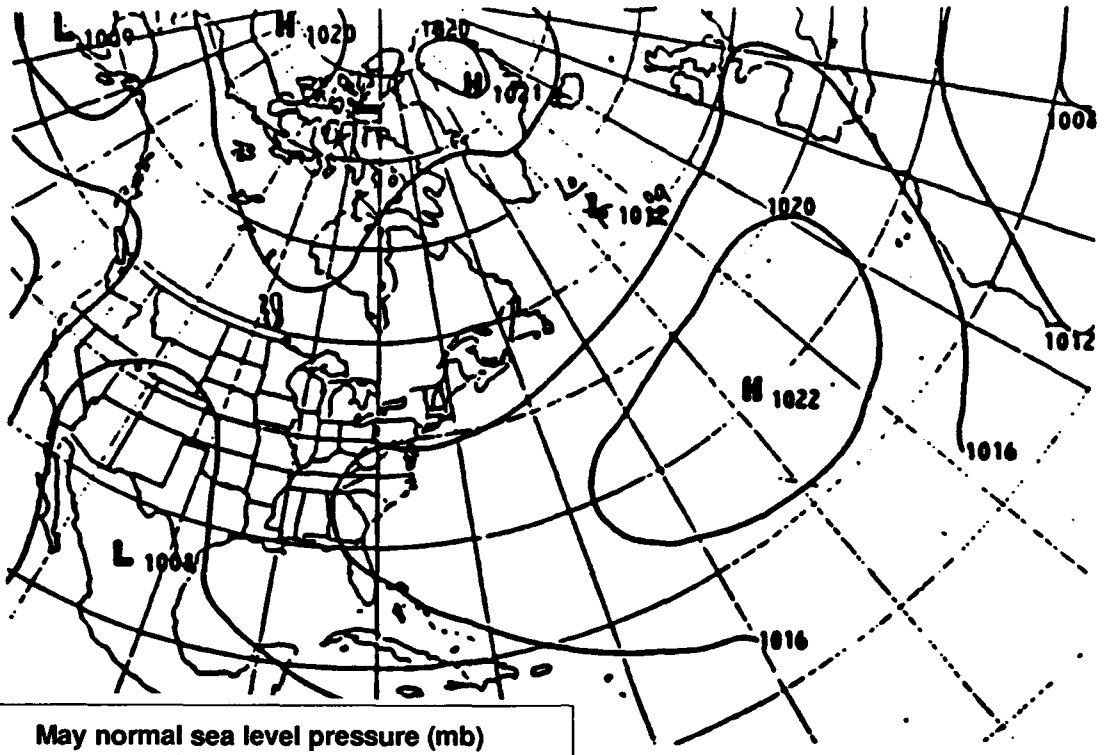

May normal sea level pressure (mb)
(1948 — 1970)

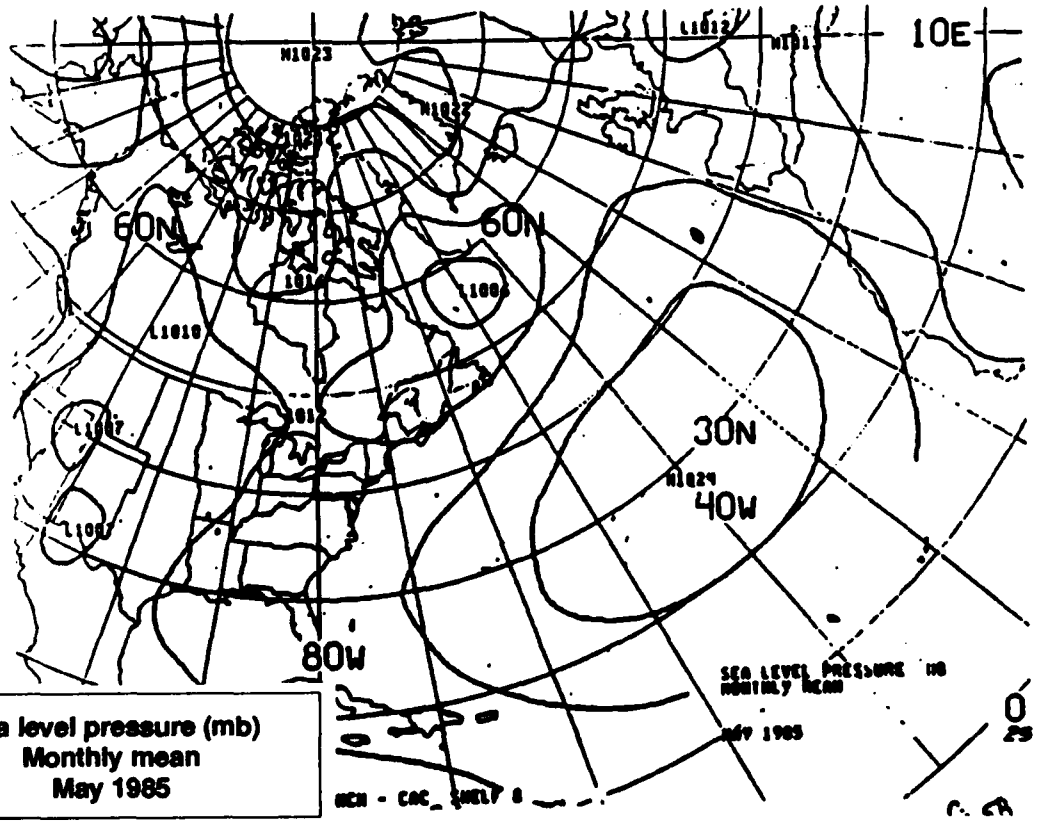

Sea level pressure (mb)
Monthly mean
May 1985

Figure 6.

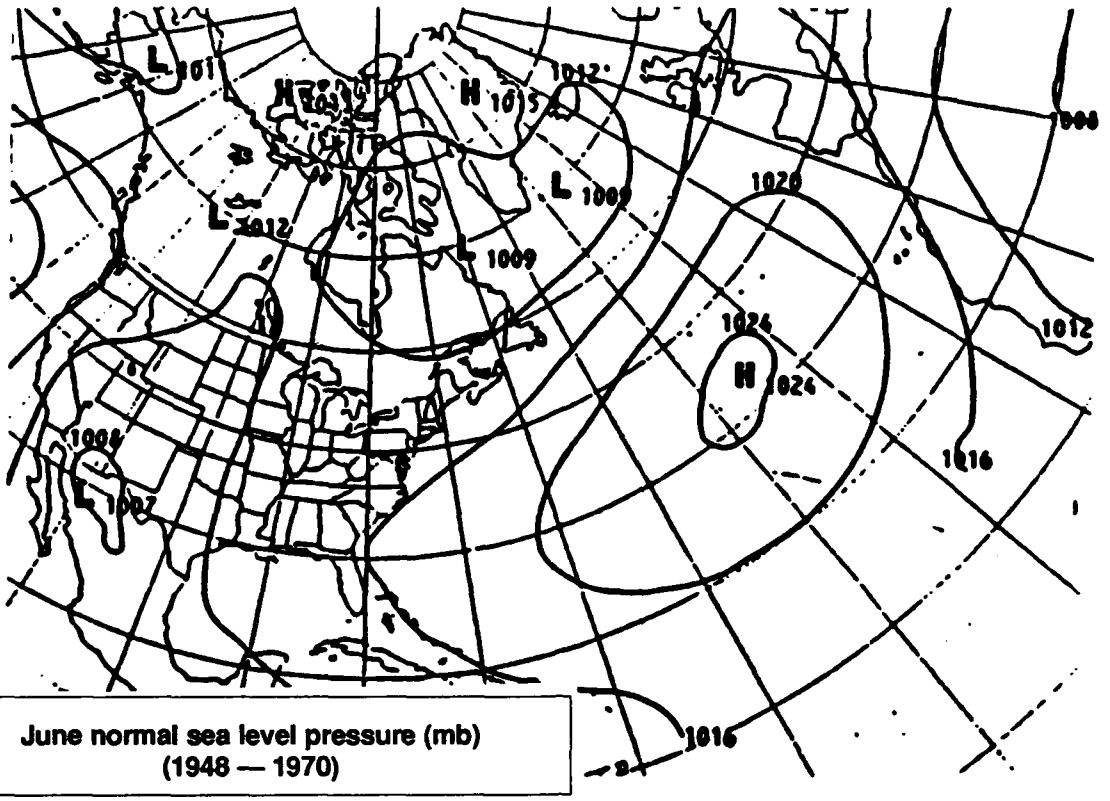

June normal sea level pressure (mb)
(1948 — 1970)

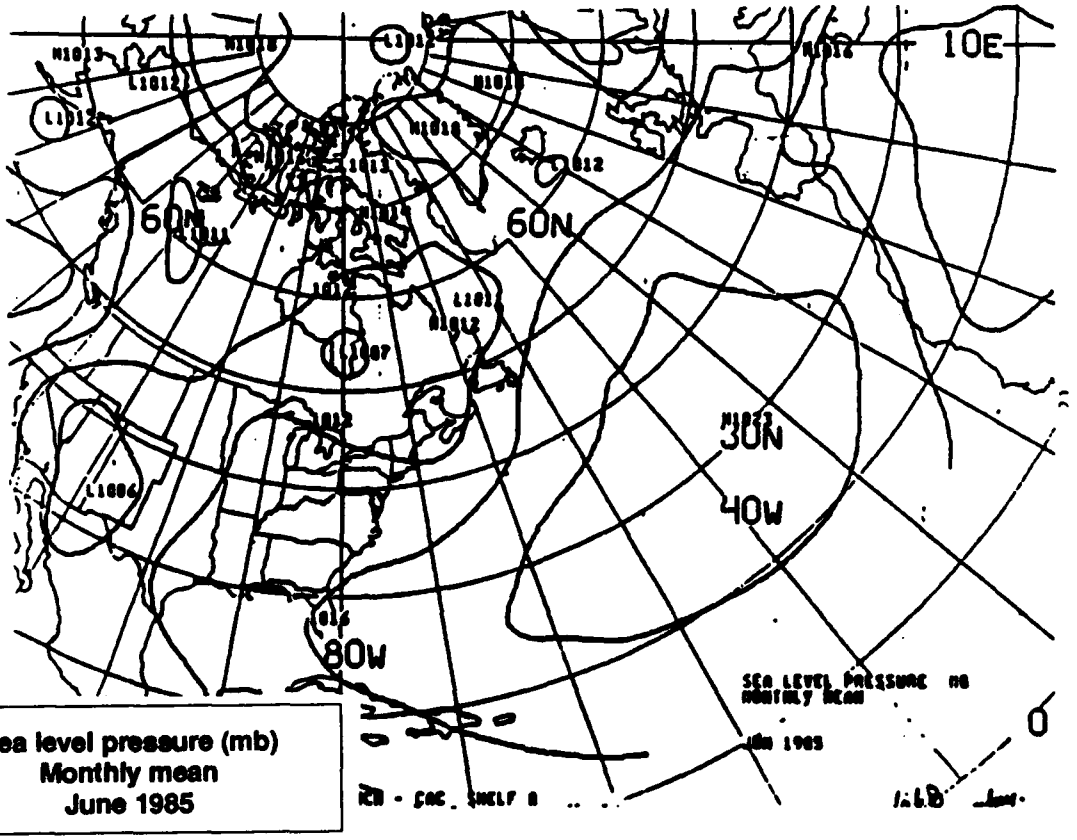

Sea level pressure (mb)
Monthly mean
June 1985

Figure 7.

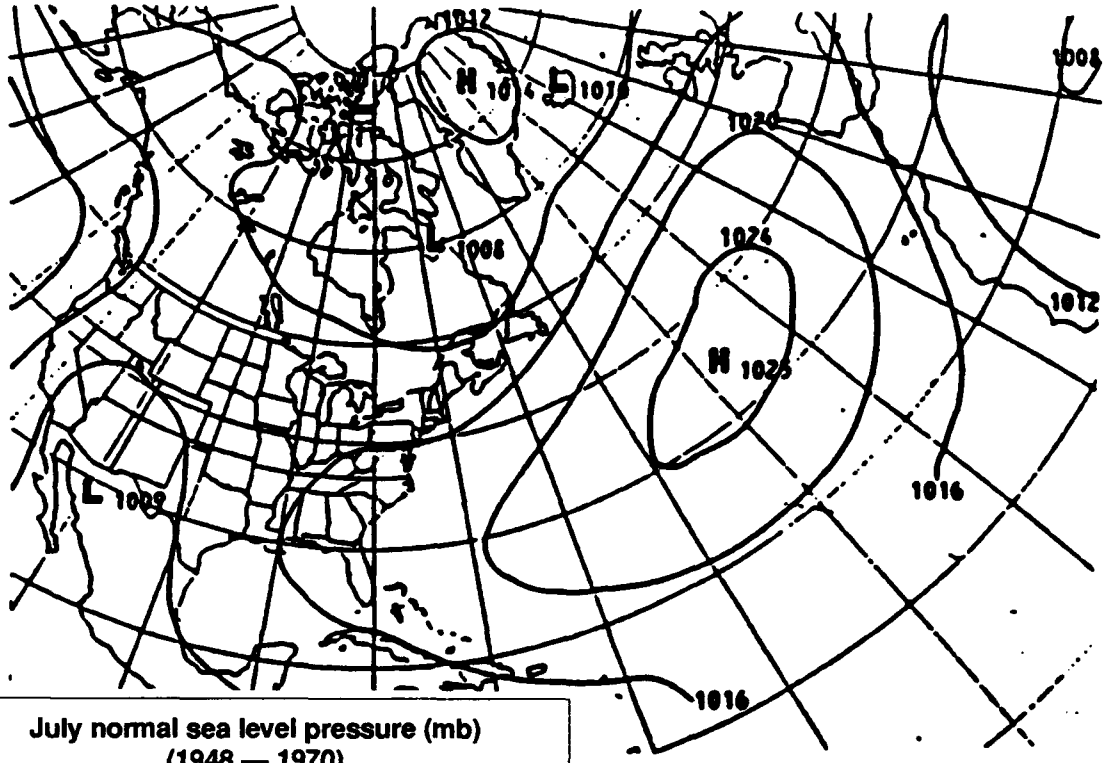

July normal sea level pressure (mb)
(1948 — 1970)

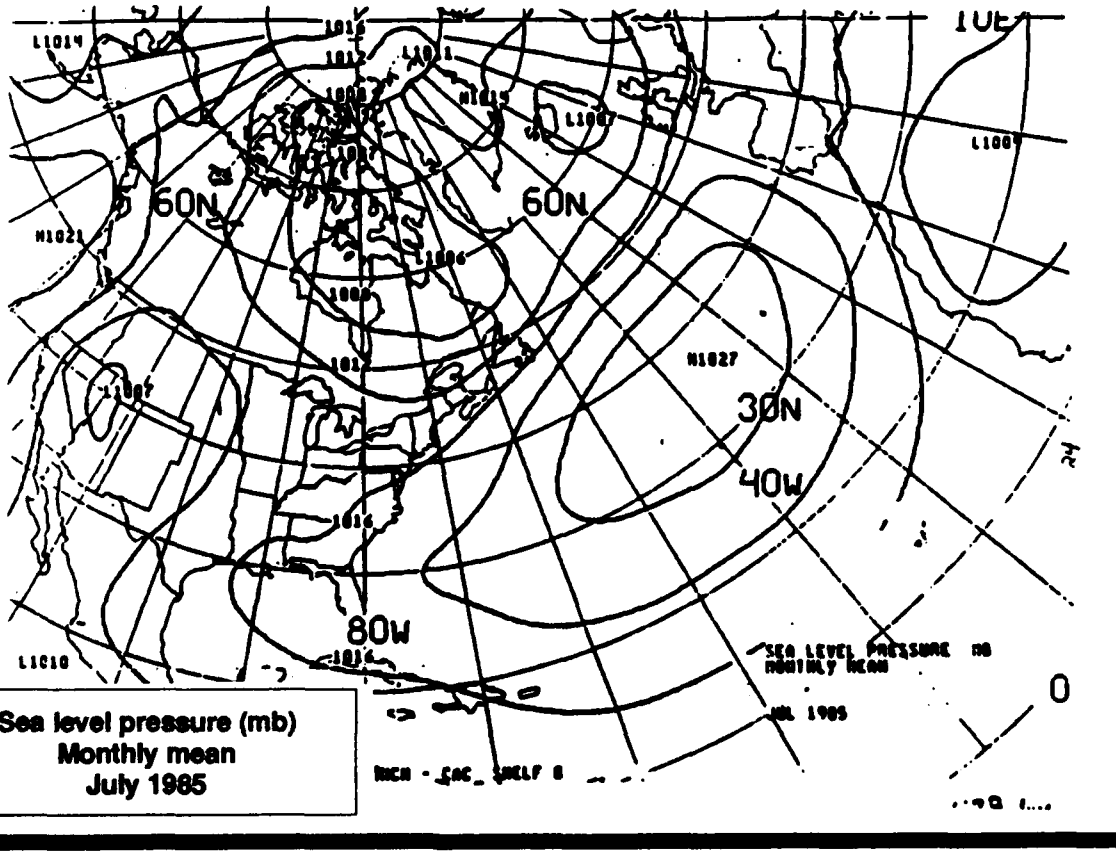

Sea level pressure (mb)
Monthly mean
July 1985

Figure 8.

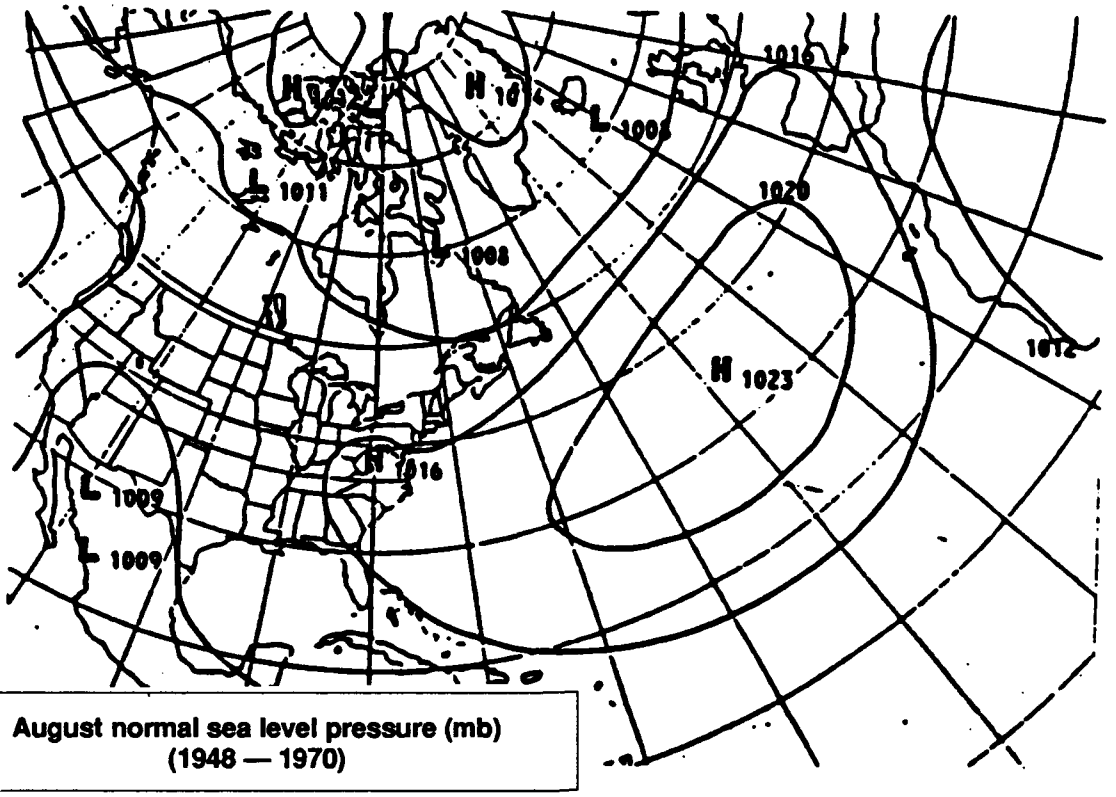

August normal sea level pressure (mb)
(1948 — 1970)

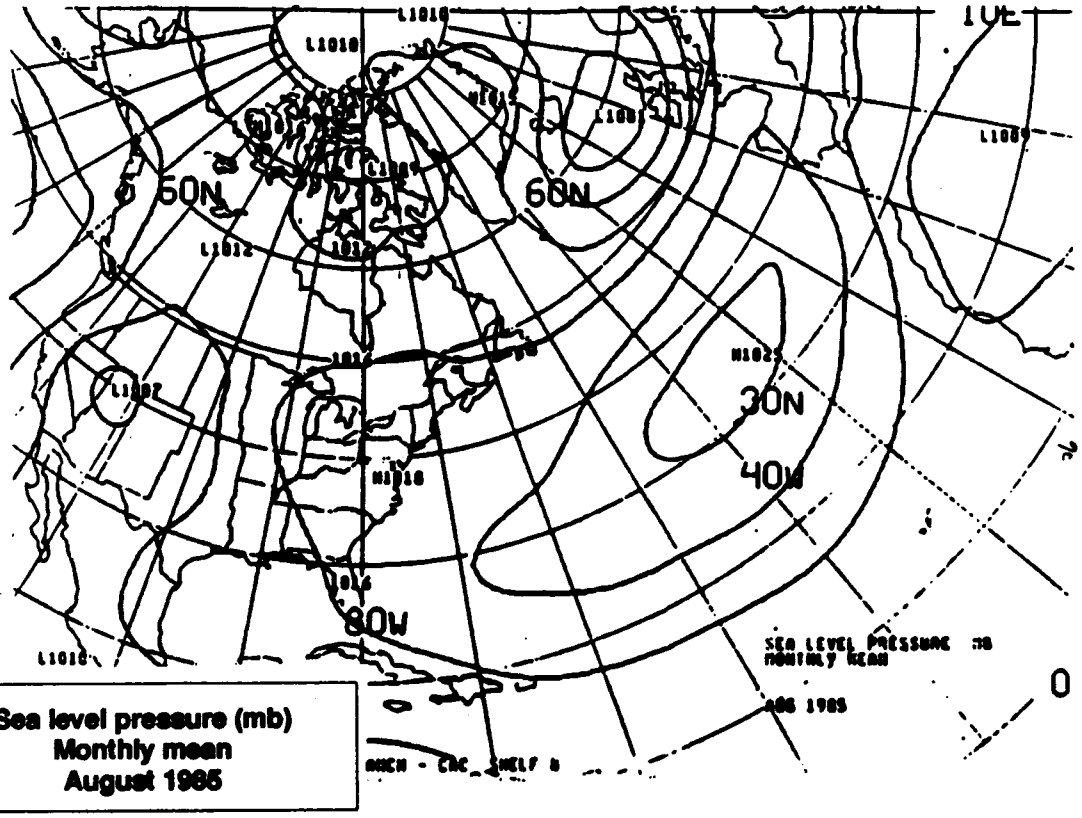

Sea level pressure (mb)
Monthly mean
August 1965

Figure 9.

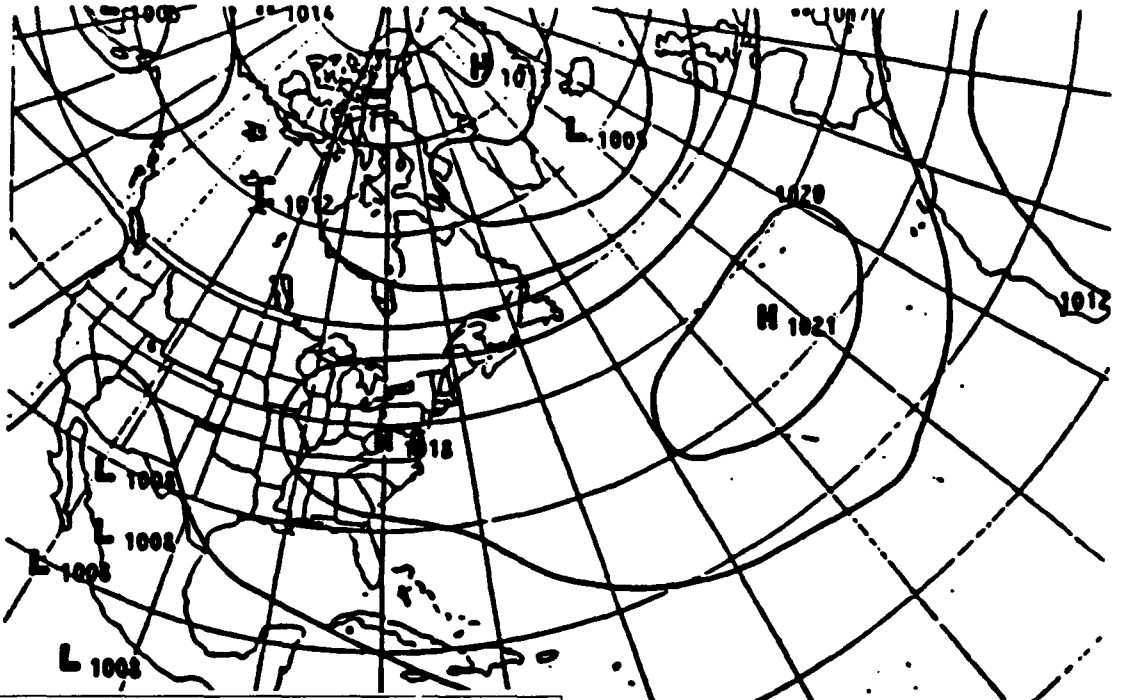

September normal sea level pressure (mb)
(1948 — 1970)

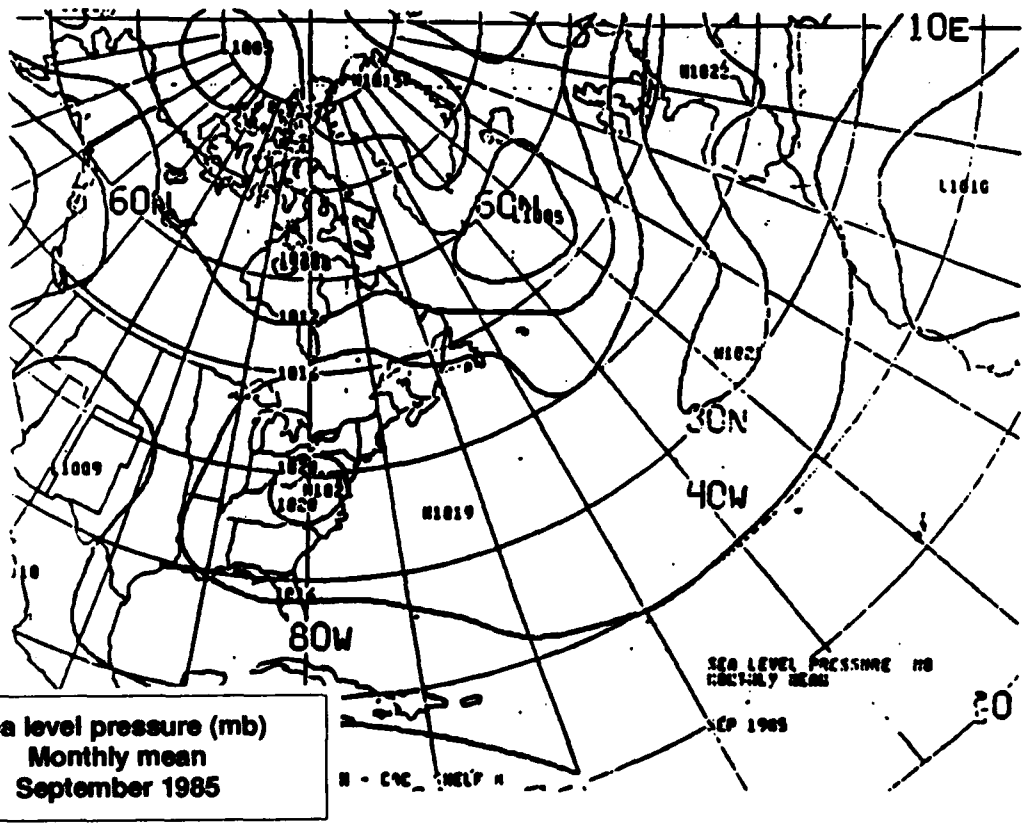

Sea level pressure (mb)
Monthly mean
September 1985

Figure 10. 16 October 1984

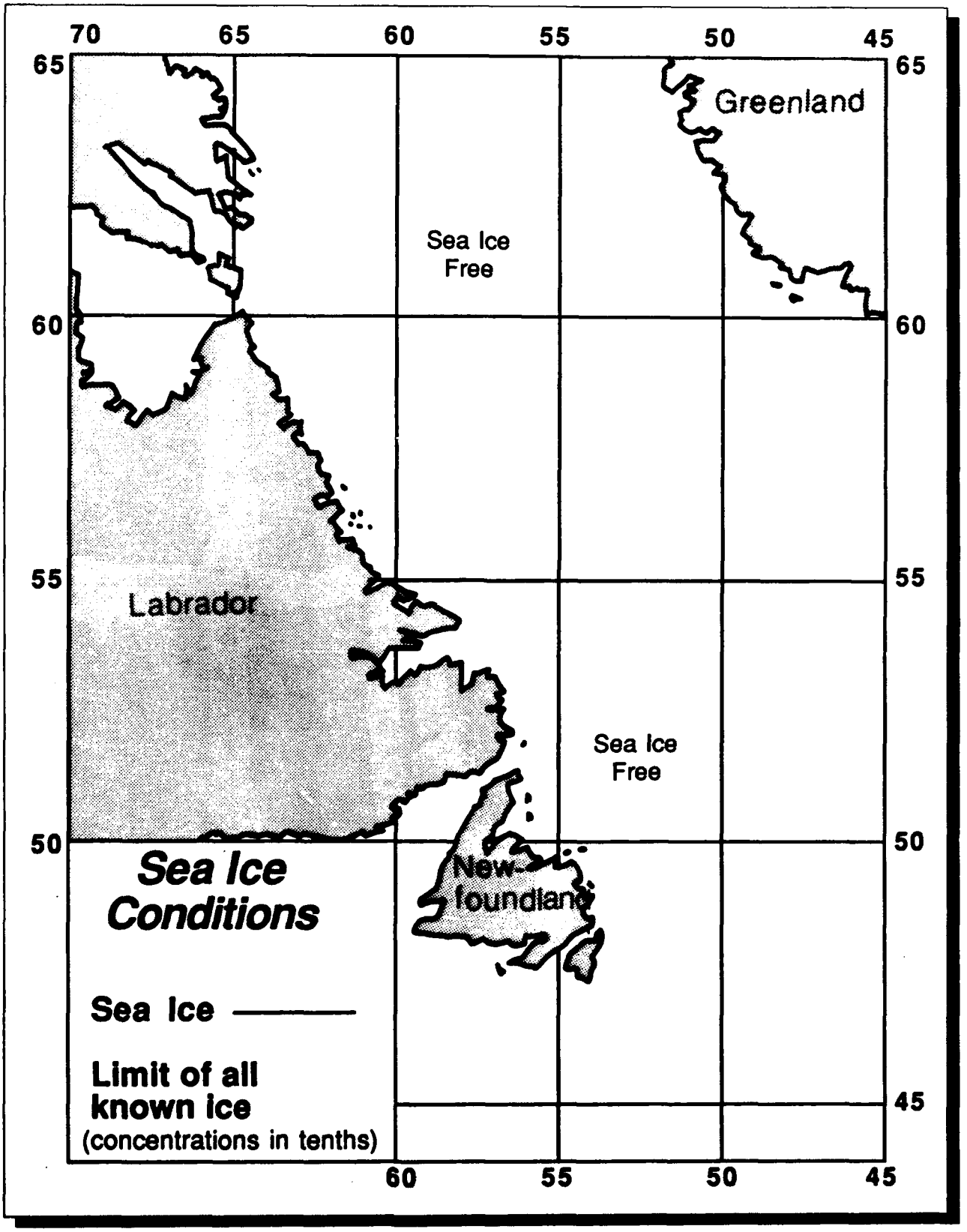

Figure 11. 13 November 1984

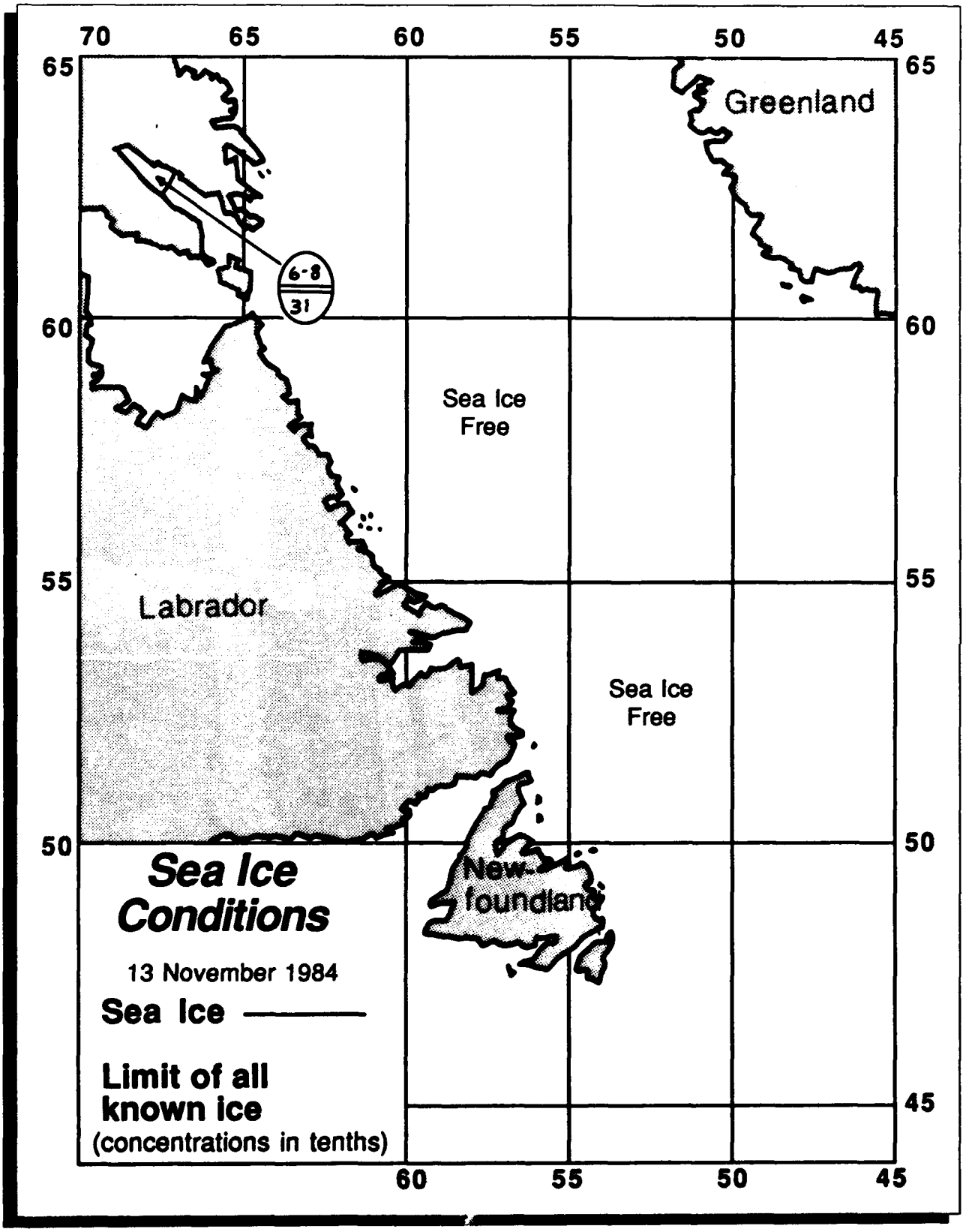

Figure 12. 18 December 1984

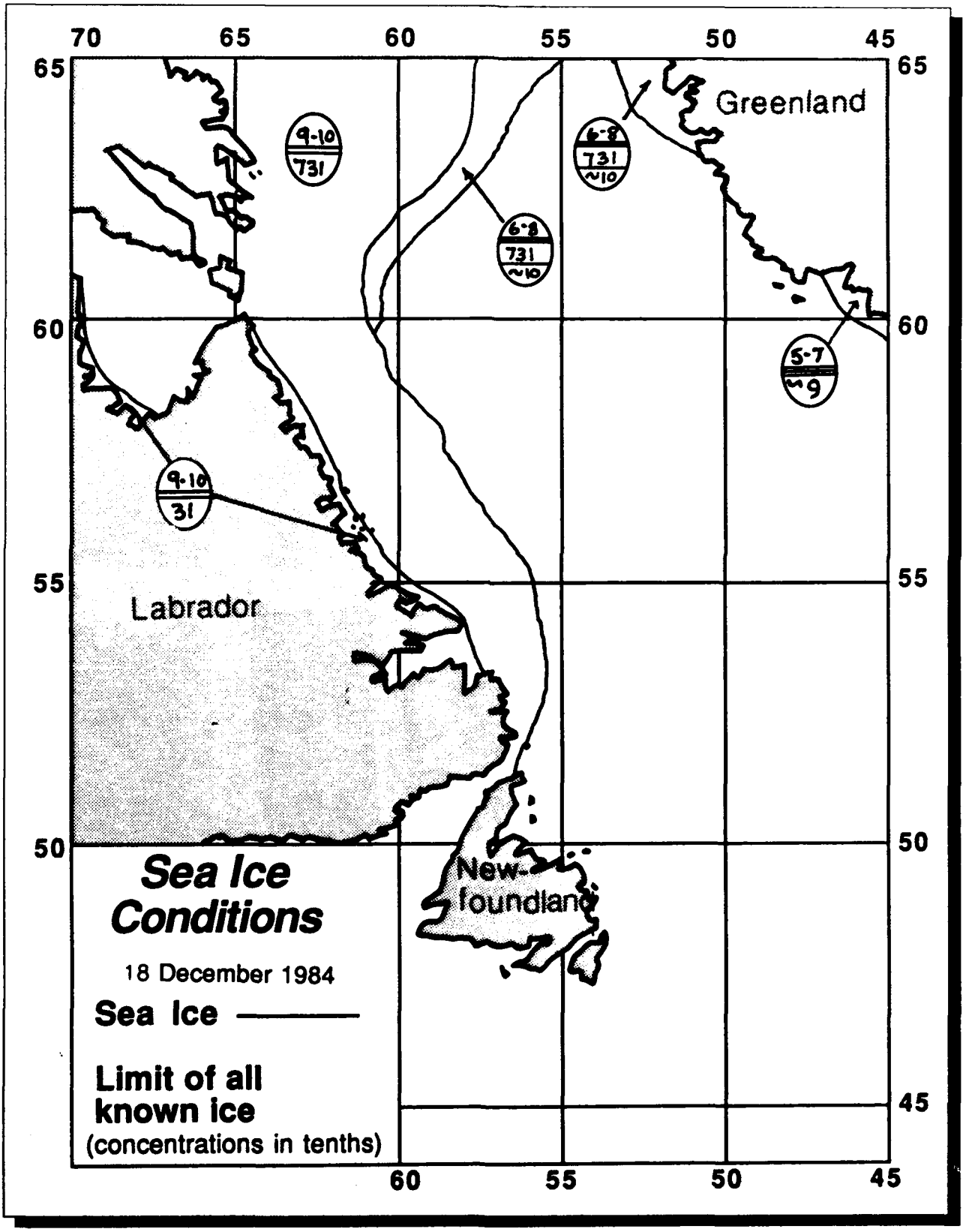

Figure 13. 15 January 1985

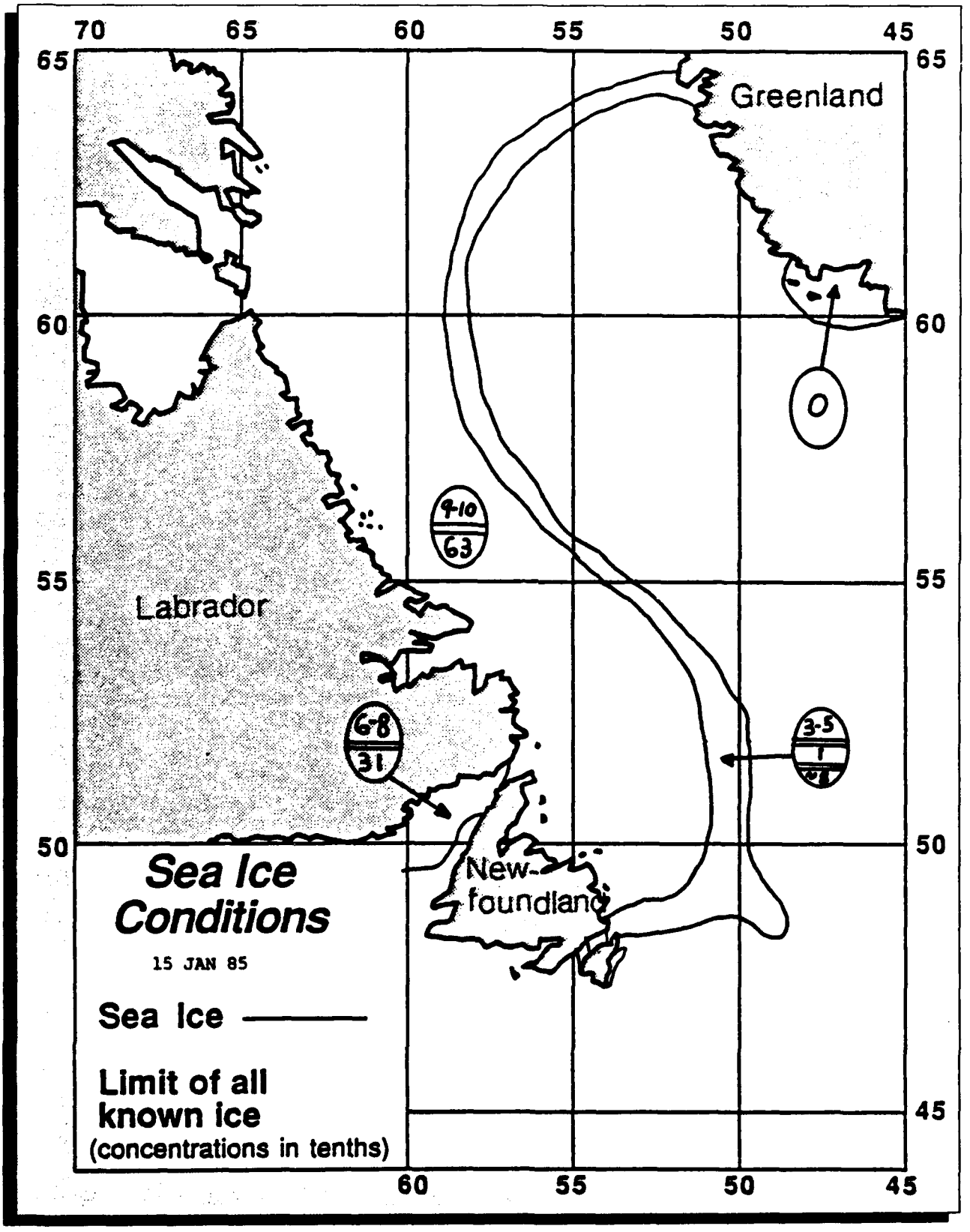

Figure 14. 12 February 1985

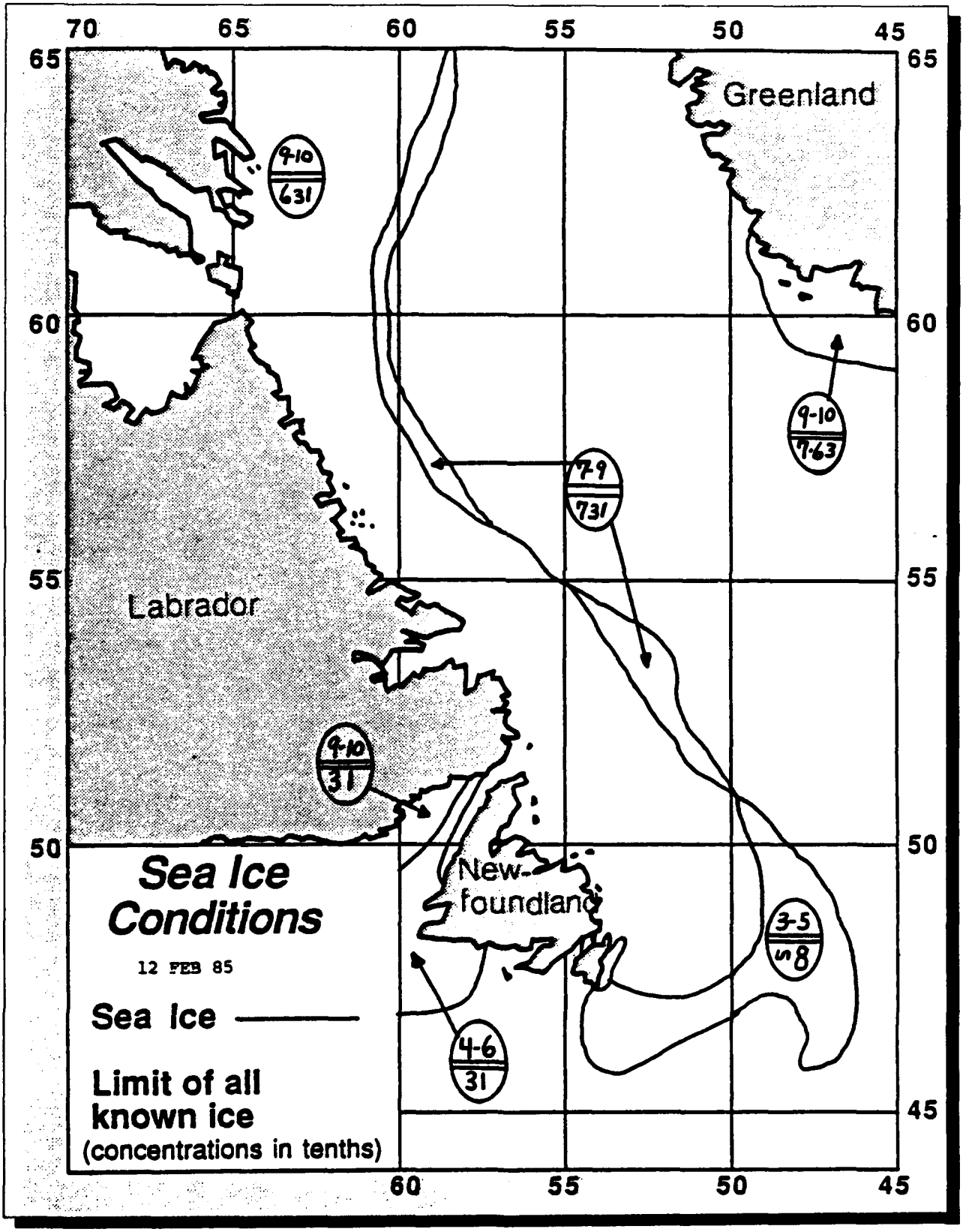

Figure 15. 12 March 1985

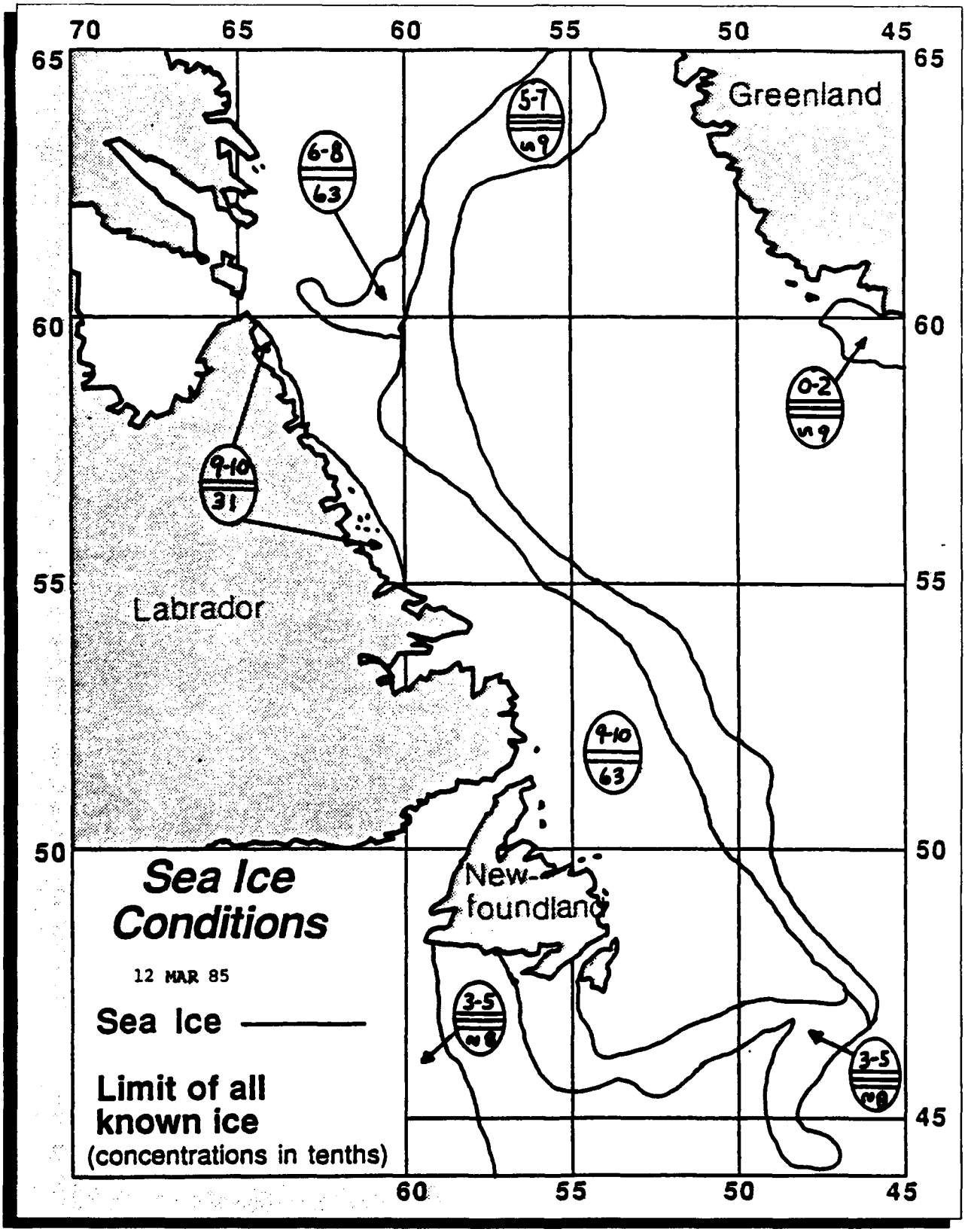

Figure 16. 16 April 1985

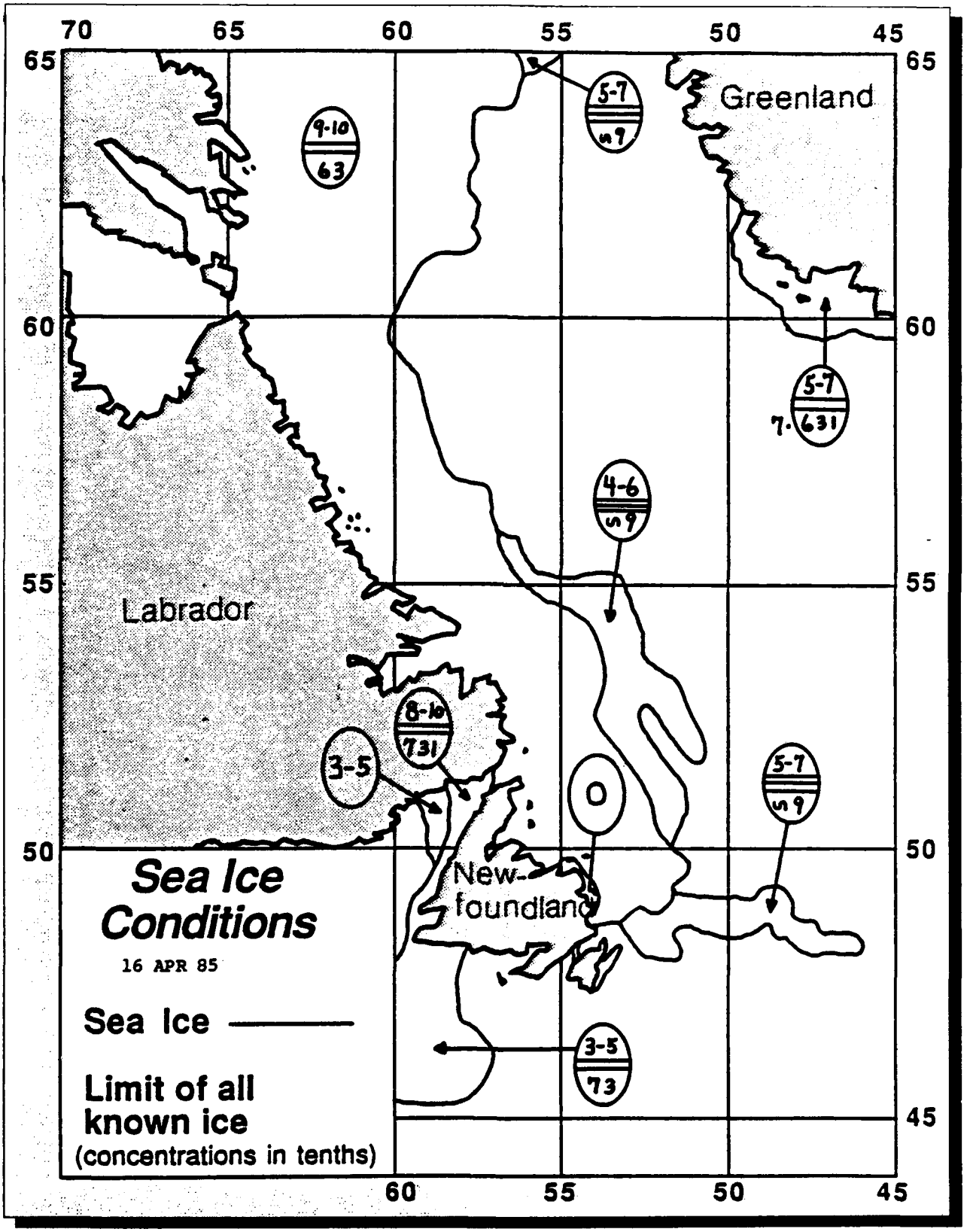

Figure 17. 14 May 1985

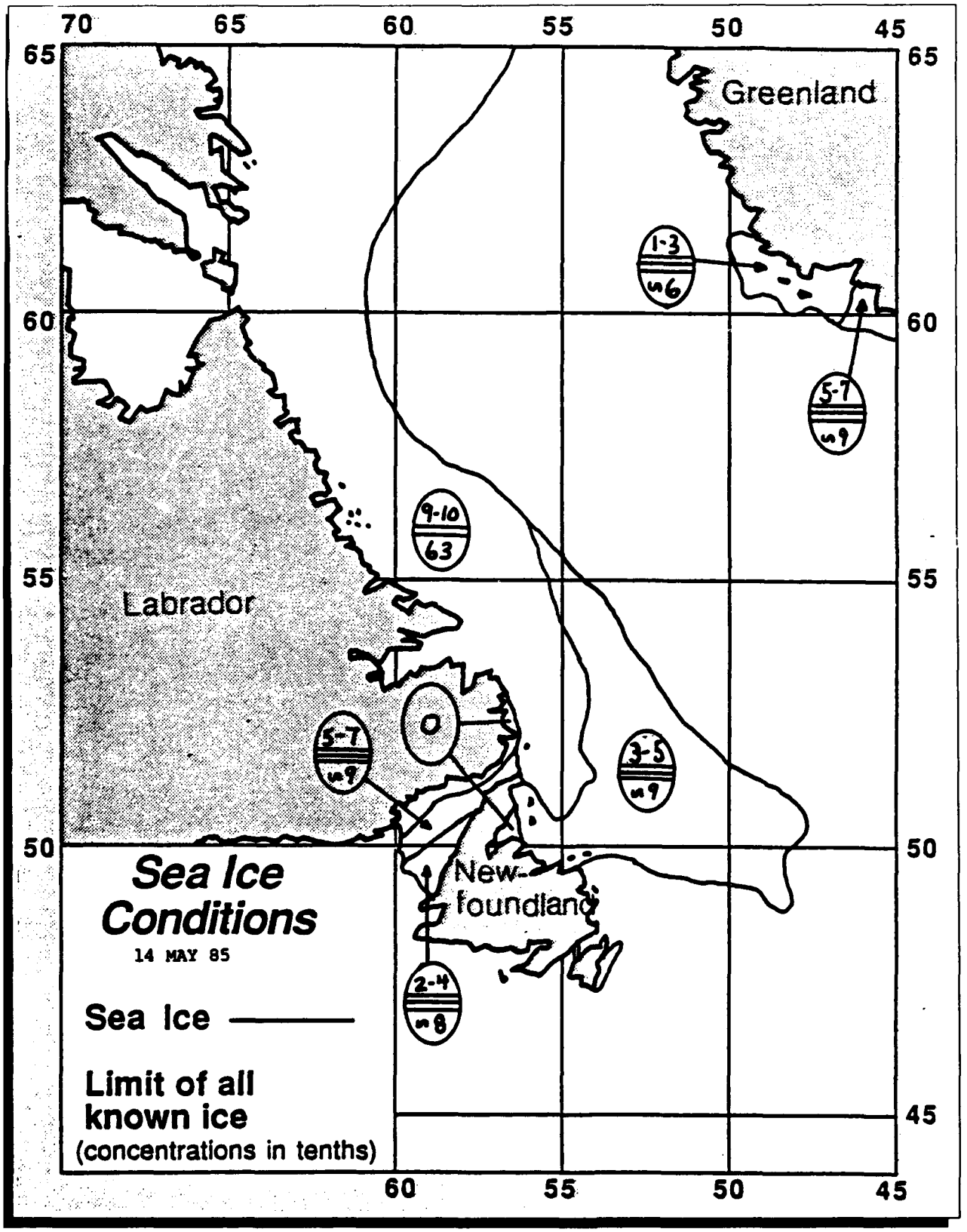

Figure 18. 18 June 1985

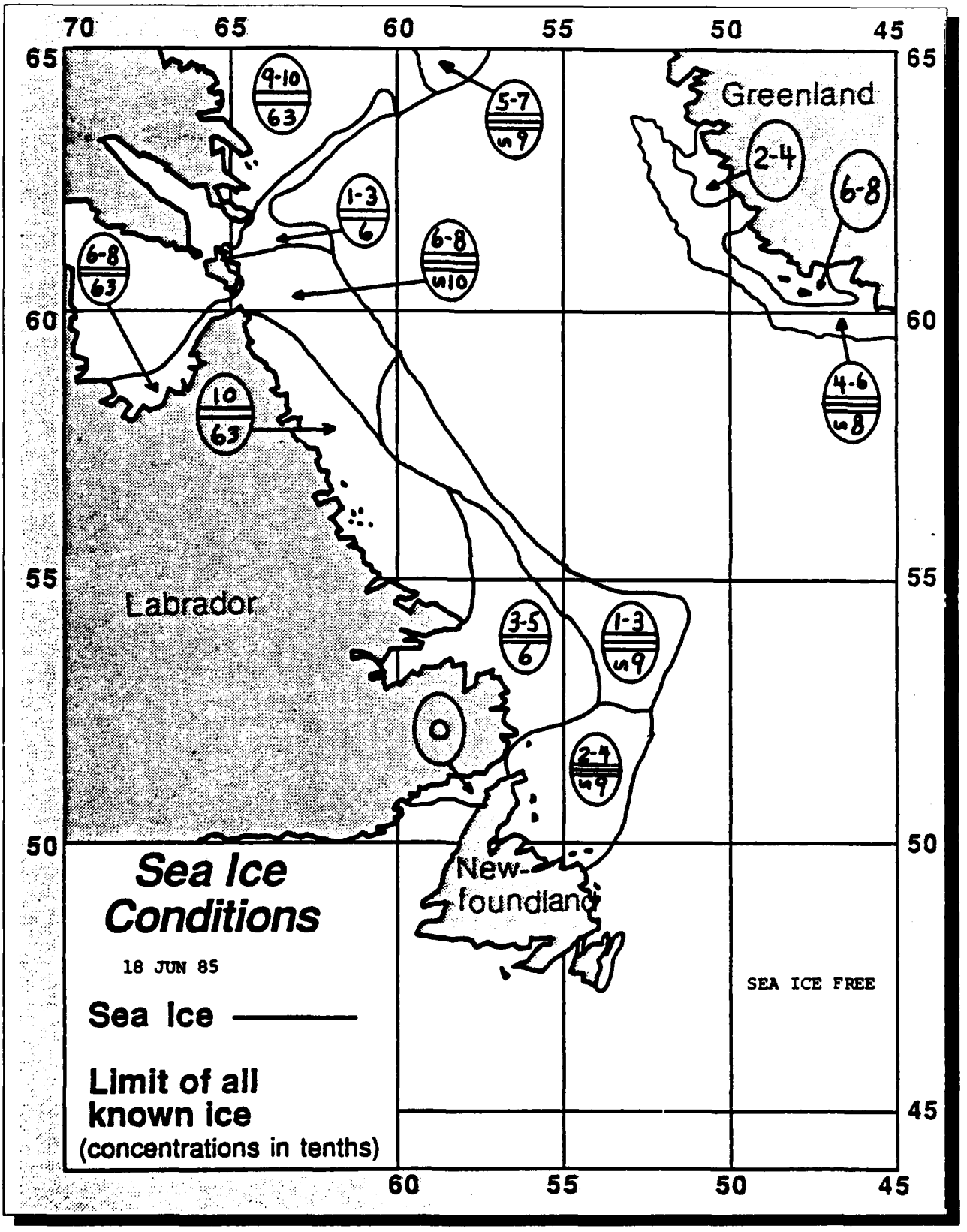

Figure 19. 16 July 1985

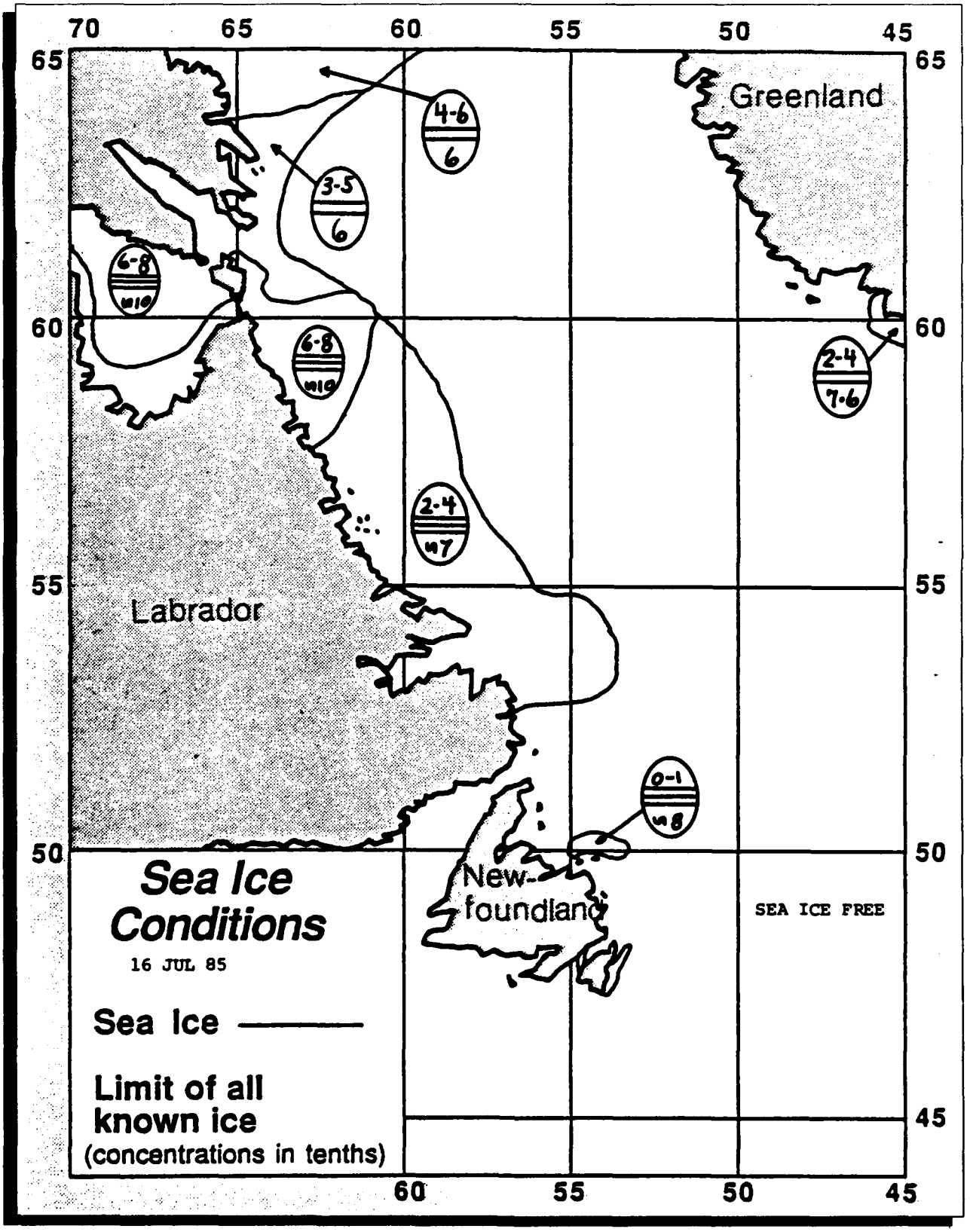

Figure 20. 13 August 1985

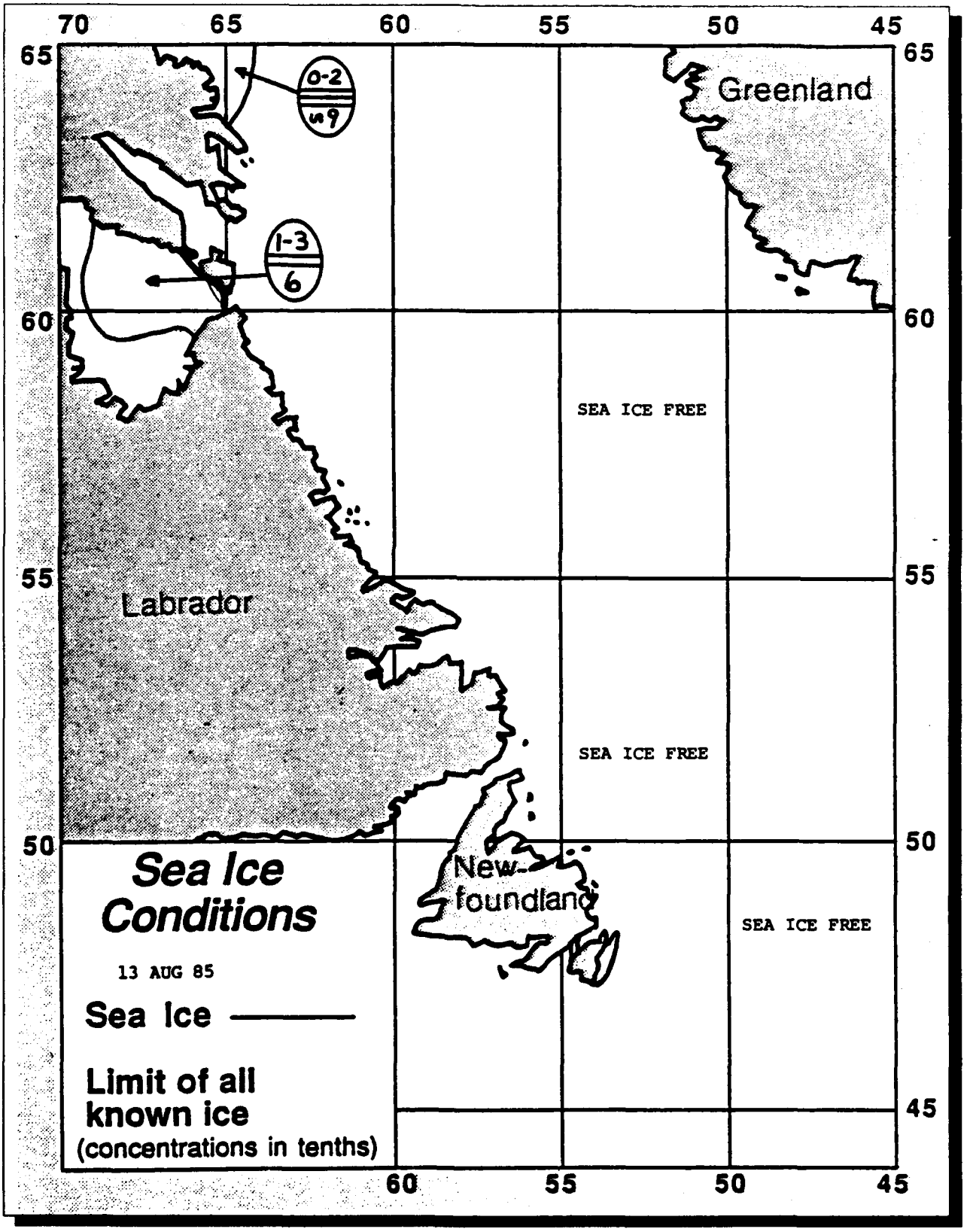

Figure 21. 17 September 1985

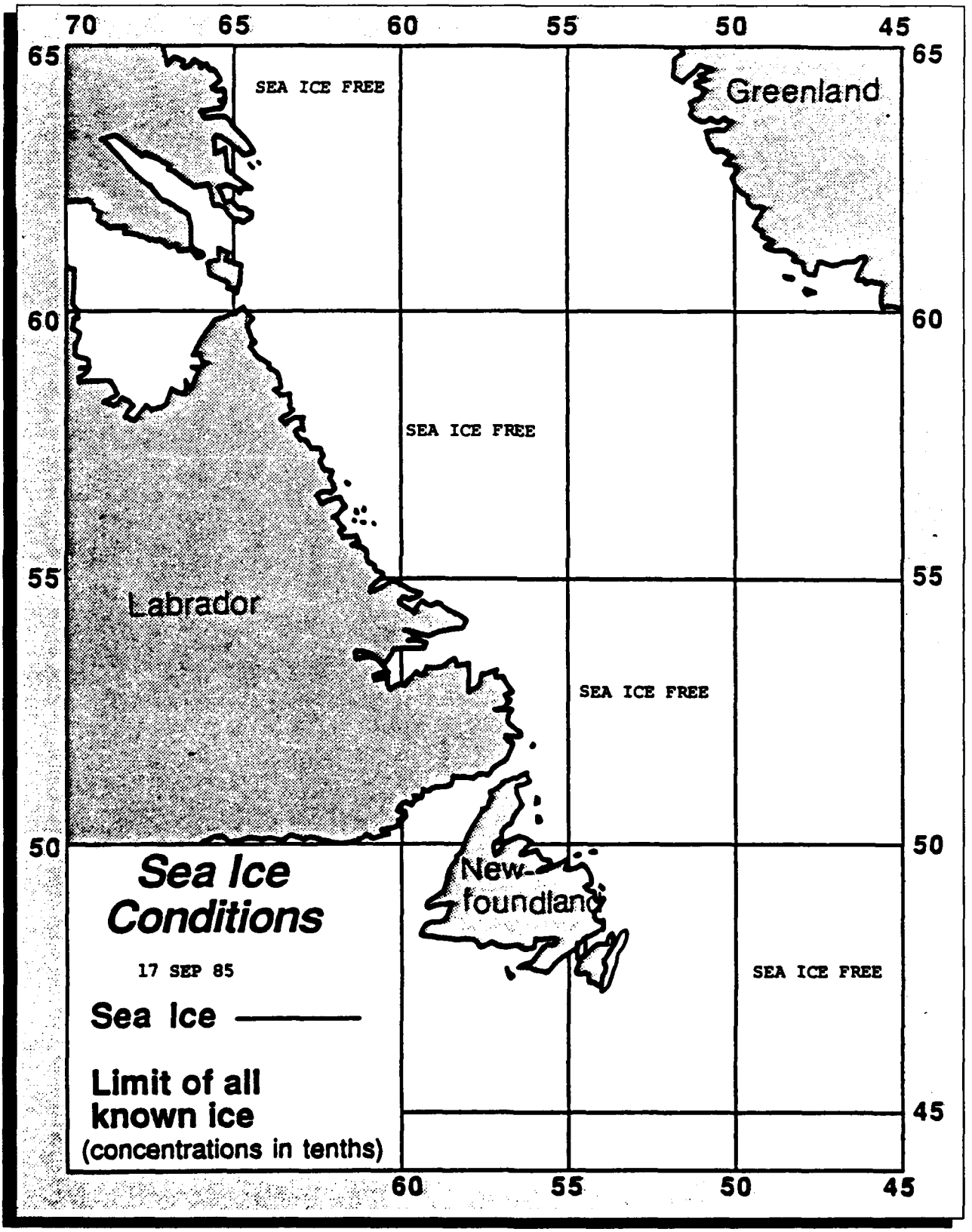

Figure 22. 15 March 1985

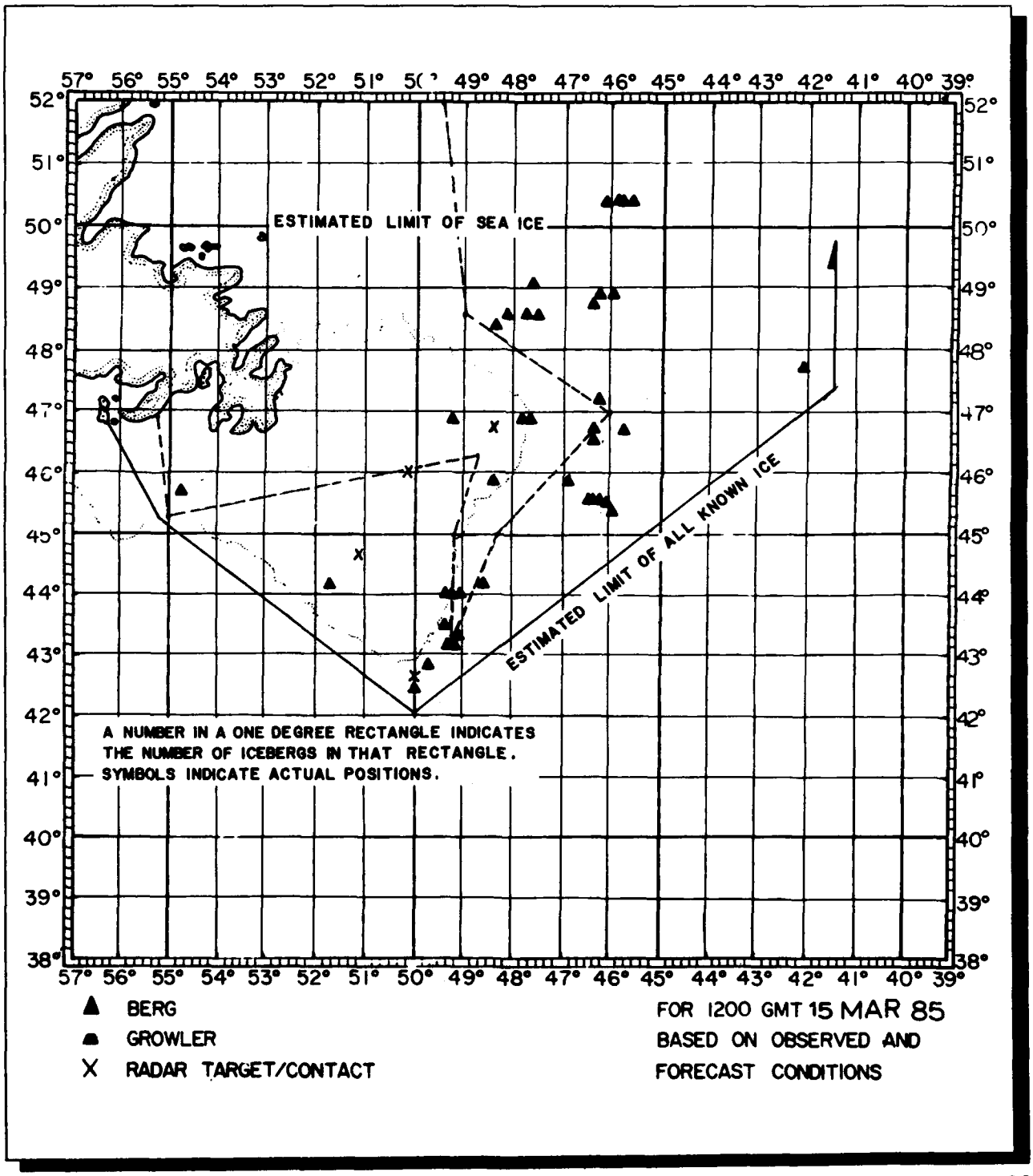

Figure 23. 30 March 1985

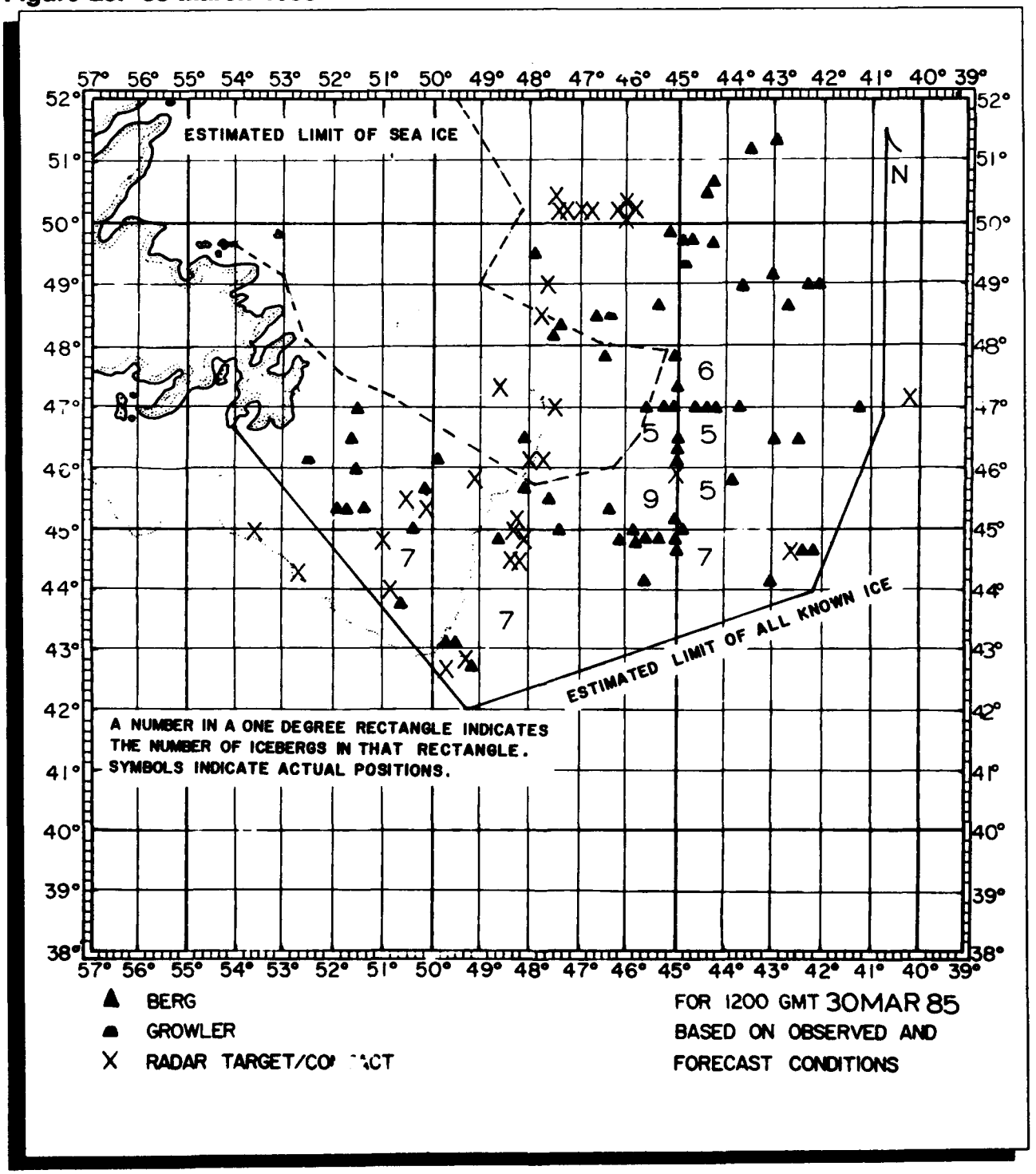

Figure 24. 15 April 1985

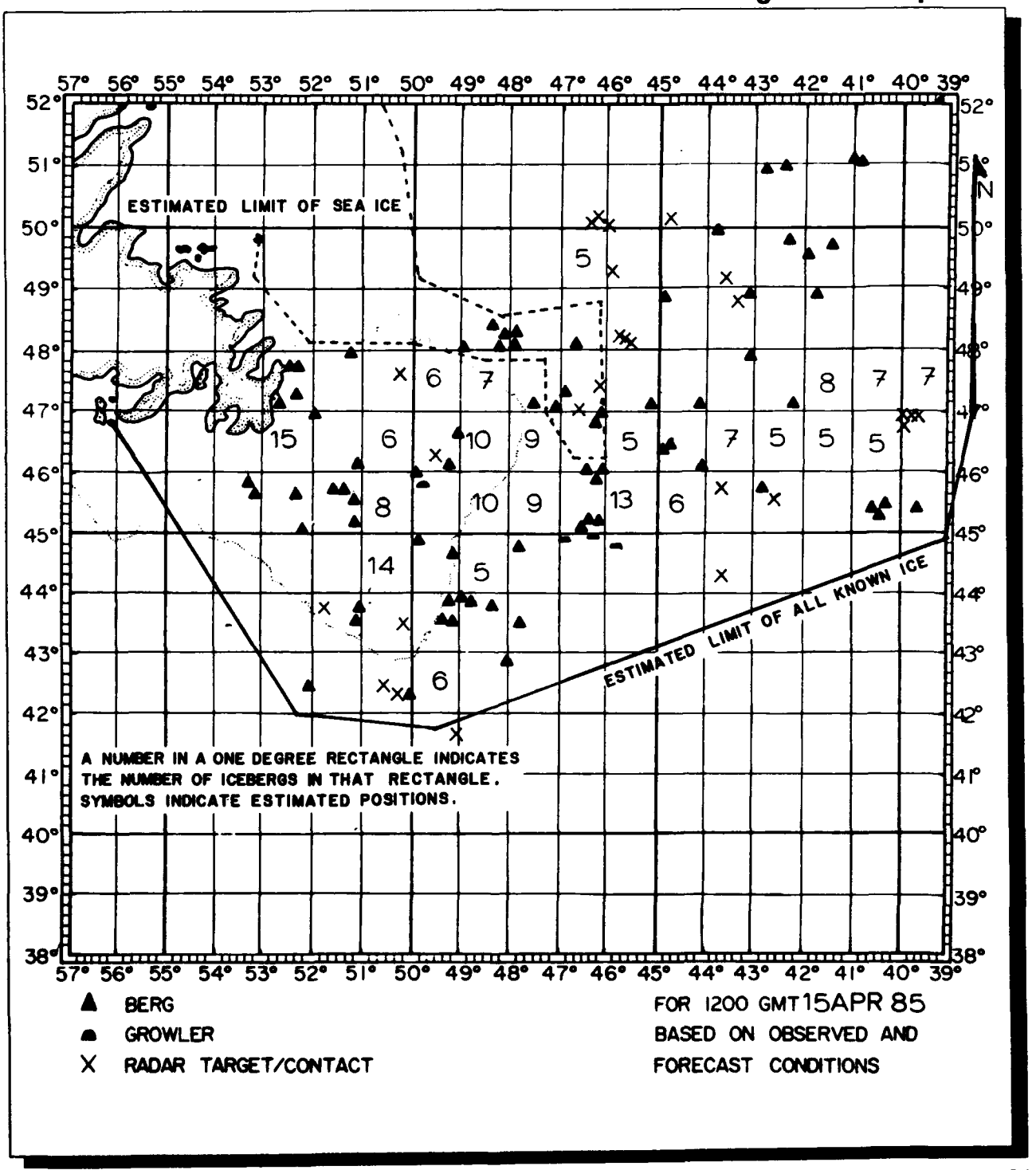

Figure 25. 30 April 1985

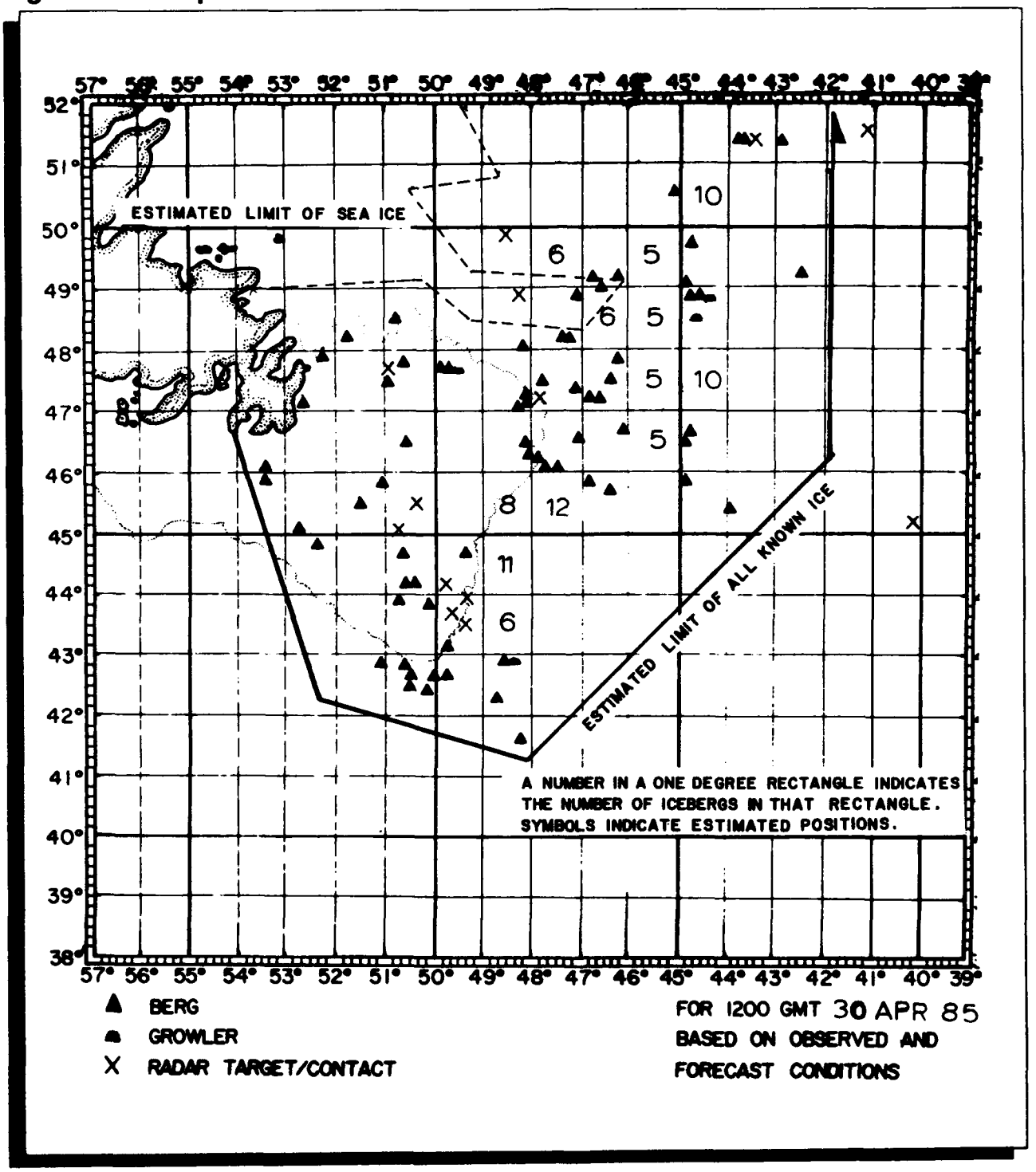

Figure 26. 15 May 1985

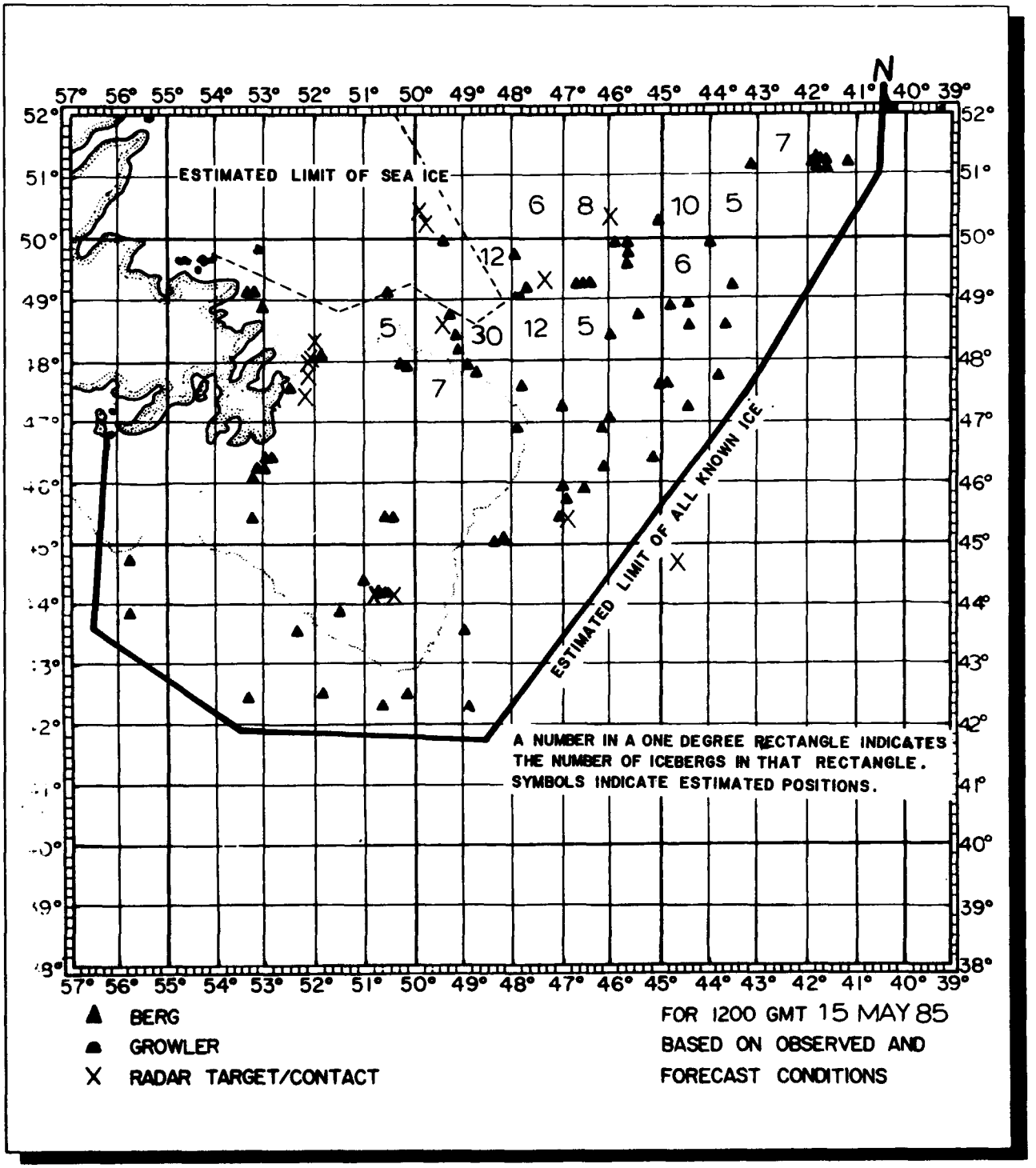

Figure 27. 30 May 1985

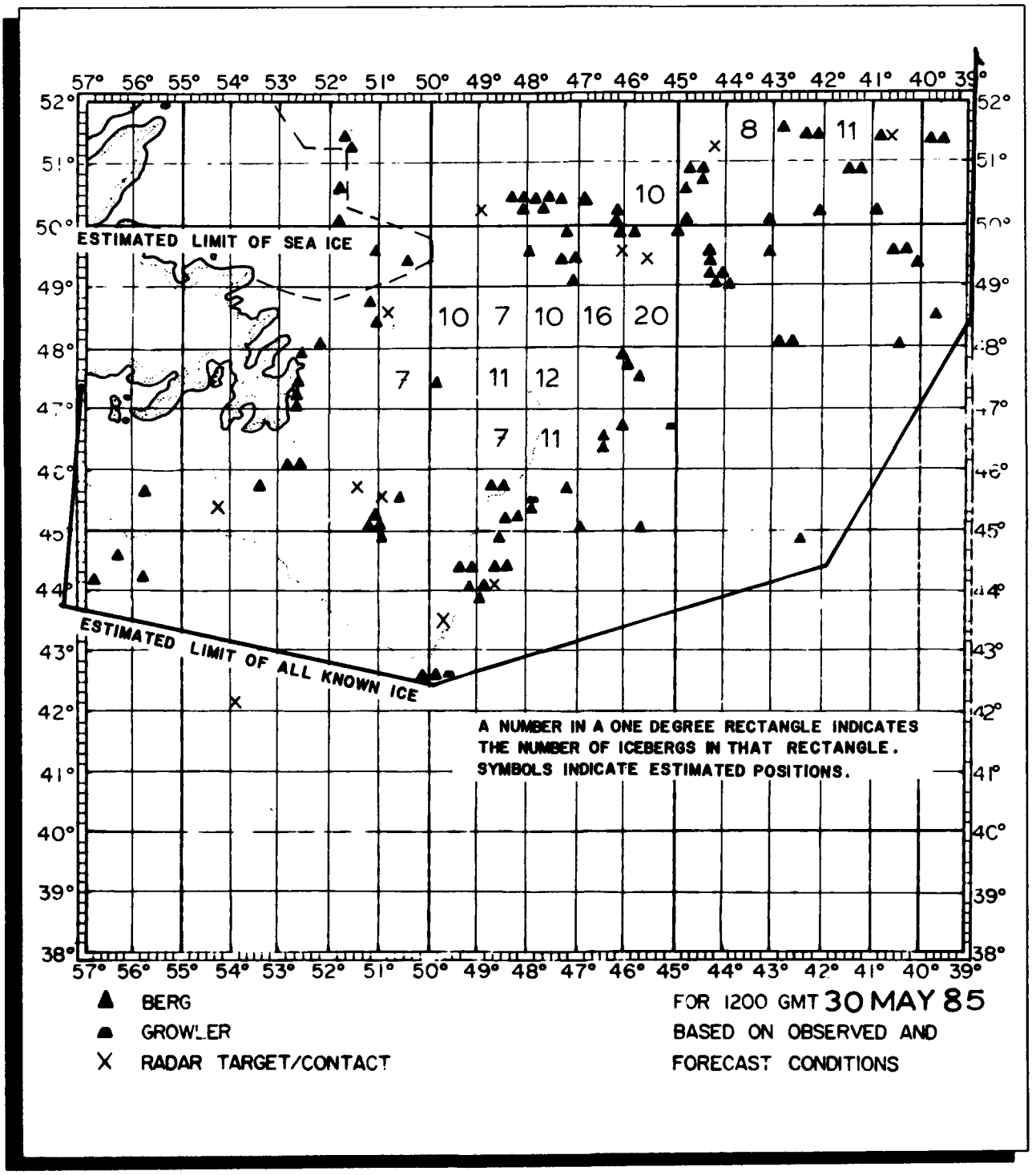

Figure 28. 15 June 1985

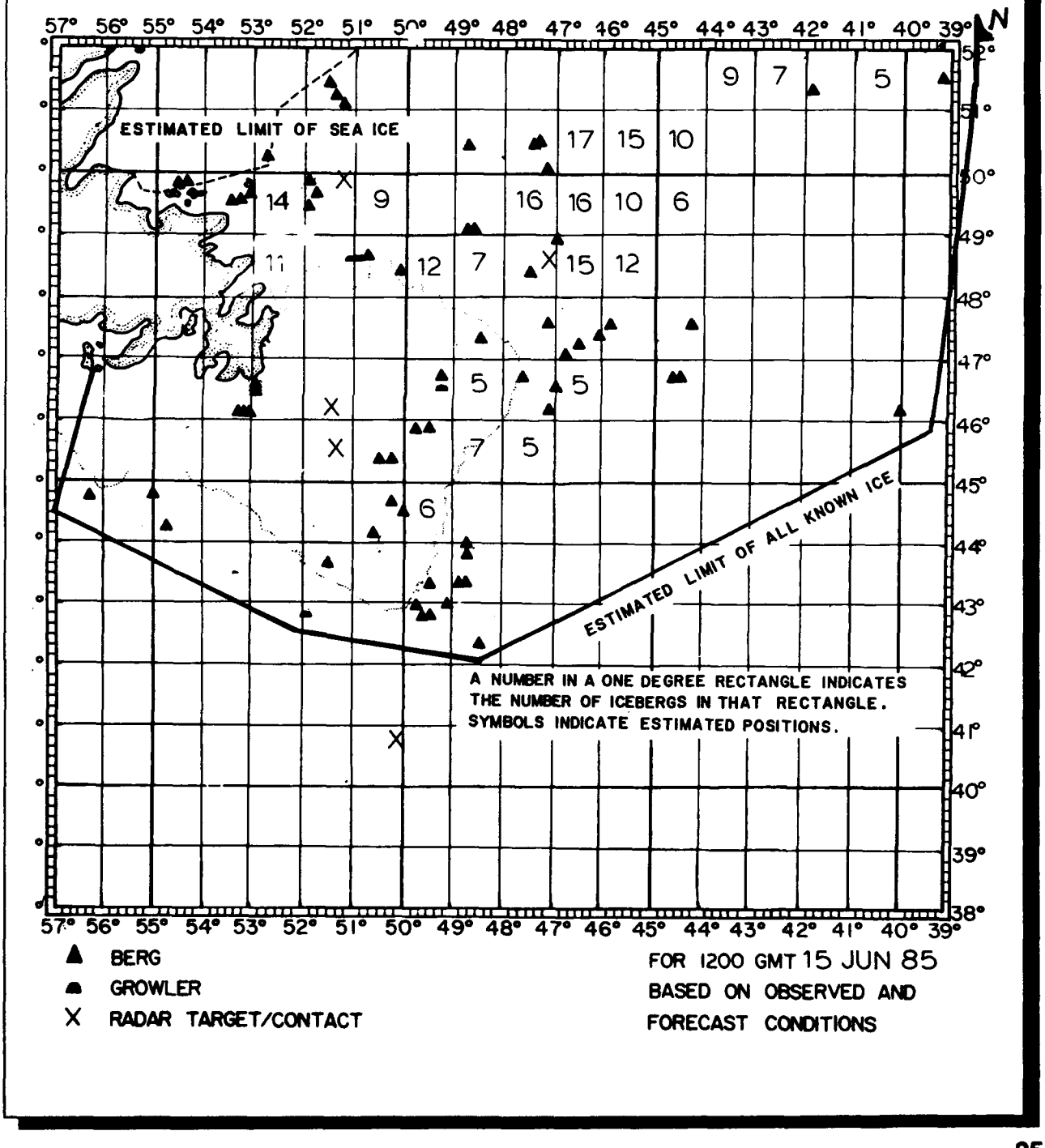

Figure 29. 30 June 1985

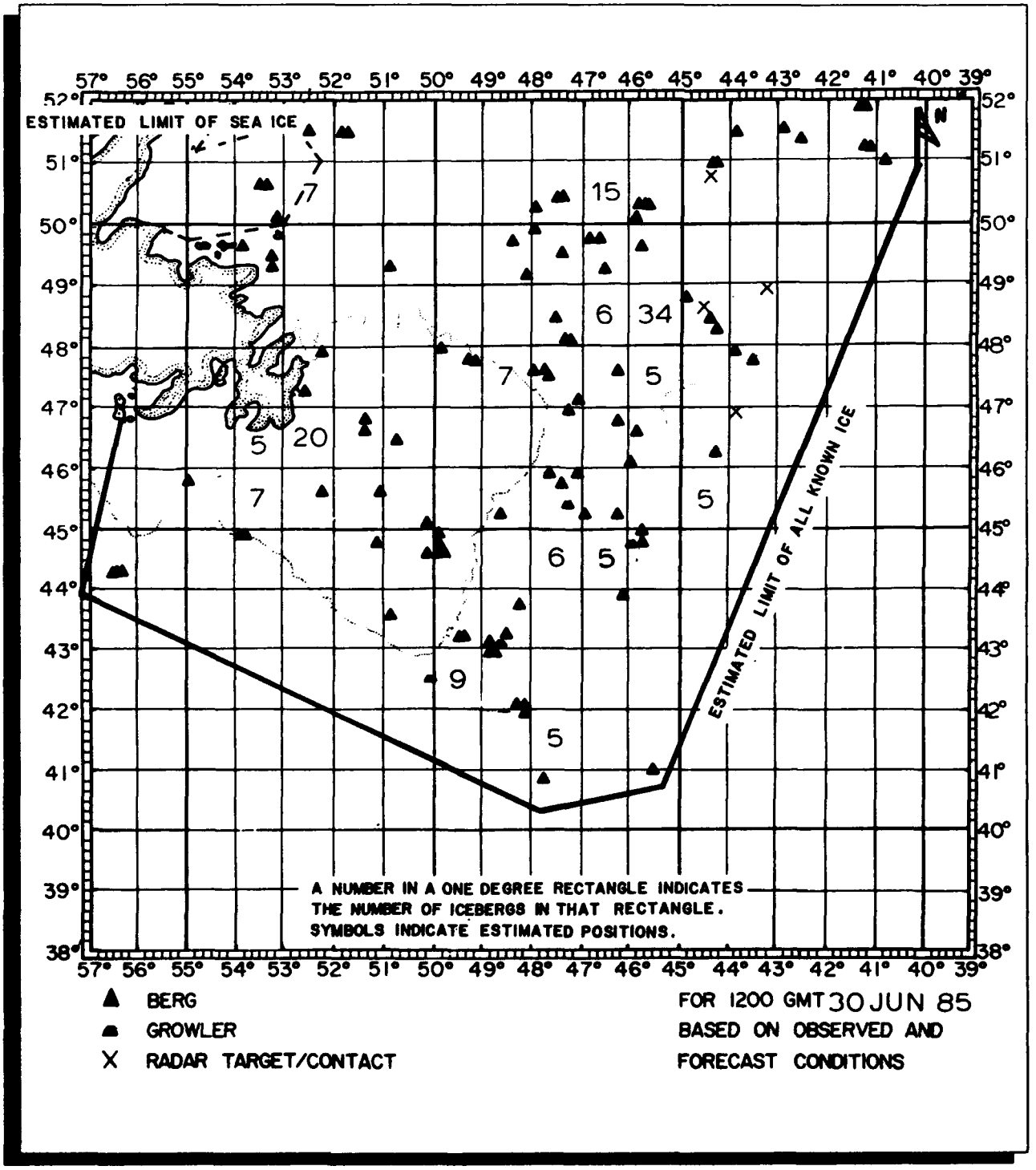

Figure 30. 15 July 1985

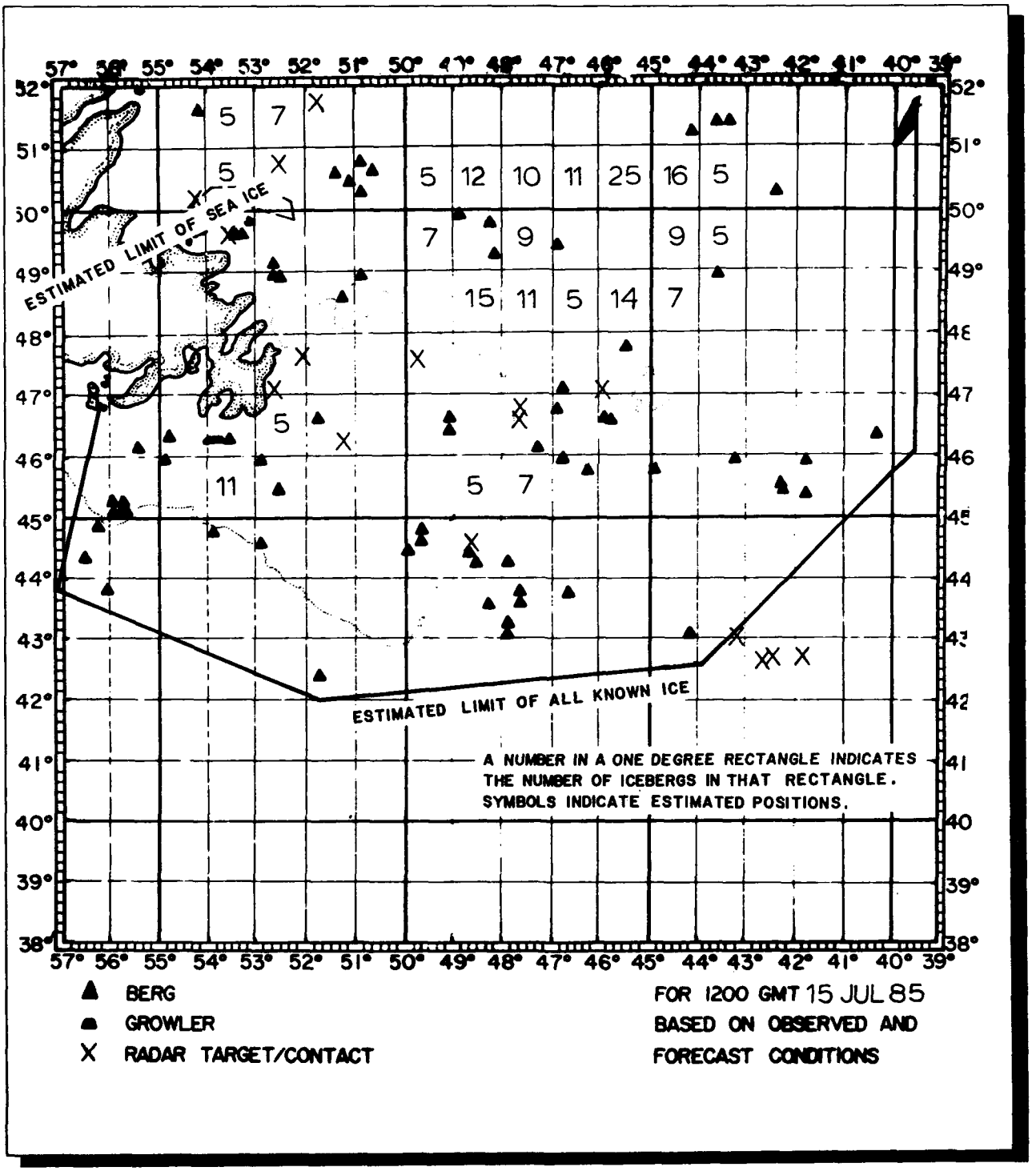

Figure 31. 30 July 1985

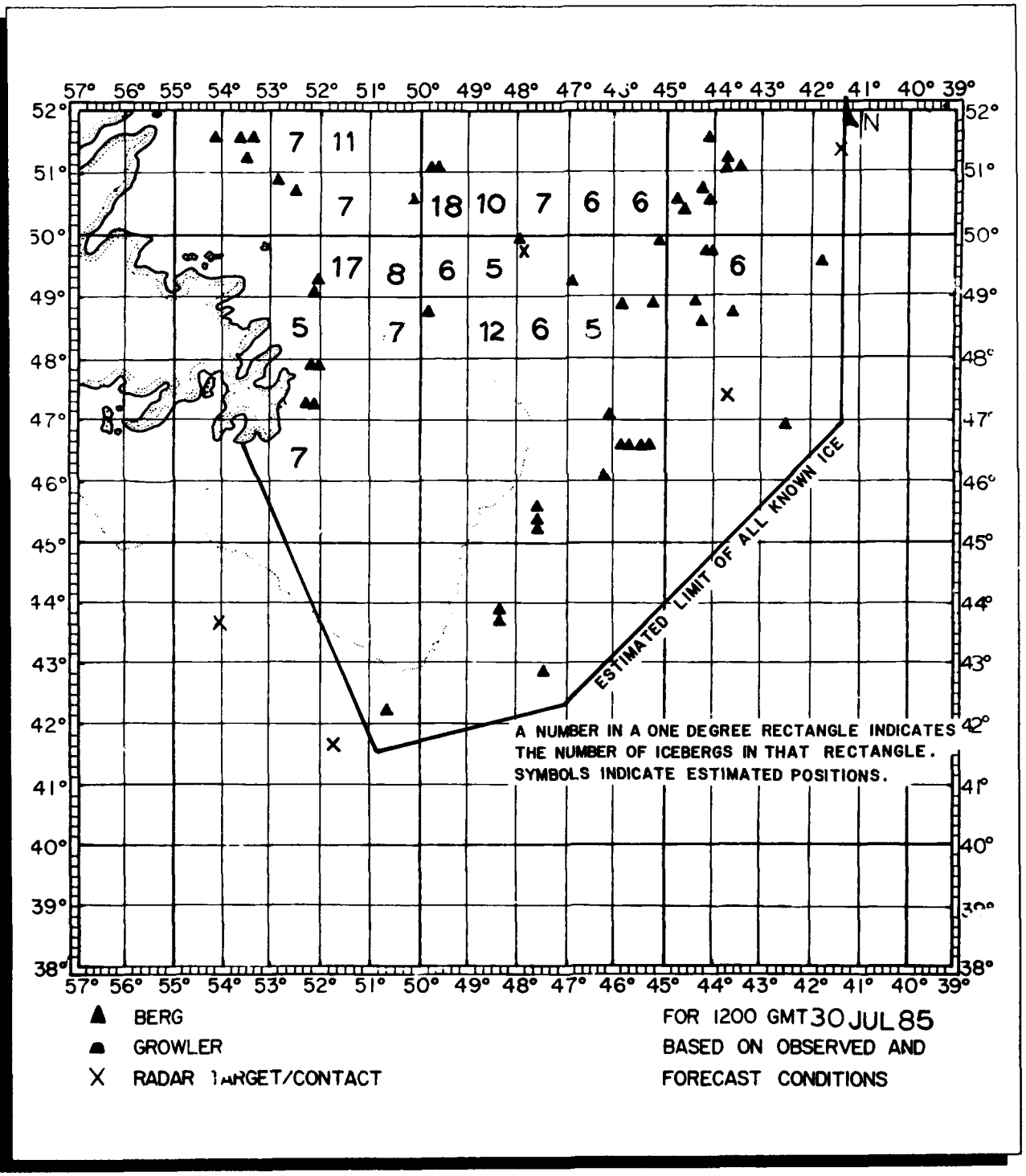

Figure 32. 15 August 1985

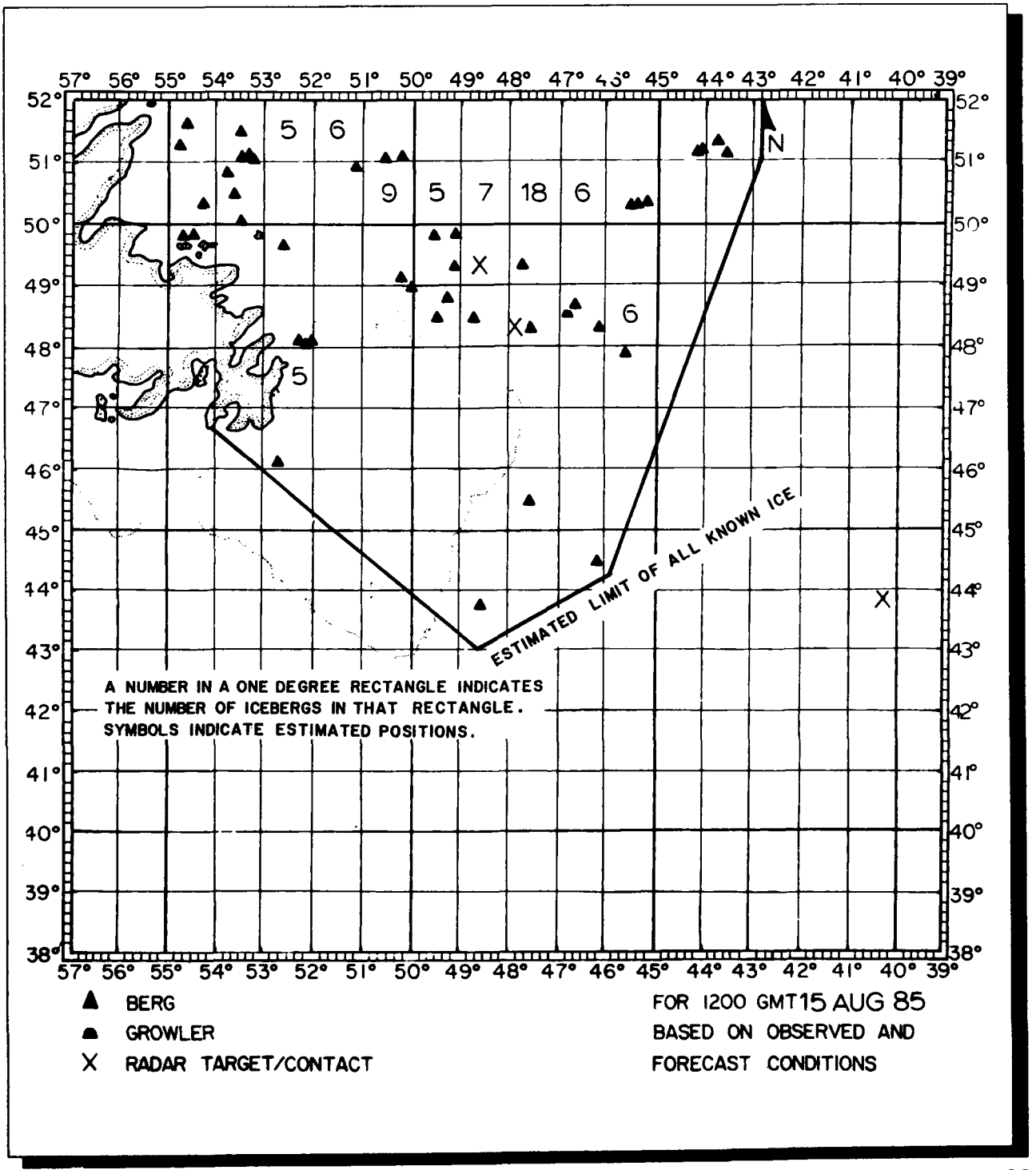

Figure 33. 29 August 1985

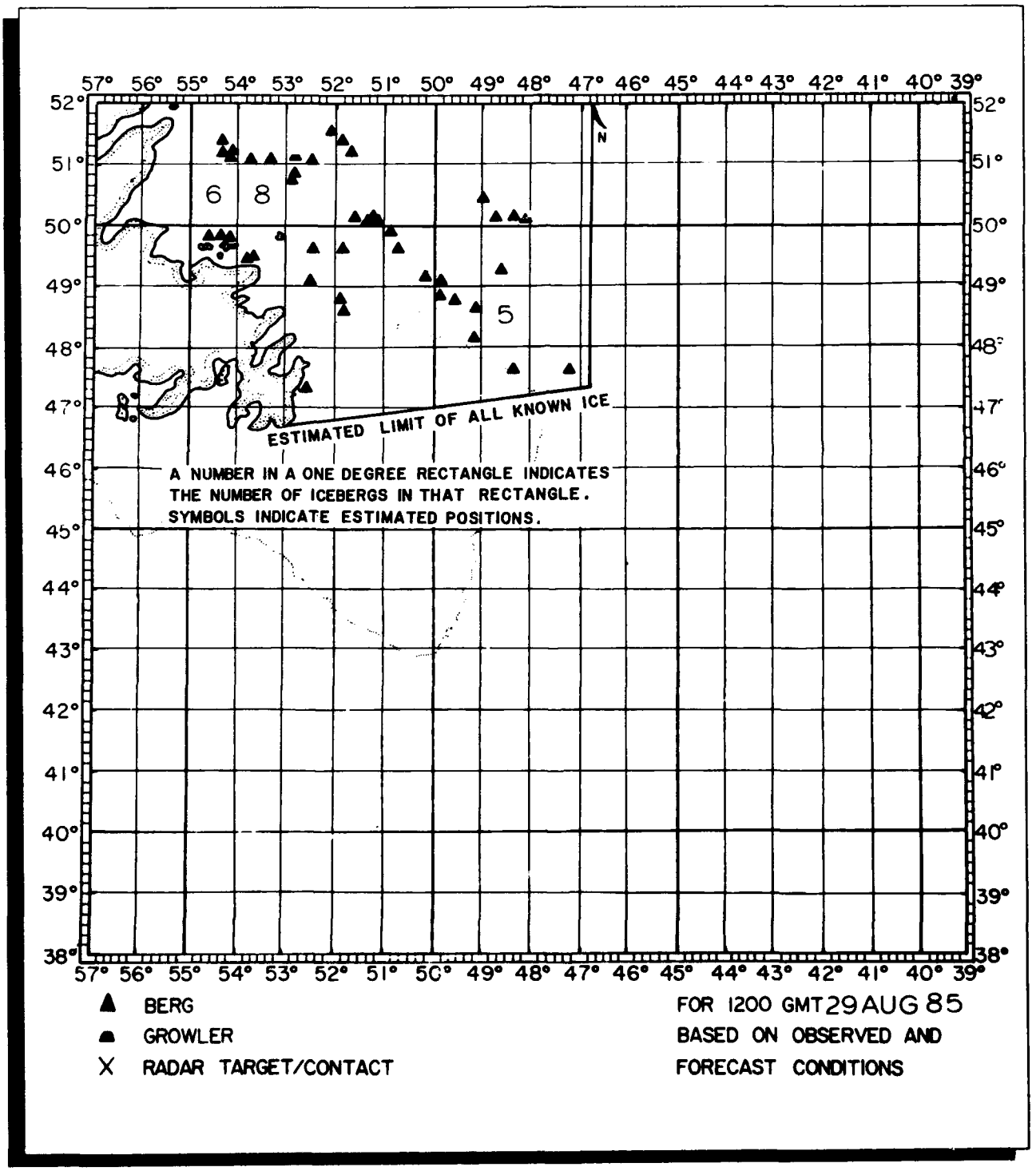

Ice Conditions 1985 Season

October - November 1984: Ice formation was delayed in October by warm temperatures (Figure 10 and Table 5). By mid-November, some ice was forming in the Foxe Basin and Frobisher Bay (Figure 11). Freeze-up continued gradually through November and by the end of the month, Ungava Bay and Hudson Strait were completely covered by light ice. Much of Hudson Bay remained ice-free. There were 14 icebergs south of 48°N during October and November, which is unusually high.

December 1984: By mid-month, sea ice had formed south along the Labrador coast and closed the Strait of Belle Isle (Figure 12). It held this position through the rest of the month with some formation beginning in the Gulf of St. Lawrence. The colder temperatures experienced in December (Table 5) and the northerly flow over the region contributed to the advance of ice. During December, 7 more icebergs were sighted south of 48°N.

January 1985: By January 15, the southern limit of sea ice had reached the vicinity of Cape Freels (Figure 13). On January 22, the sea ice had reached Cape Bonavista and a tongue of ice was being carried south in the Labrador Current to approximately 48°N 49°W. With continued low temperatures and northerly winds, sea ice formed rapidly, expanding to the Grand Banks. This provided protection for icebergs moving south and also retarded their drift so that only two icebergs drifted south of 48°N during January.

February 1985: On 12 February, a broad expanse of ice was as far south as Cape Race and extended out to 47°W from that point. A tongue of three- to five-tenths first year ice was estimated to extend approximately to 46°N 47°W (Figure 14) which terminated oil drilling operations on the Grand Banks for over 30 days. Sea ice formation progressed rapidly throughout the month and by 26 February an expanse of nine- to ten-tenths first year ice covered the area from midway between Cape St. Francis and Cape Race to approximately 45°N 46°W. Due to the number of sightings in early February, an IIP pre-season flight was made 20-25 February, during which 64 icebergs were sighted, 57 of which were south of 48°N.

March 1985: A long tongue of ice started forming in the Labrador Current during early March and by 12 March had reached 43°N 48°W (Figure 15). The first regular season ICERECDET, planned for 12 March, was delayed until 17-27 March by an aircraft mishap in Groton on 12 March. There were 129 icebergs estimated to have drifted south of 48°N during March and there were 168 icebergs on plot at IIP on 29 March (Figure 23).

April 1985: With near normal temperatures (Table 5) and westerly/southwesterly flow (Figure 4), the sea ice had receded somewhat by 16 April and a small shore lead had opened along the northeast coast of Newfoundland (Figure 16). While on an iceberg reconnaissance flight on 15 April, HC-130 CG-1504 dropped a memorial wreath at position 41°56'N 50°14'W to commemorate the tragic sinking of the RMS TITANIC 73 years earlier. During April, normally a heavy iceberg month, an estimated 208 icebergs drifted south of 48°N and 176 icebergs were on plot on 30 April (Figure 25).

May 1985: Sea ice retreated in May with a region of three- to five-tenths coverage remaining as far south as Cape Freels on 14 May (Figure 17). With the receding ice edge releasing icebergs to open water, May was a heavy iceberg month, with 205 icebergs estimated to have drifted south of 48°N. This large population of icebergs provided a good supply of experimental subjects for the detection, drift and deterioration experiments (Appendices B, C and D). There were 272 icebergs on plot on 30 May (Figure 27).

June 1985: The retreat of sea ice continued in June (Figure 18). By 25 June only strips and patches remained south of Cape Bauld. The shipping season for the Strait of Belle Isle was

delayed opening 2-3 weeks this year due to ice persisting longer than normal in the Strait. June was the heaviest iceberg month with 893 icebergs plotted by IIP during the month and 247 icebergs estimated south of 48°N. The largest number of icebergs on plot during any single day in 1985 was on 14 June (Figure 28), when there were 292 on plot. There were 242 icebergs on plot on 30 June (Figure 29).

July 1985: On 16 July, the Strait of Belle Isle was ice-free as was much of Davis Strait (Figure 19). The melt proceeded rapidly and by 30 July sea ice only extended as far south as Cape Mugford on the Labrador Coast. July also was a heavy iceberg month with 765 icebergs plotted during the month. However, only 123 icebergs were estimated to have passed south of 48°N and 227 icebergs remained on plot on 30 July (Figure 31).

August 1985: With warmer than normal temperatures (Table 5) and favorable winds, the sea ice continued to melt rapidly and the iceberg population decreased dramatically. On the 6-14 August ICERECDET deployment, only 30 icebergs were detected south of 50°N and the eastern limits of all known ice shifted 4 degrees west (Figure 32). On 13 August, Newfoundland and Labrador were nearly ice-free with some ice remaining in Hudson Strait and along the east coast of Baffin Island (Figure 20). August was a light iceberg month with only 32 icebergs south of 48°N. As a result of the final ICERECDET on 20-28 August, the limit of all known ice shifted another 4 degrees west and north and the 1985 Ice Patrol season was closed on 29 August with 64 icebergs on plot at IIP, only three of which were south of 48°N (Figure 33).

September 1985: Labrador and the Davis Strait was entirely sea ice free by 17 September (Figure 21). There were an additional 32 icebergs sighted south of 48°N during September.

Table 6.
Explanation of Sea Ice Technology Used in Figures 10-21

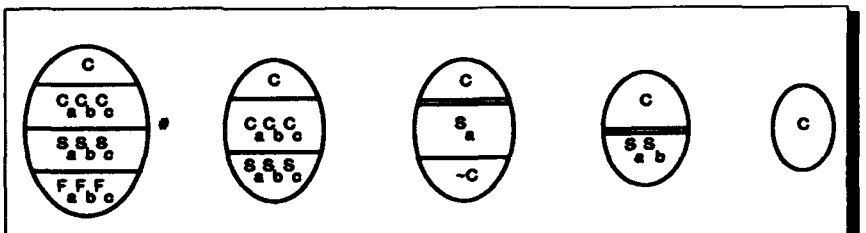

C = Total ice concentration in the area in tenths.

$C_a C_b C_c$ = Concentration of thickest (C_a), 2nd thickest (C_b), and 3rd thickest (C_c).

$S_a S_b S_c$ = Stage of development of thickest (S_a), 2nd thickest (S_b), and 3rd thickest (S_c).

~C = Concentration of ice within areas of strips and patches.

$F_a F_b F_c$ = Floe size of thickest (F_a), 2nd thickest (F_b), and 3rd thickest (F_c).

Stage of Development	
0	No stage of development
1	New ice
2	Nilas, ice rind
3	Young ice
4	Grey ice
5	Grey-white ice
6	First-year ice
7	Thin first-year ice
8	Thin first-year ice, 30-60 cm
9	Thin first-year ice, 60-70 cm
1·	Medium first-year ice
4·	Thick first-year ice
7·	Old ice
8·	Second-year ice
9·	Multi-year ice
▲	Icebergs
·	A trace of ice thicker than S_a
#	Fourth type, if $C_a C_b C_c$ do not add up to C

Floe Sizes	
0	Pancake ice
1	Brash, small ice cake
2	Ice cake
3	Small floe
4	Medium floe
5	Big floe
6	Vast floe
7	Giant floe
8	Growlers and floebergs
9	Icebergs
/	Undetermined or unknown

Discussion of Icebergs and Environmental Conditions

The number of icebergs that pass south of 48°N in the International Ice Patrol area each year is the measure by which International Ice Patrol has judged the severity of each season since 1912 (Table 1). With 1063 icebergs south of 48°N, 1985 is the seventh highest year on record.

Since the number of icebergs calved each year by Greenland's glaciers is in excess of 10,000 (Knutson and Neill, 1978), a number of icebergs exist in Baffin Bay during any year. Therefore, annual fluctuations in the generation of arctic icebergs is not a significant factor in the number of icebergs passing south of 48°N annually. The factors that determine the number of icebergs passing south of 48°N each season can be divided into those affecting iceberg transport (currents, winds, and sea ice) and those affecting iceberg deterioration (wave action, sea surface temperature, and sea ice).

Sea ice acts to impede the transport of icebergs by winds and currents and also protects icebergs from wave action, the major agent of iceberg deterioration. Although it slows current and wind transport of icebergs, sea ice is itself an active medium, for it is continually moving toward the ice edge where melt occurs. Therefore, icebergs in sea ice will eventually reach open water unless grounded. The melting of sea ice itself is affected by snow cover (which slows melting) and air and sea water temperatures. As sea ice melt accelerates in the spring and early summer, trapped icebergs are rapidly released and then become subject to normal transport and deterioration.

With sea ice extending south over the Grand Banks later than usual during the 1985 season, icebergs were protected longer than normal, making it possible for the icebergs to reach farther south than normal.

References

Knutson, K.N. and T.J. Neill, (1978); *Report of the International Ice Patrol Service in the North Atlantic Ocean for the 1977 Season*, CG-188-32, U.S. Coast Guard, Washington, DC.

Robe, R.Q., N.C. Edwards, Jr., D.L. Murphy, N.B. Thayer, G.L. Hover, and M.E. Kop, (1985); *Evaluation of Surface Craft and Ice Target Detection Performance by the AN/APS-135 Side-Looking Airborne Radar (SLAR)*, CG-D-02-86, U.S. Coast Guard, Washington, DC.

Rossiter, J.R., L.D. Arsenault, A.L. Gray, E.V. Guy, D.J. Lapp, R.O. Ramseier, and E. Wedler, (1984); *Detection of Icebergs by Airborne Imaging Radars*, Proceedings of the 9th Canadian Symposium on Remote Sensing, St. John's, Newfoundland, August 1984.

Thayer, N.B. (1984); *Effects of Side-Looking Airborne Radar (SLAR) on Iceberg Detection During the 1983 and 1984 International Ice Patrol Seasons*; from Report of the International Ice Patrol in the North Atlantic, 1984 Season, CG-188-38, U.S. Coast Guard, Washington, DC.

Acknowledgements

Commander, International Ice Patrol acknowledges the assistance and information provided by the Canadian Department of the Environment, the U.S. National Weather Service, the U.S. Naval Weather Service, and the U.S. Coast Guard Research and Development Center.

We extend our sincere appreciation to the staffs of the Canadian Coast Guard Radio Station St. John's, Newfoundland/VON and the Gander Weather Office and to the personnel of U.S. Coast Guard Air Station Elizabeth City and the USCGC EVERGREEN for their excellent support during the 1985 International Ice Patrol season.

Appendix A

International Ice Patrol Ice and SST Reports for 1985

Ship's Name	Country of Registry	Ice Reports	SST Reports
Aberdeen	Panama	3	
Abitibi Concord	Germany	7	
Acadia Forest	Liberia	1	
Aeneas	Singapore	2	
Akizuki Maru	Japan		3
Albright Explorer	United Kingdom	2	
Alcona	United States of America	1	
Alexander Henry	Canada	2	2
Alexandros F	Greece	1	1
Alfanourious	Liberia	1	1
Alfred Needler	Canada	4	
Algonquin	Korea	1	27
Altamira	Spain	3	
Altay	Union of Soviet Socialist Republics	1	
Altis	Greece	1	
Ambassador	United Kingdom	16	
Ambrose Shea	Canada	2	
Amstelwal	Netherlands	3	4
Anagell Horizon	Greece	1	
Anka D	Cyprus	1	
Annouta	Greece	4	7
Arctic	Canada	2	
Arctic Link	United Kingdom	1	
Arctic Viking	Canada	2	
Astron	Canada	2	
Atlantic Conveyer	United Kingdom	1	
Atlantic Link	United Kingdom	4	15
Atlantic Saga	Sweden	1	
Atlantic Service	France	2	
Atlantic Star	United Kingdom	2	1
August Thyssen	Liberia	2	
Australian Reefer	Bahamas		2
Azalea	Korea	2	1
Badak	Liberia	1	5
Bahia Portete	Columbia		1
Balder Hesnes	Canada	3	
Balder Vigra	Canada	1	
Balu	Sri Lanka		1
Bandazul	Spain	1	
Bart Atlantica	United Kingdom	1	
Bartlett	Canada	4	
Batna	Algeria	4	4
Beinir	Canada	1	
Belle Etoile	Mauritius	4	10
Bernhard Oldendorf	Panama		1
Bernier	United Kingdom	4	
Bilderdyk	Netherlands Antilles	1	
Biesaya Barrero	Portugal	6	
Bottenhor	Canada	4	
Bonavista Bay	Canada	3	
Boxy	Sweden	3	
Bridgewater	Germany	7	

Appendix A (cont'd.)

International Ice Patrol Ice and SST Reports for 1985

Ship's Name	Country of Registry	Ice Reports	SST Reports
Bulkness	United Kingdom	3	
Canada Marquis	Canada	1	
Canadian Explorer	Canada	10	1
Cape Roger	Canada	4	
Capetan Costis	Cyprus		9
Cast Huskey	United Kingdom	3	
Cast Muskox	United Kingdom	5	
Cast Otter	United Kingdom	5	
Cast Polar Bear	Liberia	4	6
Cavallo	Canada	1	
Chandidis	India	2	
Chateaugay	Liberia	1	
Chignecto Bay	Canada	5	
Chili	United Kingdom		2
City of Perth	United Kingdom	5	
C. Mehmet	Turkey		4
Chippewa	Liberia	2	
Commandant Guy	France	1	
Concord	United States of America		8
Condata	Honduras		1
Conta Belgica	Korea	2	
Corner Brook	Korea	2	
Danaos	Greece	4	
Daphne	Netherlands	1	
Dart Americana	United Kingdom	3	1
Dart Atlantica	United Kingdom	1	
Dart Britain	United Kingdom	3	
Diana	Brazil	1	
Dock Express	Netherlands	1	
Dora Oldendorff	Singapoore	1	
Donny	Sweden	2	
Dr D. K. Samy	Liberia	1	
Dry Sack	Spain	2	
Eastern Unicorn	Panama	8	9
Eekio	Belgium	4	
El Aalim	Liberia	1	
Elsat	Italy	1	
Elizabeth	Liberia	1	
Esso Aberdeen	United Kingdom	2	1
Eulima	Norway	1	
Europe	Belgium	8	
USCGC EVERGREEN	United States of America	8	69
Evimeria	Greece	1	2
Fairlift	Netherlands Antilles	2	
Fair Spirit	Liberia	2	
Faith	Singapore		1
Falcken	Sweden	1	
Falcon	Norway	5	
Farnes	Liberia	2	
Federal Asahi	Japan		4
Federal Danube	Belgium	4	

Appendix A (cont'd.)

International Ice Patrol Ice and SST Reports for 1985

Ship's Name	Country of Registry	Ice Reports	SST Reports
Federal Ottawa	Belgium	8	
Federal Rhine	Liberia	1	
Federal Saguenay	Liberia	1	
Federal St. Laurent	Liberia	2	
Federal Thames	Belgium	1	
Fermita	Norway		3
Filiatra Legacy	Greece		5
Filispoint	Greece	1	
Fina America	Belgium	2	
Finn Fighter	Finland	1	
Finn Fury	Finland	2	
Finnrose	Finland		2
Finn Oceania	Finland	2	
Fiona Mary	Panama	1	
Firmes	Liberia	12	
Fjord Bridge	Panama	2	1
Flora	Greece	1	1
Fogo Isle	Canada	1	
Fort Providence	United Kingdom	1	1
Fortune Ace	Panama	1	1
Fred J. Agnich	Canada	1	
Frithjof	Germany	2	7
Fuji Reefer	Japan	1	1
Garbarus Bay	Canada	9	
Genoa	Singapore	1	1
Germanic	Federal Republic of Germany	3	
Godafoss	Iceland	1	
Golden Rio	Liberia	1	10
Graigias	United Kingdom	1	
Grand Eagle	Panama	9	
Gripo	Finland	3	7
Gulf Grain	Liberia	3	1
Hassho	Panama	1	
Heide	Germany	1	
Helene	Federal Republic of Germany	1	1
Helen Schulte	Cyprus	1	2
Hercules Bulker	Liberia	3	
Hofsjoull	Iceland	1	1
Hokusetmaru	United States of America	1	1
Hual Trapper	Liberia	1	
Hudson	Canada	6	3
Hugo	Finland	1	
Imperial Bedford	Canada	2	
Imperial Quebec	Canada	2	
Imperial St. Clair	Canada	2	
Inma	Spain	1	

Appendix A (cont'd.)

International Ice Patrol Ice and SST Reports for 1985

Ship's Name	Country of Registry	Ice Reports	SST Reports
Irenes Galaxy	Panama	1	
Iroquois	Korea		8
Irving Nordic	Canada	4	
Irving Ours Pollaire	Canada	1	
Ivan Der Benev	Union of Soviet Socialist Republics	2	
Iver Libra	Liberia		1
Jackamn	Chile	1	
Jade Kim	Panama	2	
Jan Wilhelm	Germany		1
James Transport	Canada	3	
Jason	Panama	1	
Je Bernier	Canada		2
Jennifer Jane	Cyprus	2	
Jenny	United Kingdom	1	
Jijet	Yugoslavia	1	
Joao Ferreira	Portugal	2	
John	Greece		4
John A. MacDonald	Canada	4	
John M.	Federal Republic of Germany	1	
Johnson Chemstream	Singapore	1	
Jugoagent	Yugoslavia	2	14
Juventia	Panama	1	
Kaladia	India	3	
Kapitan Chukhchinche	Union of Soviet Socialist Republics	4	
Keenaviga	United Kingdom	1	
Khiko	Panama	1	
Klippergracht	Netherlands	1	
Koeln Express	Germany	10	
Korea Pacific	Korea		4
Kyoushi Waru	Japan	2	
Lake Anina	Liberia		2
Lake Biwa	United States of America	1	
Lake Shell	Canada	1	
La Pampa	United Kingdom	7	
La Richardais	France	2	3
Lamara	Singapore	1	
Larrado	Canada	2	
Laurentian	France	9	
Laurentian Forest	Panama	2	
Lena	Philippines		8
Leninak	Union of Soviet Socialist Republics	1	
Leros Challenger	Malta		1
Levantine	Liberia	1	
Liberian Badak	Liberia		1
Liquid Bulker	Panama		4
Liria	Spain	1	1
Lok Nayak	India	1	1
Lorne	Canada	1	
Louis S. St. Laurent	Canada	1	
Ludolf Oldedorff	Singapore	1	

Appendix A (cont'd.)

International Ice Patrol Ice and SST Reports for 1985

Ship's Name	Country of Registry	Ice Reports	SST Reports
Mahone Bay	Canada	1	
Maiakamd	Pakistan		4
Manchester Challenge	United Kingdom	10	2
Manga	United Kingdom	1	
Manila Triumph	Philippines	1	
Maratha Shogun	India	2	
Margit Gorthon	Sweden	3	
Maria	Germany	1	
Marine Reunion	Liberia	1	
Marine Star	United Kingdom		1
Marques Debolarque	Spain		1
Marshal Grechko	Union of Soviet Socialist Republics	3	
Meshill	Norway	2	
Meerdrecht	Netherlands	1	
Meerkatze	Germany	6	
Megastar	Sri Lanka	2	
Mela	Panama	1	4
Mesarige	Canada	1	
Metro Star	Canada	1	
Mini Lot	Panama		1
Mightious	Panama	1	1
Miyashima Maru	Japan	1	1
Mijet	Mongolia	2	
Mobil Engineer	Sweden		4
Mobil Oil Co.	Bolivia	1	
Monana D.	Liberia		6
Montcalm	United States of America	1	
Monty Python	Malta		1
Mosel Oreck	Liberia	1	
Moshrouk	Norway	1	
Mouthaina	Greece	3	
M. Soveron	Singapore	1	
Musashi	Greece	2	
Musson	Union of Soviet Socialist Republics	1	
Nancy Bartlet	Canada	1	
Navtroll	Liberia	1	2
Neckarore	Liberia	1	
Noble Supporter	Panama	1	
Norderlor	Liberia	1	12
Nordheide	Canada	3	
Nordic Sun	Singapore	4	
Nordkap	Liberia	3	
Norshwian	Cyprus	1	7
Northern Lynx	Liberia	1	
USCGC NORTHWIND	United States Of America	7	6
Nosira Lin	United Kingdom	1	51
Nosira Madeleine	United Kingdom	3	
Nürnberg Express	Germany	4	
Ocean King	Greece	1	
Osolemio	Liberia		5
Overseas Argonaut	United Kingdom	1	2

Appendix A (cont'd.)

International Ice Patrol Ice and SST Reports for 1985

Ship's Name	Country of Registry	Ice Reports	SST Reports
Pacific Challenger	United Kingdom	1	
Pacific Courage	United Kingdom	1	
Pacific Defender	Liberia		9
Pacific Express	Liberia	1	
Pacifico Mexicano	Panama	1	
Pan Crystal	Korea	1	
Pantazis	Greece	1	
Pavel Vavilov	Union of Soviet Socialist Republics	1	
Pawnee	United Kingdom		12
Petrodvorets	Union of Soviet Socialist Republics	4	
Philippeld	France	1	
Placentia Bay	Canada	1	
Planeta	Germany	1	
Polar Bear	Liberia		2
Polar Circle	Canada	2	
USCGC POLAR SEA	United States of America	1	
Port St. Jean	Canada	2	
Premnitz	Germany	2	
President Quezon	Philippines	1	
Priimorsk	United Kingdom	2	
Prins Maurits	Netherlands	2	
Pristina	Yugoslavia	1	
Proteus	United Kingdoom	1	
Puhos	Finland	3	5
Quadra	Canada	4	
Queen Ellizabeth II	United Kingdom	2	
Quest	Canada	1	
Reginas	Greece	1	
Ruebens	United Kingdom	1	
Rio Frio	Netherlands	1	
Rio Plasta	Liberia	1	
Saar lore	Liberia	2	
Salvia Star	Philippines	2	
Saskatchewan Pioneer	Canada	1	
Scandinavia Maru	Japan	1	
Schnoorturm	Canada	4	
Seaforth Atlantic	Canada	3	
Seaforth Atlantic Cartwright I	Canada	1	
Sea Fortune	Panama	3	
Sealand Express	United States of America	1	
Sealand Independence	Mexico	1	
Seijin Maru	Japan		5
Selkirk Settler	Canada	1	
Senhora Das Candeias	Portugal	4	
Sentinel 2	France	1	
Silverland	Sweden		2
Sir Robert Bond	Canada	7	
Sir W. Alexander	Canada	1	
Sitia Glory	Panama	2	
Skaftefell	Iceland	1	
Stefan Batory	Poland	9	2
Stefan Starzynski	Poland	4	

Appendix A (cont'd.)

International Ice Patrol Ice and SST Reports for 1985

Ship's Name	Country of Registry	Ice Reports	SST Reports
Stolt Castle	France	1	
Stolt Excellence	Liberia	1	
Stratus	Liberia		4
Stuttgart Express	Germany	3	
Suvretta	Panama	1	
Tadeusz Kosciuszzko	Poland	1	
Takapu	Canada	1	
Teamhada	Singapore		2
Techno St., Laurent	Canada	1	
Terra Nordica	Canada	4	
Thuleland	Singapore	1	
Tina	Cyprus		1
Toanui	Canada	2	
Tobruk	Poland	1	
Tokiarrow	United Kingdom	1	
Torrent	Liberia	1	
Trans Reefer	Panama		1
Traquair	United Kingdom		9
Travemar Africa	Spain	1	6
Trinity Bay	Canada	9	
Tsukubamaru	Japan	1	1
Tuber	Canada	1	
Tuffias	Sweden	1	
Tulsidas	India	1	
Uniwersytet Slasky	Poland	1	
Uority Dolgarufiy	Union of Soviet Socialist Republics	1	
Vamand Wave	United Kingdom	1	
Vanil	Sweden	1	5
Varjakka	Finland		2
Vimieiro	Portugal	1	
Vascaya	Norway	1	
Wanderer	United Kingdom		4
Warnemundie	Union of Soviet Socialist Republics	3	
Wilfred Templeman	Canada	2	
Wise	Cyprus		6
World Agamemnon	Greece		1
World Argonaut	Greece	1	
World Nancy	Panama	1	
Yannis	Greece	1	
Yukona	Liberia	3	1
Zeepaard	Bahamas	1	
Ziemia Opolska	Poland	2	
Ziemia Zamojska	Poland	3	4

Appendix B

Iceberg / Ship Target Discrimination with Side-Looking Airborne Radar

LTJG N. B. Thayer, USCGR
CDR N. C. Edwards, USCG

Introduction

Since 1983, the International Ice Patrol (IIP) has been using a Motorola AN/APS-135 Side-Looking Airborne Multi-Mission Radar (SLAMMR) as its primary method of iceberg reconnaissance in the North Atlantic. The ability to detect icebergs with a side-looking airborne radar (SLAR) in poor or zero visibility, plus the ability to search larger areas, has resulted in a significant increase in the number of icebergs tracked by IIP.

Because SLAR can be used with the sea surface obscured by clouds, IIP frequently conducts reconnaissance flights when visual confirmation of SLAR targets is not possible. Without visual confirmation, distinguishing between icebergs and vessels is sometimes difficult.

Without visible cues on the SLAR film (target movement, wakes, brash, radar shadows, strength of return) which improve target identification, it is difficult to distinguish between targets with similar radar return, e.g., small icebergs and vessels. IIP has planned its search legs and the track spacing equal to one-half the total SLAR sweep width (i.e., 25 nm). This type of search plan gives 200% coverage between parallel legs and provides two views of each target within the search area. Despite these efforts to maximize cues, it is still sometimes difficult to distinguish vessels from small and medium icebergs. For example, fishing vessels often drift or move slowly, producing no wake and showing little or no movement between looks. In addition, the search legs going to and from the search area as well as the outlying legs of the search itself do not afford double SLAR coverage. As a result, approximately 35% of the search area is seen only once on SLAR, eliminating the chance to detect movement and decreasing the probability of picking up other cues from SLAR images.

This study measures the error rate in SLAR target identification, using single looks at individual iceberg and ship targets without visual cues.

Methods

To conduct this study, it was necessary to find a source of SLAR targets with visual confirmation. The best source of targets with positive identification of both target size and type was the BERGSEARCH '84 (Rossiter, *et al.*, 1984) data and the 1985 SLAR experiment conducted by IIP and the Coast Guard Research and Development Center (Robe, *et al.*, 1985). These two sources provided SLAR film from 7 days of IIP operations with shipboard ground truth data, 160 ship and iceberg targets in all. All of the film used in this study was collected at an altitude of 8,000 feet on the 50 km SLAR range scale, standard conditions during IIP iceberg reconnaissance.

The films were duplicated and the duplicate films were examined for suitable targets for the study. All targets without obvious cues were used. Although targets were not selected for ambiguity, all of those used were quite ambiguous, since they were all single targets without accompanying visual cues. With the limited number of vessels and icebergs involved in the two source experiments, some targets were used more than once, but separate SLAR passes

provided different looks so that each image was used only once.

To isolate individual targets and at the same time give the SLAR interpreters a surrounding piece of film to examine for background, each target was cut from a duplicate film and mounted on a 2 1/4" photo slide mount. Each target was randomly assigned a 2-3 digit identification number and each slide mount was labelled with that number, the lateral range to the target from the aircraft, and the sea conditions (from ship ground truth).

These 74 slides (35 icebergs and 39 ships) were taken to U. S. Coast Guard Air Station Elizabeth City, North Carolina, for viewing by the Coast Guard Avionics Technicians who are the IIP's SLAR interpreters, operators and technicians during ice reconnaissance flights. Four experienced technicians separately viewed the slides on a light table using an optical magnifier, conditions approximating the normal IIP post-flight analysis. Each technician was asked to identify each target as either a ship or an iceberg.

Results

Table B-1 presents the raw test results, divided into the two target types: ships and icebergs. The "correct" column under each target type represents the number of times each observer identified that target correctly, while "incorrect" represents the number of times that type of target was misidentified.

The data was subjected to Chi-square analysis (Lapin, 1975) to identify statistically significant differences in the error rates between the observers, and to look for differences in how the two target types were treated. The analysis revealed that there was too much difference in error rate and target treatment between the four observers to allow combining all the data. Also, observers 1 through 3 showed a bias toward icebergs, i.e., a tendency to identify ships as icebergs. This is a reflection of their IIP experience, since observers are taught to be conservative and identify doubtful targets as icebergs. Observers 1 and 3 were sufficiently similar in their treatment of the targets to allow combining their data. Finally, observer 4 showed no bias toward icebergs.

The results from observers 1 and 3 probably offer the most representative sample, since the bias they show toward icebergs reflects their IIP experience. Actually, while selection of different subsets of the data can be made based on bias shown or statistical judgements, the error rate for all targets is in the range of 40-45%, as shown in Table B-2.

While these data sets cannot be combined or compared for statistical reasons, selecting any one of them yields essentially the same result, i.e., that the observers correctly identified all targets 55-60% of the time. Applied directly to all IIP SLAR detections, a possible 45% error rate would have alarming implications. The targets used in this study, however, represent only a subset of IIP SLAR targets. There are characteristics that limit the size of that subset and mitigate the 45% figure.

First, the sizes of icebergs in BERGSEARCH '84 and the

Table B-1. Target Identification

	Iceberg		Ship	
Observer	Correct	Incorrect	Correct	Incorrect
1	31	4	15	24
2	23	12	7	32
3	28	7	15	24
4	20	15	24	15
TOTAL	102	38	61	95

Table B-2. Error Rates

Observer(s)	Error Rate (Ships & Icebergs)
1-4	45%
1,3	40% (Iceberg Bias)
4	40% (No Bias)

Table B-3. Iceberg Size Distribution (SLAR) 1984 - 1985

Year	Growler	Small	Medium	Large	Radar	Total
1984	370 (25%)	441 (30%)	418 (29%)	211 (14%)	21 (1%)	1461
1985	65 (11%)	194 (34%)	182 (32%)	113 (20%)	10 (1%)	564
1960-1982	8393 (15%)	21353 (37%)	15461 (27%)	4854 (8%)	7711 (13%)	57772

1985 IIP experiment range from growler through medium. The targets selected for this study were small and medium icebergs (ground truthed by on-scene vessels) and ship targets of similar radar return. Small and medium icebergs represent 59% of the icebergs recorded by IIP SLAR in 1984 and 66% in 1985, as shown in Table B-3. These percentages are comparable to the pre-SLAR value of 64% for the period 1960 through 1982.

The second mitigating factor is the ambiguity of the targets used, i.e., the absence of cues. Since the methods of this study eliminated these cues, the targets used represented the most ambiguous available.

In order to assess the impact of these results on IIP iceberg reconnaissance, it is necessary to estimate the proportion of IIP SLAR targets that are cueless. It can be conservatively assumed that 40% of SLAR targets are cueless, based on IIP operational experience. Indications that this is a reasonably conservative assumption are that the data set used for this study in which 74 of 160 targets (46%) were cueless, and the fact that 65% of IIP search flight mileage offers 200% search coverage, which is assumed to greatly increase the probability of cues being present. A further assumption is that the presence of cues results in 100% correct identification

Applying a worst-case error rate of 45% to the (estimated) cueless 40% of the small and medium icebergs detected by SLAR, yields an estimated SLAR error of 161 and 68 misidentified icebergs in 1984 and 1985, in the small and medium size range.

Conclusions

The probability of correctly identifying ambiguous (cueless) iceberg and ship SLAR targets is just above chance (55-60%). Therefore, the International Ice Patrol uses search tactics to maximize cues and visual confirmation during SLAR reconnaissance.

Based on this limited study of cueless SLAR targets, the SLAR error rate and iceberg bias of SLAR operators could inflate the number of icebergs that IIP reports. This inflation is insignificant when compared with the increased efficiency that SLAR provides iceberg reconnaissance. Even though visual searches provide unquestionable identification, they were historically flown only on 50% of the deployment time and each visual flight covered one-third less area than a SLAR flight does.

An important issue not addressed by this study is the SLAR identification error rate for unambiguous targets, i.e., targets with cues. If this error is quantified by further study, a better estimate of the overall error rate would be possible.

References

Lapin, L. 1975. *Statistics: Meaning and Methods.* Harcourt, Brace and Janovich. New York.

Robe, R.Q., N. C. Edwards, Jr., D. L. Murphy, N. B. Thayer, G. L. Hover, M. E. Kop. 1985. *Evaluation of Surface Craft and Ice Target Detection Performance by the AN/APS-135 Side-Looking Airborne Radar (SLAR),* CG-D-02-86. U. S. Coast Guard, Washington, DC

Rossiter, J. R., L. D. Arsenault, A. L. Gray, E. V. Guy, D. J. Lapp, R. O. Ramseier, E. Wedler. 1984. *Detection of Icebergs by Airborne Imaging Radars,* Proceedings of the 9th Canadian Symposium on Remote Sensing, St. John's, Newfoundland, Canada

Appendix C

Oceanographic Conditions on the Grand Banks During the 1985 IIP Season

LT I. Anderson, USCG

Introduction

During the 1985 International Ice Patrol (IIP) season, twelve satellite-tracked TIROS Oceanographic Drifters (TODs) were deployed in the IIP operating region. Ten of the TODs were deployed from an HC-130 aircraft during regular ice reconnaissance flights. The data from these TODs are discussed below. The remaining two TODs were deployed and recovered five times each from the USCGC EVERGREEN as part of an iceberg drift and deterioration study. This is the first time IIP has deployed TODs with the expressed intent of recovery. The tracks of the two ship-deployed TODs are discussed in Appendix D.

Two oceanographic cruises were planned during the 1985 IIP season. The first cruise was on the USCGC EVERGREEN (WMEC 295) from 10 April until 10 May 1985. The objectives of obtaining iceberg drift, deterioration and detection data were met. The results of the EVERGREEN cruise drift data are discussed in Appendix D and the detection data results are discussed in Appendix B. The iceberg deterioration data will be discussed below. The second cruise planned for USCGC NORTHWIND (WAGB 282) was cancelled because of ship's main engine problems.

TIROS Oceanographic Drifter Tracks

IIP uses TODs to provide real time current information to update the historical current field used by our iceberg drift model. TODs are deployed in areas of high iceberg density and in areas of high variability in the current field in order to improve drift prediction.

All ten of the air-dropped TODs have a 3 meter long spar-shaped hull with a 1 meter diameter flotation collar and are equipped with a sea surface temperature (SST) sensor, a drogue tension sensor, and a battery voltage monitor. Each TOD is deployed with a 2 meter by 10 meter window shade drogue attached to the TOD by either a 30 or 50m tether (Table C-1). An average of 7.4 positions per day from each TOD were obtained through Service ARGOS. The distribution of the positions and sensor data points are evenly distributed in time except for the period between 0000Z and 0400Z where virtually no data is received. This null data period is due to the orbits of the NOAA/TIROS N-series satellites.

Table C-1. 1985 IIP TIROS Oceanographic Drifters

TOD #	Date Deployed	Deployment Position		Tether Length	Par. Rel.	Deploy SST	Date Left IIP Area	Ave/ Day
4526	10 APRIL	46°15.6N	46°28.8W	30M	NO	-0.8	22 JULY	7.2+
4536	7 MAY	45°42.0N	48°09.6W	50M	NO	-0.6	5 AUG *	6.4
4527	30 MAY	46°34.8N	47°22.8W	30M	NO	0.0	17 SEP**	7.1
4537	3 JUNE	47°40.0N	48°00.0W	50M	NO	---	---------	---
4548	26 JULY	47°00.6N	47°17.4W	50M	NO	10.2	8 AUG *	7.7
4529	28 JULY	48°21.0N	46°48.0W	30M	NO	10.0	17 OCT	7.9
4550	29 JULY	50°30.0N	50°29.4W	50M	YES	8.3	2 OCT	7.6
4546	10 AUGUST	47°00.0N	47°30.0W	50M	NO	---	--------	---
4541	11 AUGUST	48°17.4N	47°00.6W	50M	NO	12.6	11 SEP	8.7
4544	26 AUGUST	50°07.2N	50°29.4W	50M	YES	8.8	***	6.6

PAR. REL.: Visually confirmed release of parachute at deployment

+: INCLUDES DATA FROM 3 JUNE ONLY
*: PICKED UP BY FISHING VESSELS. 4536 HAS BEEN RETURNED TO IIP AND 4548 IN MURMANSK, USSR
**: TOD FAILED ON 17 SEPTEMBER WHILE IN IIP REGION
***: STILL IN IIP REGION AS OF 30 OCTOBER 1985

Figure C-1. Drift tracks for International Ice Patrol's 1985 TODs.
Tracks presented include data through 30 October 1985. The symbol ( ) indicates deployment position of the TOD. The julian dates beside the tick marks correspond to events discussed in the text.

As of 30 October, only one of the TODs (#4544) remained in the IIP region (Figure C-1). Two of the TODs (#4537 and #4546) failed on deployment. TOD #4526 was deployed on 10 April. Between 11 April and 3 June, only one position was received. After 3 June, TOD #4526 performed without problem. Two TODs (#4536 and #4548) were recovered by fishing vessels. Four of the TODs (#4529, #4541, #4544 and #4550) are still drifting and providing data while two other TODs failed after 110 days (#4527) and 178 days (#4526).

Only two of the parachute release mechanisms (TODs #4550 and #4544) were observed to operate following deployment. The actual fate of the remaining TOD parachutes is uncertain. We assume that when the parachute collapsed, it settled into the water and, at worst, ended up acting as a near-surface drogue. TOD #4536 was observed from CG-1504 on 18 July, more than two months after deployment, with the parachute wrapped abound the TOD hull. The parachute was still attached to the TOD when it was recovered by a fishing vessel on 5 August. There are no significant differences in the velocity distributions for TODs with confirmed parachute releases and those without, suggesting the parachute, even if it remains attached to the TOD does not significantly affect the drift of the TOD (Figure C-2).

The below discussions include TOD data through 30 October

Figure C-1a

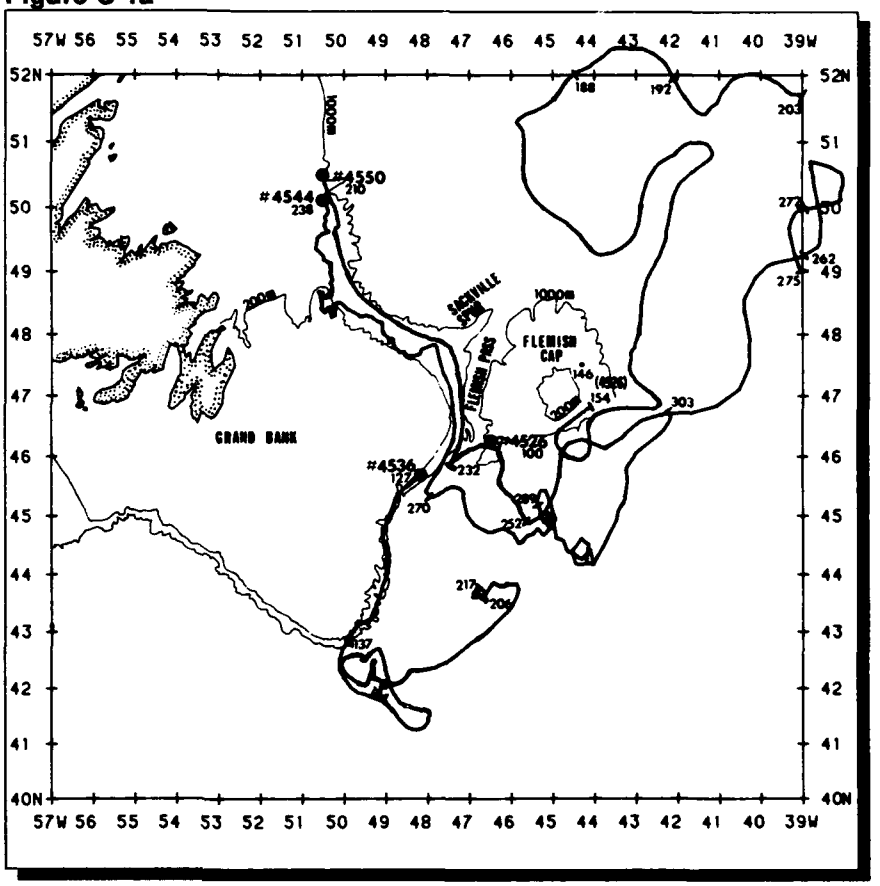

Figure C-1b

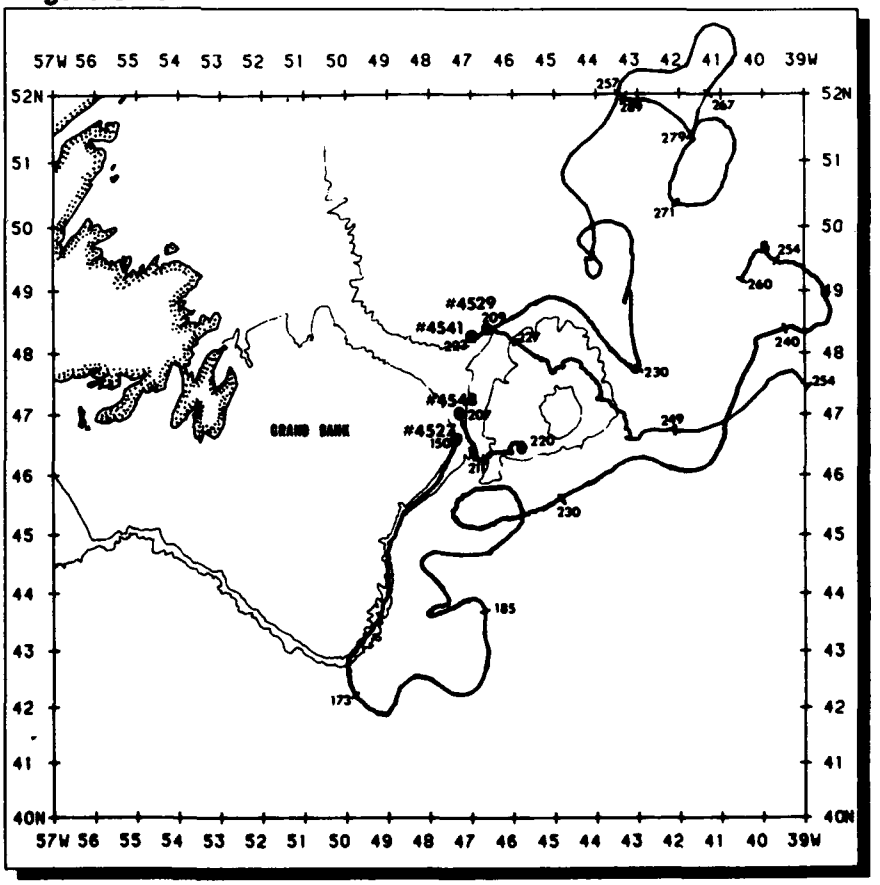

1985. The drift tracks of the TODs will be discussed below in chronological order according to when they were deployed. The number in parenthesis following dates are Julian dates and correspond to the dates on Figure C-1.

TOD #4526

TOD #4526 was deployed on 10 April (100) in the Flemish Pass in position 46°15.6'N 46°28.8'W (Figure C-1). Between 11 April and 3 June (154), only one position was received from TOD #4526. This position on 26 May (146) at 47°35.4'N 44°15.0'W indicated TOD #4526 drifted north around Flemish Cap. From 3 June (154) to 7 June, TOD #4526 drifted from 46°48.6'N 44°07.2'W in a southwesterly direction at an average velocity of 27 cm/s until it entered the North Atlantic Current. On 7 June (158), the sea surface temperature reading from TOD #4536 increased from 3°C to 5°C. Although TOD #4526 briefly drifted north of the IIP region between 7 July (188) and 11 July (192), the drift track of TOD #4526 after 7 June corresponds well with the isotherm pattern as depicted by the Canadian METOC SST charts (Figure C-3). An average velocity of 51 cm/s was maintained while TOD #4526 was in the North Atlantic Current until exiting the IIP region to the east on 22 July (203).

During June when TOD #4526 was drifting north of Flemish Cap in the North Atlantic Current, the 8°C isotherm apparently indicated the western edge of this branch of the North Atlantic Current. TOD #4526 continued to return data as it drifted across the Atlantic until its failure on 5 October. Throughout the period from 3 June until 5 October, the drogue sensor indicated the drogue was disconnected.

Figure C-2. Velocity distributions for International Ice Patrol's 1985 TODs

Figure C-2a

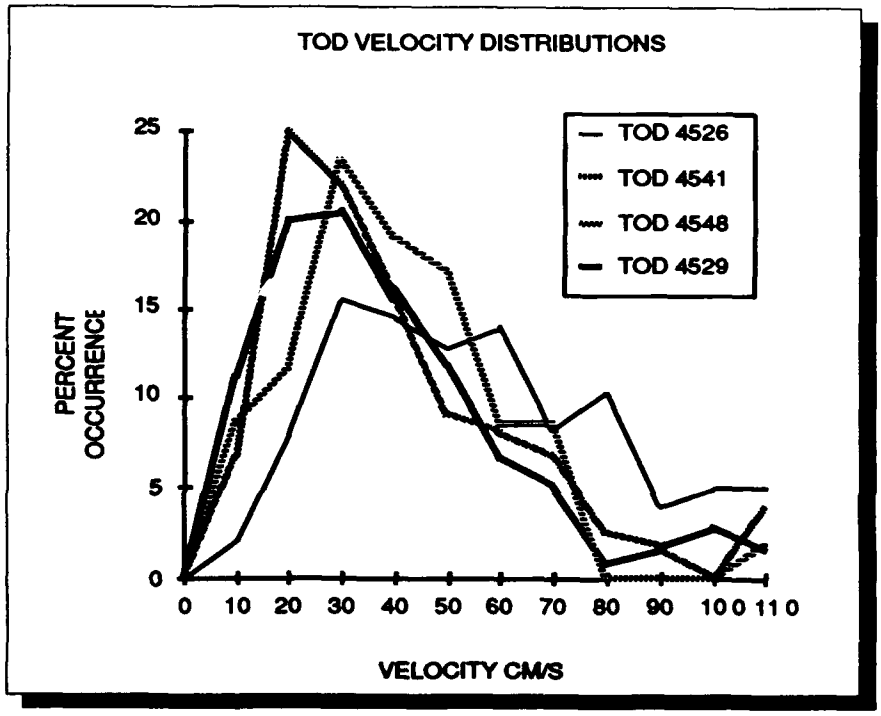

Figure C-2b

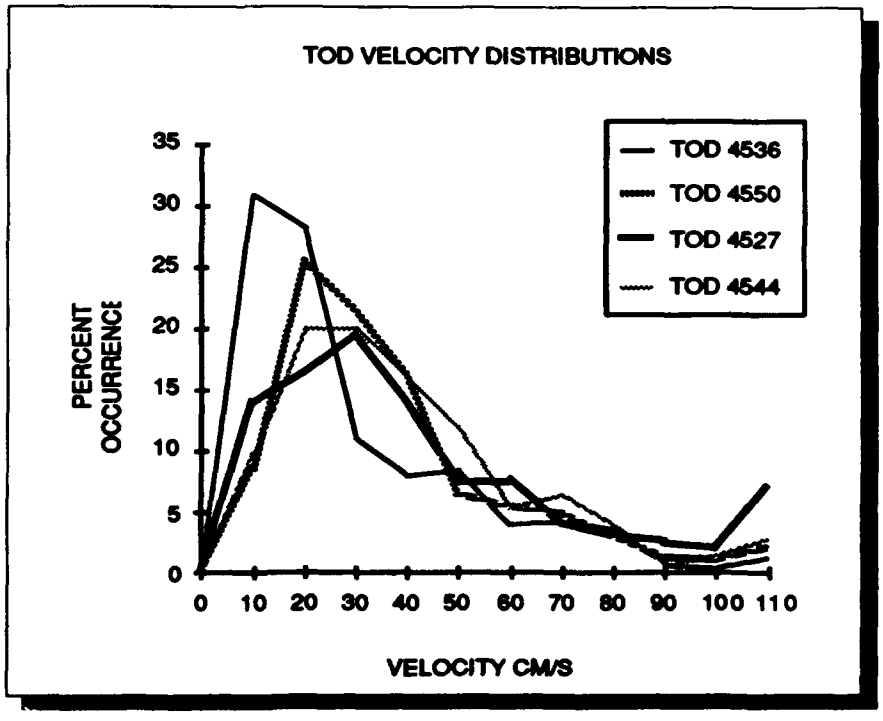

TOD #4536

TOD #4536 was deployed on 7 May (127) in 500m of water on the eastern edge of the Grand Bank south of Flemish Pass in position 45°42.0'N 48°09.6'W (Figure C-1). TOD #4536 was carried south by the Labrador Current roughly following the 500m contour at an average velocity of 44 cm/s until passing south of the Tail of the Bank on 17 May (137). Between 17 May and 3 July (184), TOD #4536 meandered along the front between the Labrador Current and the North Atlantic Current at an average velocity of 32 cm/s. The location of the front is particularly evident near 42°N 47°W along the 10°C isotherm in the METOC SST chart of 14-17 June (Figure C-3). The large amount of time (47 days) that TOD #4536 spent in this relatively slow moving area explains the shift of the velocity distribution curve to the left (Figure C-2).

On 3 July (184), the water temperature increased from 9°C to 11°C and the velocity increased significantly from about 20 to 60 cm/s indicating TOD #4536 had been caught up in the North Atlantic Current. It remained in the North Atlantic Current until 25 July (206). From 25 July until 5 August (217), TOD #4536 drifted slowly at an average velocity of 10 cm/s.

On 5 August, TOD #4536 was picked up by a fishing vessel working out of New Bedford, Massachusetts and the TOD was subsequently returned to the Ice Patrol. The exact date TOD #4536 was picked up by the fishing vessel is not certain. The drogue was attached to the TOD when it was recovered.

TOD #4527

TOD #4527 was deployed between the 200m and 500m contours along the eastern Grand Bank in position 46°34.8'N 47°22.8'W on 30 May (150) (Figure C-1). It drifted south with the Labrador Current at an average velocity of 29 cm/s along the edge of the shelf until entering the North Atlantic Current on about 22 June (173). It remained in the North Atlantic Current travelling in a generally northeasterly direction at 47 cm/s until 4 July (185). Between 4 July and 18 August (230), TOD #4527 meandered generally northward at 26 cm/s completing one large cyclonic circle south of the Flemish Cap. This period of time was spent between the Labrador Current and the North Atlantic Current.

On 18 August (230), TOD #4527 re-entered the North Atlantic Current and was carried again to the northeast at 74 cm/s. On 28 August (240), TOD #4527 began a slow cyclonic motion that followed the isotherm pattern at an average velocity of 27 cm/s (Figure C-3). TOD #4527 exited and re-entered the IIP region during this section of the drift. It continued this motion until the TOD failed on 17 September (260). The drogue sensor indicated the drogue remained attached until 11 September (254).

TOD #4529

TOD #4529 was deployed on the north side of Sackville Spur in about 1000m of water on 28 July (209) in position 48°21.0'N 46°48.0'W (Figure C-1). It drifted around the top of Flemish Cap at an average velocity of 21 cm/s until 18 August (230) when it was caught up in the North Atlantic Current. TOD #4529 was carried in a generally northerly direction at 36 cm/s until it exited the IIP region on 14 September (257). This northward drift corresponds well with the 12°C isotherm as depicted on the 15-19 August METOC SST chart

Table C-2.
1984 IIP TIROS Oceanographic Drifters Grounding in Europe

TOD #	Deployment Date	Deployment Position	Grounding Date	Grounding Position
4512	27 APR 84	47°51.6N 47°30.0W	27 SEP 85	49°36.6N 01°38.4W
4528	5 AUG 84	50°59.4N 51°01.2W	12 OCT 85	57°03.0N 06°29.4W
4530	6 AUG 84	46°46.8N 46°54.4W	28 AUG 85	50°01.2N 05°15.6W

Figure C-3. Canadian METOC Seas Surface Temperature Charts for the indicated periods

(Figure C-3). The SST sensor on TOD #4529 indicated between 11°C and 13°C during this time period.

TOD #4529 drifted to the northeast before turning south and re-entering the IIP region on 24 September (267). After re-entry, TOD #4529 drifted south until 28 September (271) when it turned cyclonically completing an ellipse with a major axis length of about 140 km on 6 October (279). The average velocity during the elliptical drift was 39 cm/s. TOD #4529 then drifted slowly to the northwest exiting the IIP region on 17 October (289). As of 30 October, TOD #4529 was still transmitting and the drogue sensor indicated the drogue was still attached.

TOD #4550

TOD #4550 was deployed in about 750m of water north of the Grand Bank on 29 July (210) in position 50°30.0'N 50°29.4'W (Figure C-1). It drifted southeast and then south with the Labrador Current through the Flemish Pass following the bathymetry until 20 August (232). During this bathymetrically guided drift period, the average velocity was 34 cm/s. TOD #4550 meandered in a southeasterly direction at an average velocity of 18 cm/s until 9 September (252). The SST values returned from TOD #4550 rose from 12°C to 17°C between 9 and 10 September indicating TOD #4550 had been caught up in the North Atlantic Current.

The North Atlantic Current carried TOD #4550 to the northeast at an average velocity of 97 cm/s until it

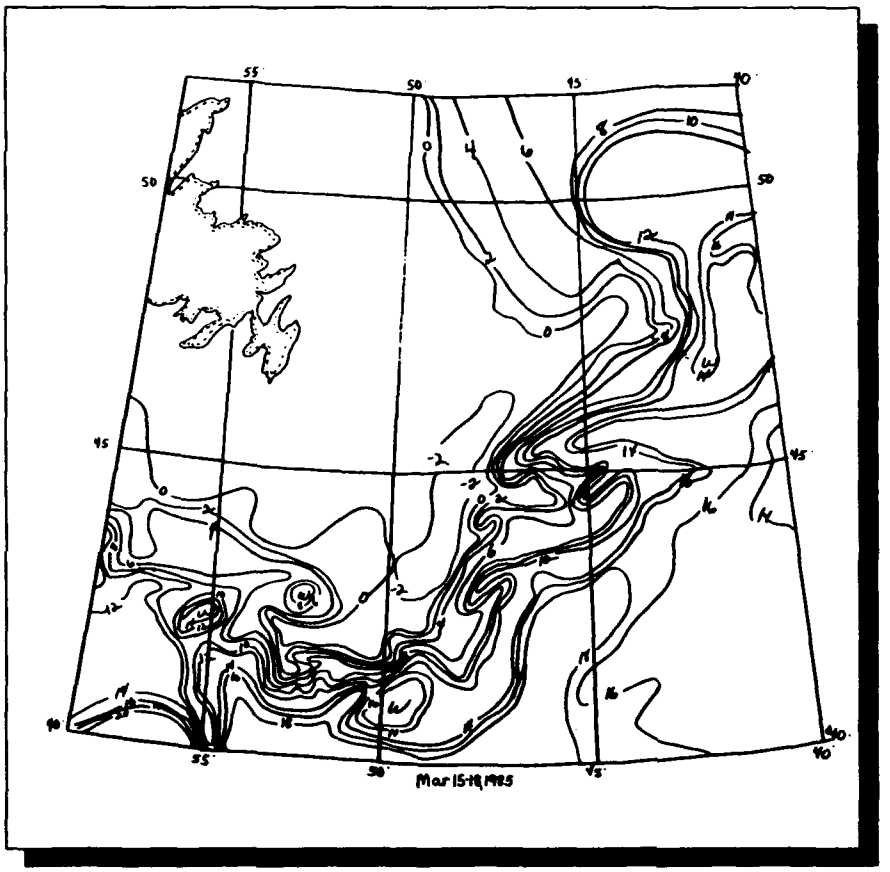

Figure C-3a. March 15-18, 1985

Figure C-3b. April 12-15, 1985

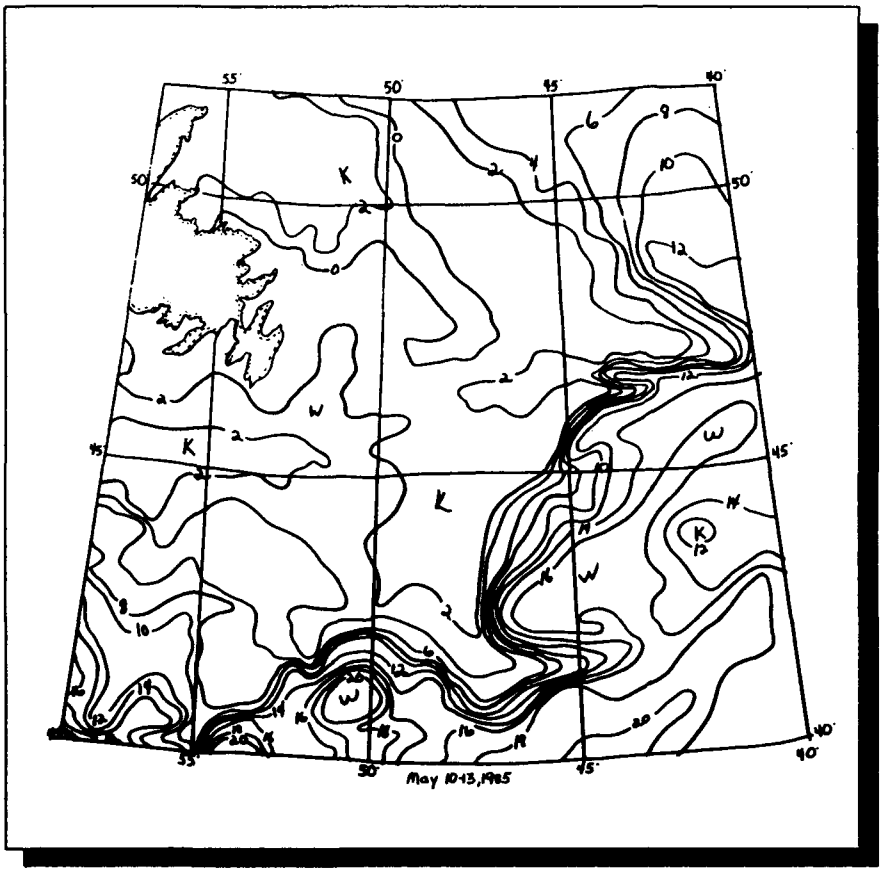

Figure C-3c. May 10-13, 1985

Figure C-3D. June 14-17, 1985

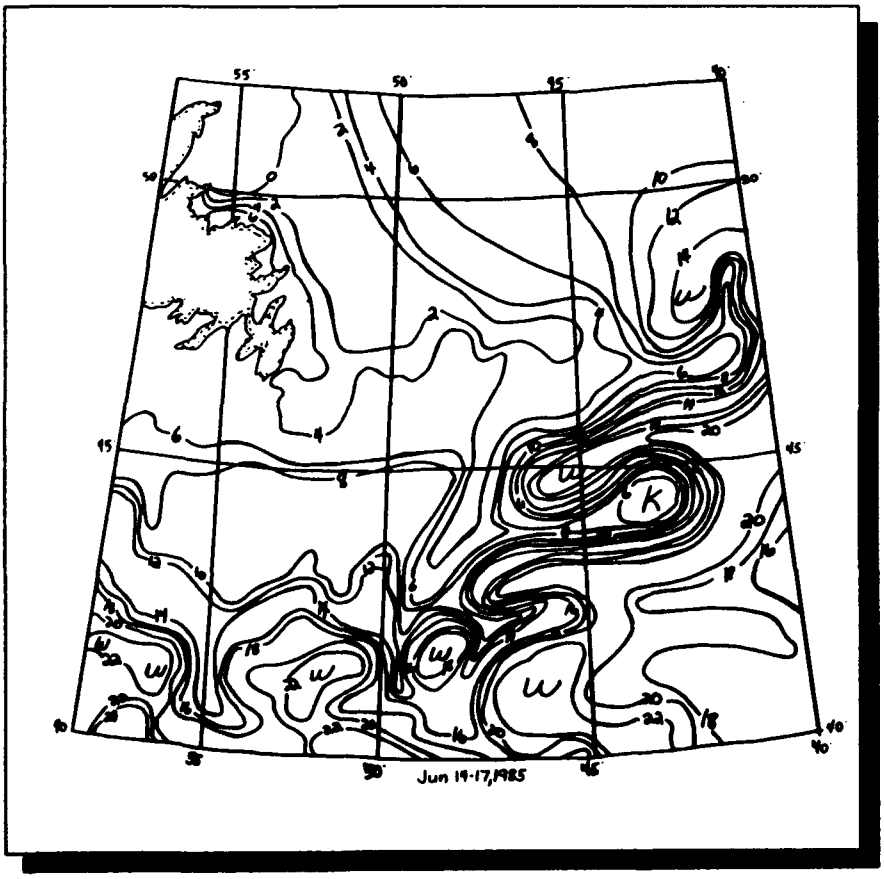

exited the IIP region on 19 September (262). TOD #4550 re-entered the IIP region briefly between 29 September (272) and 2 October (275). The drogue sensor indicated the drogue became disconnected from the TOD on 6 October. TOD #4550 is still transmitting.

TOD #4541

TOD #4541 was deployed north of Sackville Spur in about 1000m of water on 11 August (223) in position 48°17.4'N 47°00.6'W (Figure C-1). The drogue sensor indicated the drogue became disconnected on 15 August (227). TOD #4541 drifted to the southeast across the top of Flemish Cap, crossing isobaths, at an average velocity of 27 cm/s until 6 September (249). Between 6 and 8 September, the SST readings from TOD #4541 rose from 12°C to 16°C indicating TOD #4541 had entered the North Atlantic Current. From 6 September until TOD #4541 left the IIP region on 11 September (254), it drifted in an easterly direction at 70 cm/s. As of 30 October, TOD #4541 was still transmitting.

TOD #4544

To determine the drift of the last concentration of icebergs for the season, TOD #4544 was deployed north of the Grand Banks in 500m of water on 26 August (238) in position 50°07.2'N 50°29.4'W (Figure C-1). TOD #4544 drifted with the Labrador Current, following the bathymetry, through the Flemish Pass at an average velocity of 34 cm/s until 27 September (270). The drogue sensor indicated the drogue was attached only between 28 and 30 August.

From 27 September (270) until 16 October (289), TOD #4544 drifted in a southeasterly direction at 26 cm/s until it was caught in the North Atlantic Current. Between 16 October (289) and 30 October (303), TOD #4544 drifted with the North Atlantic Current at 53 cm/s. As of 30 October, TOD #4544 was still transmitting from within the IIP region.

TOD Results and Conclusions

The variability of the flow in the IIP region is again well-depicted by this year's TOD drift tracks. The areas northeast and south of Flemish Cap, in particular, illustrate the variability that exists in the IIP region making drift prediction so difficult without near-real-time inputs. As shown in previous years, the bathymetry of the Grand Bank and Flemish Cap plays a major role in guiding the drifts of TODs (Anderson, 1984). The only TOD (#4541) not apparently guided bathymetrically in this area apparently had lost its drogue.

TODs continue to supply IIP with needed real-time current information that is required to improve iceberg drift prediction. IIP intends to continue using TODs operationally. The data from all future TODs will be entered into the Global Telecommunications System (GTS). The historical current file east and north of Flemish Cap will be examined for possible changes based upon accumulated TOD drift tracks.

As a footnote, three of the TODs released in 1984 have grounded in Europe. TOD #4512 ran aground near Cherborg, France on 27 September 1985 and was taken to Brest, France, TOD #4528 grounded on the island of

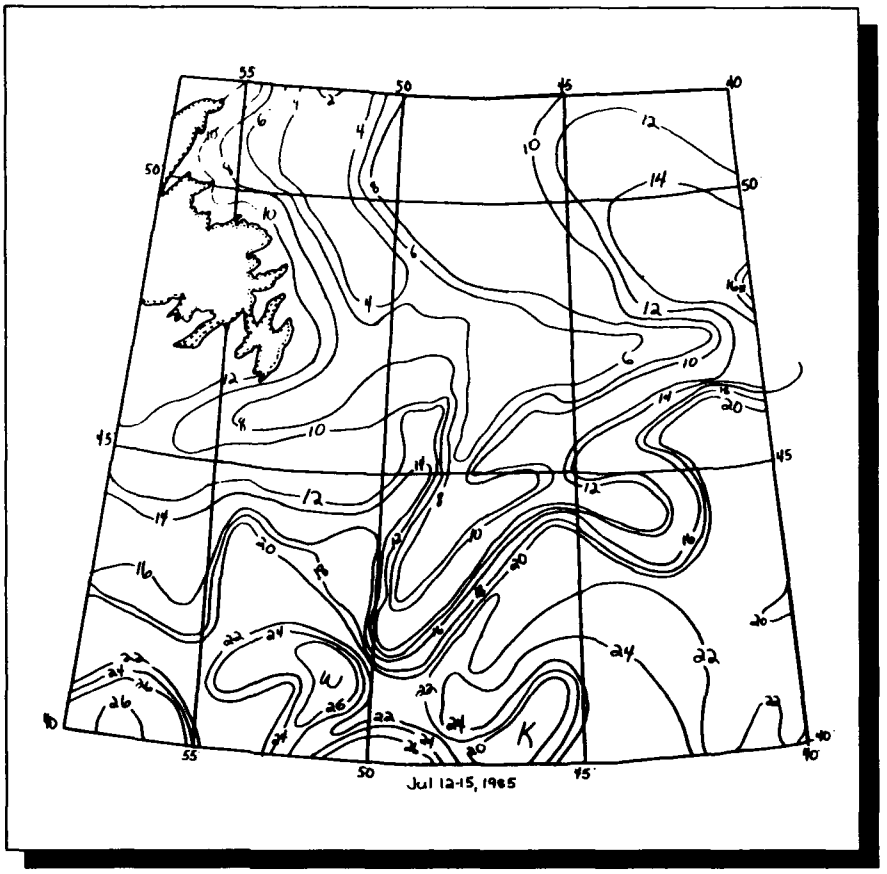

Figure C-3e. July 12-15, 1985

Figure C-3f. August 16-19, 1985

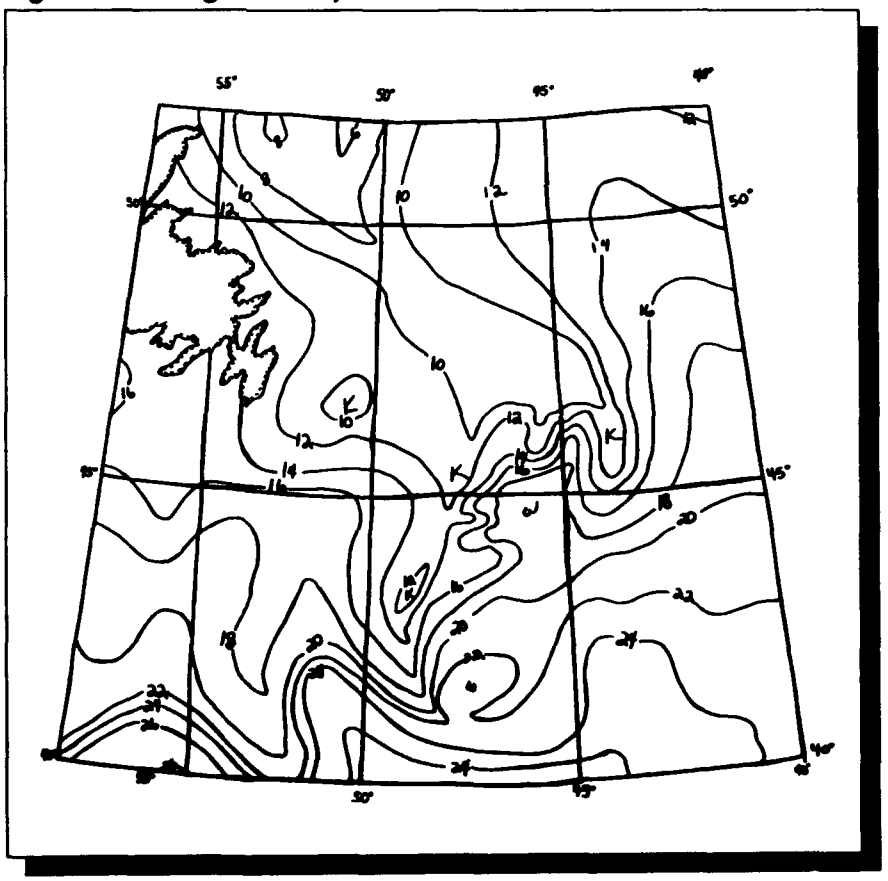

Rhum in the Sea of The Herbides off Scotland on 12 October 1985, and TOD #4530 ran aground near Helston, England (near Lands End) on 28 August 1985 (Table C-2). With the cooperation of the Royal Navy and the Military Airlift Command, TOD #4530 is being returned to Ice Patrol.

1985 Iceberg Deterioration Observations

In 1983 International Ice Patrol began using a computer model to predict iceberg deterioration. The model, based on White, *et al.*, 1980, uses melting due to insolation, vertical buoyant convection, wind-forced convection, and wave erosion to reduce the length of each iceberg. The details of the equations used by IIP to model these four processes can be found in Anderson, 1983.

During the EVERGREEN cruise, measurements of the observed icebergs were made using a reticulated laser range finder. Measurements were made twice a day separated by 12 hours, weather and other operations permitting. Photographs of the iceberg were taken in conjunction with the measurements. Length and mass estimates were made from the measurements and photographs. These methods can lead to a large error in mass estimation, since none of the underside of the iceberg was observed. Sea surface temperature (SST), significant wave height and period data were also collected. The observed environmental data were used as the inputs for the deterioration model in the discussions that follow. In the operational use of the model, the required environmental data is received

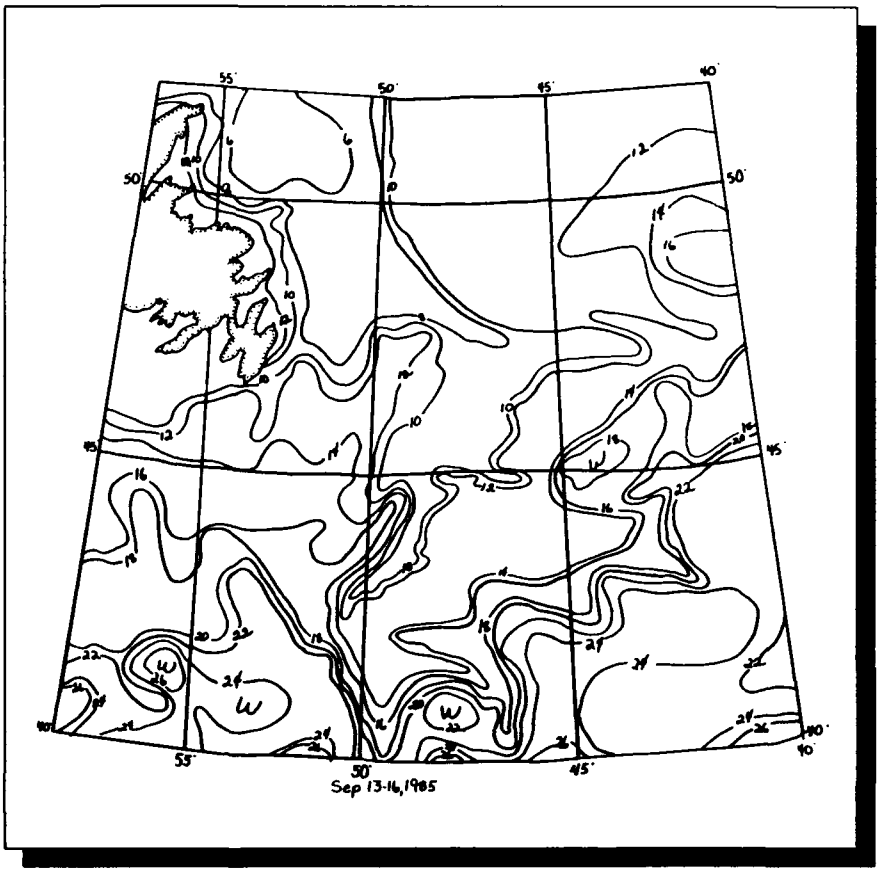

Figure C-3g. September 13-16, 1985

Figure C-4. Iceberg #1, 19 April 1985, 0930Z. Est length,129 m.

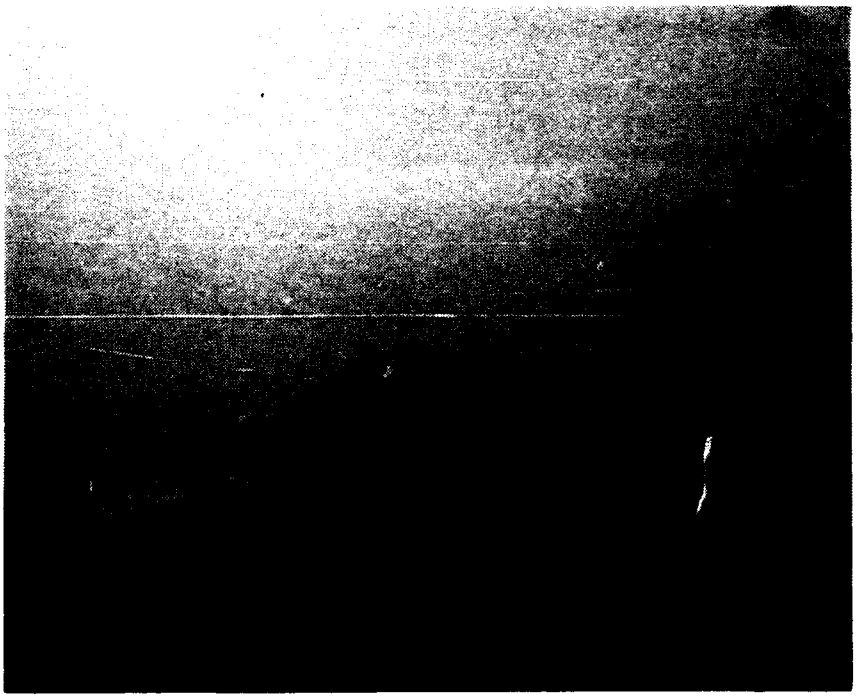

from Fleet Numerical Oceanography Center (FNOC) in Monterey, CA. FNOC provides SST data in °C and wave heights in feet. For consistency, the following discussion uses the same units.

Due to IIP's reconnaissance methods, iceberg length (not mass) is the characteristic used to evaluate deterioration. Each of the four sizes of icebergs used by IIP is assigned a characteristic length based on our size definitions (Table C-3). Before each iceberg is eliminated from our list of active icebergs because of deterioration, it is allowed to melt to 175% of its original length. This figure, although selected arbitrarily, is used conservatively to ensure the iceberg has melted before elimination. In order to reduce this figure and still ensure complete deterioration before an iceberg is eliminated, field measurements of the deterioration of three icebergs were observed during the 1985 EVERGREEN cruise, one during the first phase and two during the second phase. Comparisons of these observations to the predictions of the deterioration model are discussed below.

The two icebergs observed during the second phase of the EVERGREEN cruise were used as targets for a side-looking airborne radar (SLAR) detection and identification experiment conducted between 27 April and 5 May 1985. In order for the iceberg to be tracked during the SLAR experiment, it had to be detectable up to at least 5 nm (9 km) on EVERGREEN's surface search radar.

Table C-3. Characteristic Length of Iceberg Sizes

Size	IIP Definitions	Melt Model Length
Growler	less than 16 m.	16
Small	greater than 16 m but less than 60 m	60
Medium	greater than 60 m but less than 122 m	120
Large	greater than 122 m	225

Figure C-5. Observed Vs. Model Predicted Iceberg Length

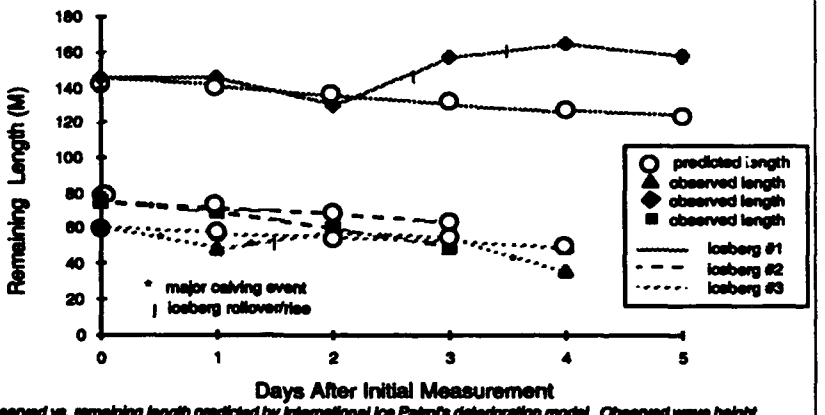

Observed vs. remaining length predicted by International Ice Patrol's deterioration model. Observed wave height and sea surface temperature were used as the model inputs. The tick marks indicate observed instances of iceberg rollover or rise while the asterisks indicate observed major calving events.

Fig. C-6. Iceberg #2 at 1000Z 28 April 1985. Est length 73m.

Figure C-7. Iceberg #3 at 2145Z 2 May 1985. Est length 48m.

Figure C-8. Observed vs. FNOC sea surface temperature (SST). *The rise in observed SST between 30 April and 1 May was due to change in location of EVERGREEN*

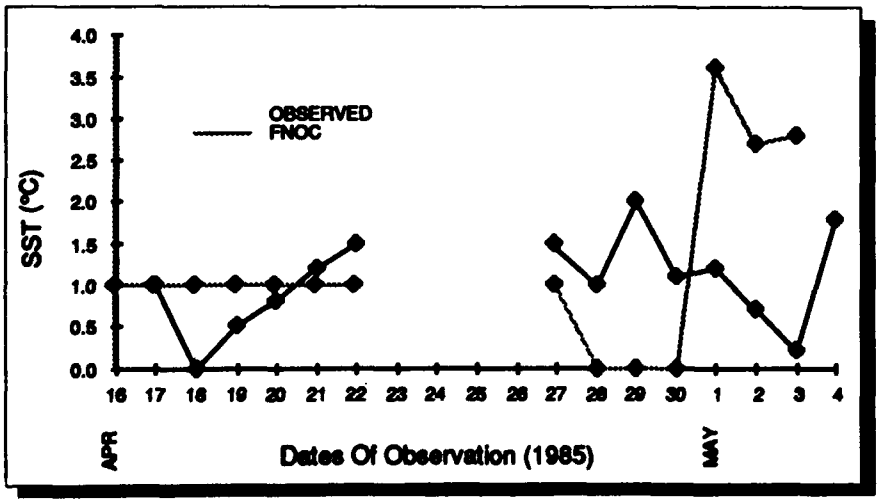

Iceberg #1

A large pinnacled iceberg with an initial length and estimated mass of about 150m and 800,000 metric tons was located in Lilly Canyon in position 44°57'N 49°03'W along the eastern edge of the Grand Bank on 16 April during the first phase of the cruise (Figure C-4). Subsequent position calculations showed that this iceberg was intermittently grounded, never drifting more than about 10 nm from the original sighted position. Poor visibility prevented the collection of size data on 16 April. Data on this iceberg were collected 17-22 April. The model-predicted waterline length matched the observed length fairly closely until the iceberg rolled on 19 April (Figure C-5).

During the evening of 19 April, the iceberg rolled, increasing the maximum observed waterline from 129m to 157m. Due to continued deterioration on 19 April, part of the iceberg rose as it tilted, allowing the iceberg to increase in length again. Although the iceberg increased in length between 17 and 22 April, it was observed to lose approximately 15% of its mass during the same period. Throughout the observation period, only a few minor calving events were observed. The average wave height and period were 5 feet and 4 to 5 seconds and the SST averaged 1.2°C.

Iceberg #2

A medium drydock iceberg was located south of Flemish Cap in position 46°12'N 46°14'W on 27 April during the second phase of the EVERGREEN cruise (Figure C-6). The initial length of the iceberg was approximately 75m. Due to the highly irregular shape, no quantitative estimates of the mass were made. Due to fog, no measurements were made on 29 April. The iceberg was observed until 30 April when it no longer was an acceptable target for the SLAR experiment.

During the observation period, there were no observed incidents of iceberg roll over. Major calving events were observed on 27 April and 30 April. The event of 30 April caused a considerable loss of mass. The model predicted a slower deterioration than was actually observed (Figure C-5). SST averaged about 1.5°C while the average wave height and period were 3 feet and 4 seconds for the observation period.

Iceberg #3

The last iceberg observed during the EVERGREEN cruise was a small drydock iceberg located in position 45°12'N 48°28'W on 1 May (Figure C-7). The initial length and mass were 60m and 35,000 metric tons respectively. Although this iceberg was never observed to have rolled over, there were frequent major calving events. A calving between 2 and 3 May caused a rise in the iceberg resulting in an increase in water-line length. The model does a fair job of predicting the deterioration rate until day 4 (5 May) when a major calving event significantly reduced the size of the iceberg (Figure C-5). On 5 May, the iceberg calved 7 large pieces of ice with the largest being 20m in length and having a mass of about 4,000 metric tons. The mass of the iceberg after this event was reduced to about 8,000 metric tons. The average significant wave height for the duration of the obser-vations was 4 feet with a 5- to 6-second period. SST averaged about 1.0°C.

Observed vs. FNOC Environmental Model Inputs

Comparisons were made between the observed and FNOC SST and wave height data. Six hour averages before the synoptic hour of the observed data were used in the comparisons below. The FNOC SST is reasonably close to the observed data (Figure C-8). The largest difference was 0.4°C. The magnitude of this difference is consistent with past comparisons (Anderson, 1983). The change in FNOC SST between 30 April and 1 May was due to EVERGREEN's change in position as iceberg #2 deteriorated substantially and iceberg #3 was located (Figure C-5). The largest error of 2.5°C occurred during the observation of iceberg #3 on 1 May.

The highest waves observed during the EVERGREEN cruise were 8 feet on 18 April (Figure C-9). FNOC predicted the wave height for EVERGREEN's position on 18 April to be 25 feet. The observed wave heights never were greater than one half of the wave height predicted by FNOC with the average error being about 10 feet. These differences between the predicted and observed wave heights are consistent with comparisons made by IIP in previous years (Anderson, 1983).

Figure C-9.
Observed vs. FNOC predicted wave heights.

Note the consistent over-estimation of wave height by FNOC for the observed period.

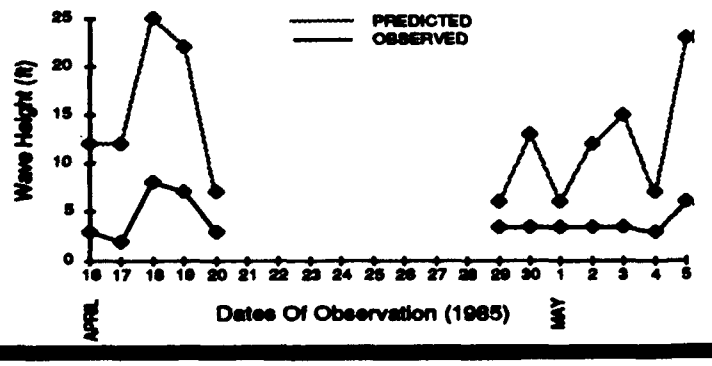

Iceberg Deterioration Discussion and Conclusions

Of the four physical processes used in the IIP model to predict deterioration, wave erosion is responsible for the vast majority of the predicted erosion. This equation is dependent on SST, wave height, and period. (Calving of growlers from an iceberg is not directly modelled but is dependent on wave erosion.) The SST and wave heights experienced by the three icebergs observed in 1985 were not significantly different.

The amount of wave-induced erosion of an iceberg of a given length under the same environmental conditions is dependent on the shape of the iceberg and the amount of surface area exposed to wave action. The shape of an opening, large or small, in an iceberg can concentrate the wave energy on a small area creating faster erosion and subsequent calving. If an iceberg has a large exposed waterline-to-mass ratio, as did icebergs #2 and #3, wave erosion with associated calving is a more effective deterioration force than on an iceberg (like iceberg #1) with a relatively small exposed waterline-to-mass ratio.

The model-predicted deteriorations for icebergs #2 and #3 were less than the observed rate over the entire obeservation period. The instances where the observed icebergs deteriorated much more rapidly than predicted by the model are correlated with observed calving events and no associated rollover or rise of the iceberg (Figure C-5). The model-predicted deterioration for iceberg #1 was greater than that observed over the entire observation period. Iceberg #1 had no observed major calving events. The major reason for the model's poor performance with iceberg #1 was the increase in maximum length due to rollover. Before the iceberg rolled over, the model-predicted deterioration closely matched the observed deterioration, and after it stabilized on day 4, the observed deterioration again closely matched the model-predicted deterioration.

Under operational conditions, the required environmental data for the deterioration model are supplied by FNOC. On their own, the observed errors in the wave height data would increase the modelled deterioration rate significantly. Part of this increase is, however, offset by the increased period of the bigger waves. (Wave height is in numerator while wave period is in the denominator of the wave erosion equation (Anderson, 1983).) During the largest error in FNOC wave height (17 feet), the deterioration rate would have been increased by about 25 percent.

Given accurate environmental data, the iceberg prediction model used by IIP predicts the deterioration reasonably well. Because of errors introduced by our present methods of operation (FNOC data errors and SLAR sizing errors), IIP will continue its conservative approach and will require that an iceberg deteriorate175% of its original length before it is eliminated. Future IIP cruises will continue to gather iceberg drift and deterioration data to further evaluate the performance of the models.

References

Anderson, I. (1983); *Iceberg Deterioration Model*, Appendix C of the Report of the International Ice Patrol Service in the North Atlantic. Bulletin No. 69., CG-188-38, International Ice Patrol, Avery Pt., Groton, CT 06340-6096

Anderson, I. (1984); *Oceanographic Conditions on the Grand Banks During the 1984 International Ice Patrol Season*, Appendix B of the Report of the International Ice Patrol Service in the North Atlantic. Bulletin No. 70., CG-188-39. International Ice Patrol, Avery Pt., Groton, CT 06340-6096.

White, F. M., M. L. Spaulding, and L. Gominho (1980); *Theoretical Estimates of the Various Mechanisms Involved in Iceberg Deterioration in the Open Ocean Environment*, U. S. Coast Guard Research and Development Center Report CG-D-62-80, 126pp.

Appendix D

An Evaluation of the International Ice Patrol Drift Model

D. L. Murphy
LT I. Anderson, USCG

Introduction

Since 1979, International Ice Patrol (IIP) has been using an iceberg drift model as an integral part of its iceberg tracking operations. During the season of maximum iceberg threat, typically March through August, IIP conducts aerial reconnaissance of its operations area (40° - 52°N, 39° - 57°W) on alternate weeks. During the week that the IIP Ice Reconnaissance Detachment (ICERECDET) is deployed to Gander, Newfoundland (IIP field operations base), daily flights are conducted on five consecutive days, each covering only a small portion of the IIP operations area. As a result of this reconnaissance schedule, IIP must often rely on the model predictions to set the limits of iceberg danger during periods when no ice reconnaissance is being conducted. In addition, the model drift predictions are used to help recognize icebergs that have been previously sighted, either by the ICERECDET or merchant vessels. Lacking this ability to recognize iceberg resights has the effect of inflating the numbers of icebergs south of 48°N, the traditional indicator of the severity of an iceberg season.

Despite the reliance that IIP places on the accuracy of the drift model results, relatively little testing of the model has been possible, primarily because adequate iceberg drift data, with accompanying environmental data, are expensive and often difficult to obtain. Moreover, only in the last few years has navigation in the operations area been accurate and reliable enough to permit the collection of good data.

Mountain (1980) tested the model using the tracks of two large tabular icebergs, a large pinnacle iceberg, and a freely-drifting satellite-tracked buoy. The drift durations were from 3 to 25 days. The results were quite variable, ranging from a small 9km error for the 3-day drift to a constant 90-150km drift error in the 25-day case. Although he recognizes the limitations of this small data set, he suggests that the primary cause of the model error is due to inaccurate inputs, i.e., winds and currents.

This report describes the results of four case studies in which the performance of the IIP iceberg drift model was examined at four different locations (Figure D-1) in the IIP operations area. The objectives were twofold: first, to test the accuracy of the drift predictions of the operational IIP iceberg drift model, and second, to investigate how the accuracy changes when on-scene measured wind and current data are used to drive the model.

Model Description

Mountain (1980) describes the details of the IIP operational drift model; thus, only a brief outline is presented here. The fundamental model balance is between iceberg acceleration, air and water drag, the Coriolis acceleration and a sea surface slope term. The resulting differential equations are solved using a fourth-order Runge-Kutta algorithm. The model is driven by a water current which combines a depth- and time-independent geostrophic flow with a depth- and time-dependent current driven by the local wind (time-dependent Ekman flow).

When used operationally, the IIP drift model employs a mean geostrophic current field based on many years of hydrographic surveys (Scobie and Schultz, 1976). It is on a grid of 20 minutes of latitude by 20 minutes of longitude, except for the Labrador Current, which is defined on a more detailed grid of 10 minutes of longitude. Wind data, on a 1 degree of latitude by 2 degrees of longitude grid, are provided to the model every 12 hours from the surface-wind analysis of the U. S. Navy Fleet Numerical Oceanography Center (FNOC).

Finally, the model requires as input the mass and cross-sectional area of the drifting iceberg. Obviously, IIP reconnaissance operations do not permit precise measurement of each detected iceberg. Often, IIP locates icebergs using the side-looking airborne radar

(SLAR) with no visual confirmation. As a result, IIP can only classify icebergs into the broad categories of growler, small, medium, and large, and assume characteristic mass and cross-sectional areas for each category. When visual confirmation is available, it is possible to distinguish between tabular and non-tabular icebergs, resulting in somewhat different mass and cross-sectional areas. Regardless of the size and shape of the iceberg, both the air and water drag coefficients are set to 1.5.

Currently, IIP estimates that the model drift error is 10nm (~18.5km) for the first 24-hour period and an additional 5nm (~9km) for each additional 24 hours of drift, up to a maximum error of 30nm (~56km). The accuracy of this error estimate is evaluated in this report.

In 1983 IIP began using observed-current data derived from the trajectories of freely-drifting satellite-tracked buoys to modify the mean geostrophic field (Summy and Anderson, 1983) during operational model runs. The modifications are both temporary and localized in that they are only applicable during the period that a buoy is in that specific region, after which the currents revert back to the mean geostrophic currents. It is not the intent of the present report to address this practice directly, but rather to compare the drift-model accuracy using two sets of input data: mean geostrophic data with FNOC wind and on-scene measured data. In doing so, the importance of using on-scene data becomes clear.

Figure D-1. Area of Study

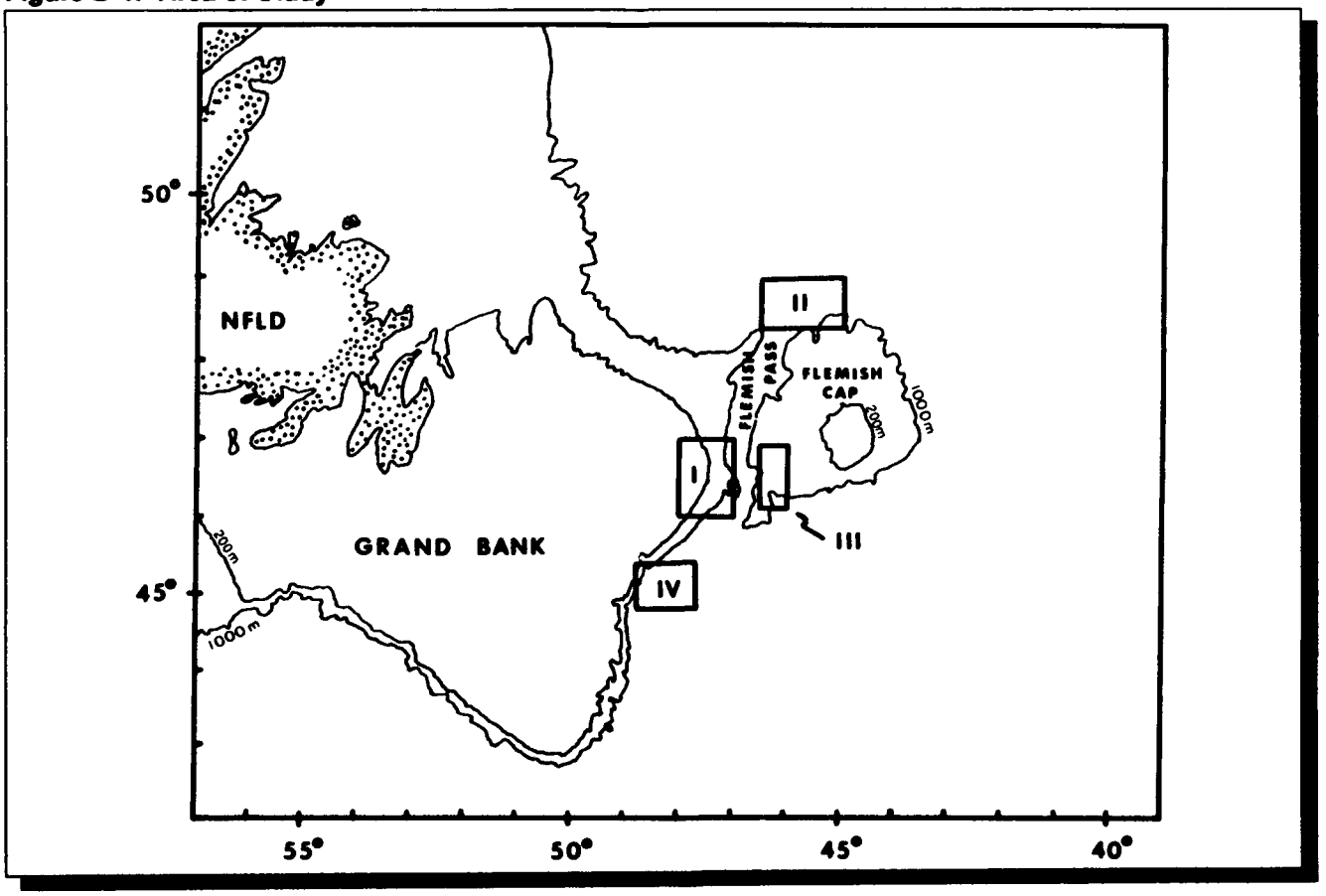

Figure D-2. Iceberg and TOD trajectories for Case I (1983)

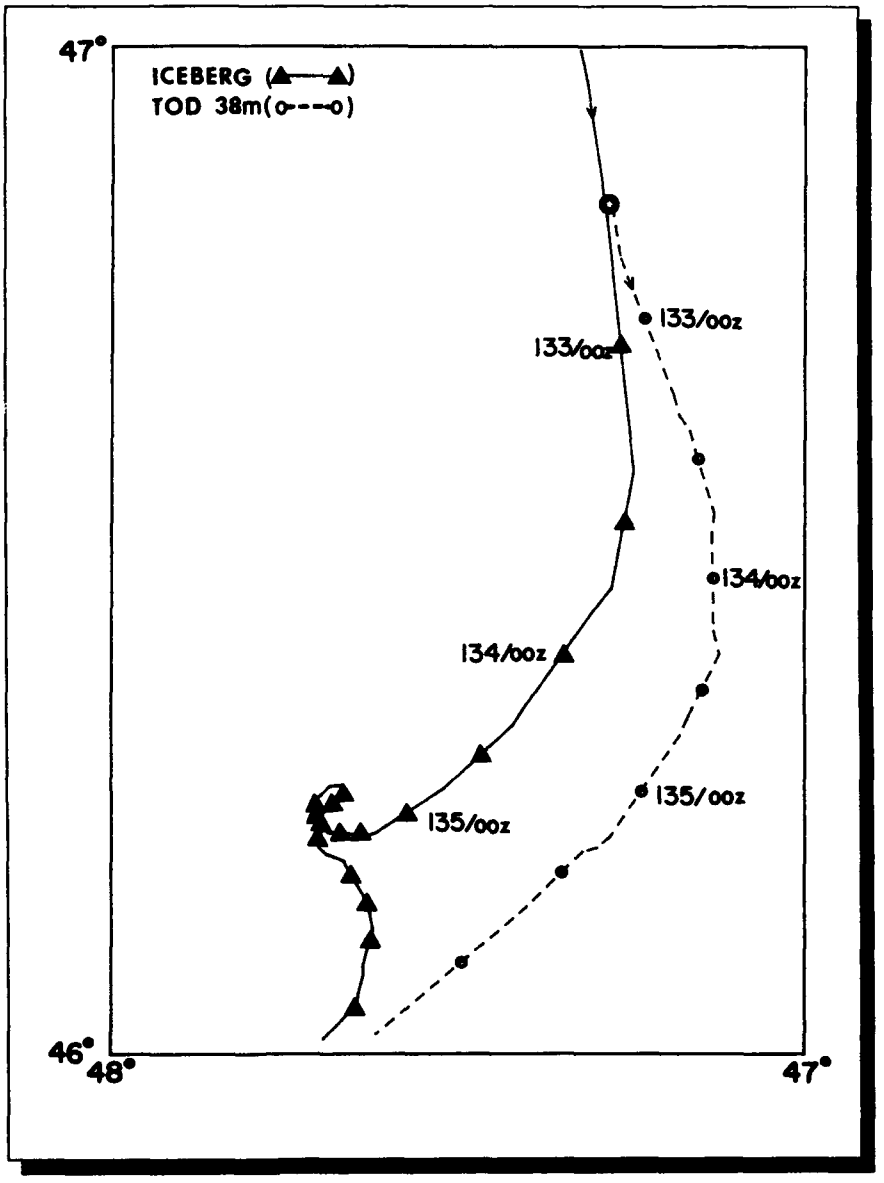

Data Description

The data used in this study were collected from 1983 through 1985. All of the cases were drifts of short duration, with a maximum drift period of 4.5 days. In all four cases, the drifting iceberg was close to at least one freely-drifting TIROS Oceanographic Drifter (TOD), from which local currents were determined. The TOD hull was a 3m spar and was fitted with a 2m x 10m window-shade drogue at the end of a tether. The drogue depths presented here refer to the depth of the center of the drogue. The TOD's were tracked by the NOAA/TIROS series satellites and the data provided to IIP by Service ARGOS, with a position accuracy well within 500m (Bessis, 1981).

In three of the cases (II, III, and IV), a surface vessel near the iceberg was collecting local wind data. The data for each case are discussed separately. The numbers in parentheses after each date are Julian year dates, that is, dates numbered sequentially from 1 January.

Case I

This case consists of a 2.5-day drift of a large tabular iceberg with a TIROS Arctic Drifter (TAD) aboard. The TAD, which is essentially a TOD with different packaging, had been deployed onto the iceberg on 27 March 1983 (86) by IIP, in cooperation with the U. S. Coast Guard Research and Development Center (R&DC).

The test period began at 1600Z on 12 May 1983 (132) when a TOD, drogued at 38m, was air-deployed from a HC-130 aircraft at a location approximately 1km from the iceberg, which at the time was moving southward in the Labrador Current (Figure D-2).

The test period ended on 15 May (135) shortly before the iceberg grounded for a 4-day period. The iceberg was last sighted with the TAD aboard on 21 May (141) by Mobil Oil Company, Canada (Anderson, 1983). On this date the iceberg was still classified as large, with estimated dimensions of 150mx110mx30m. During the test period, the maximum separation between the TAD (iceberg) and the TOD was less than 25km. No on-scene wind data were available.

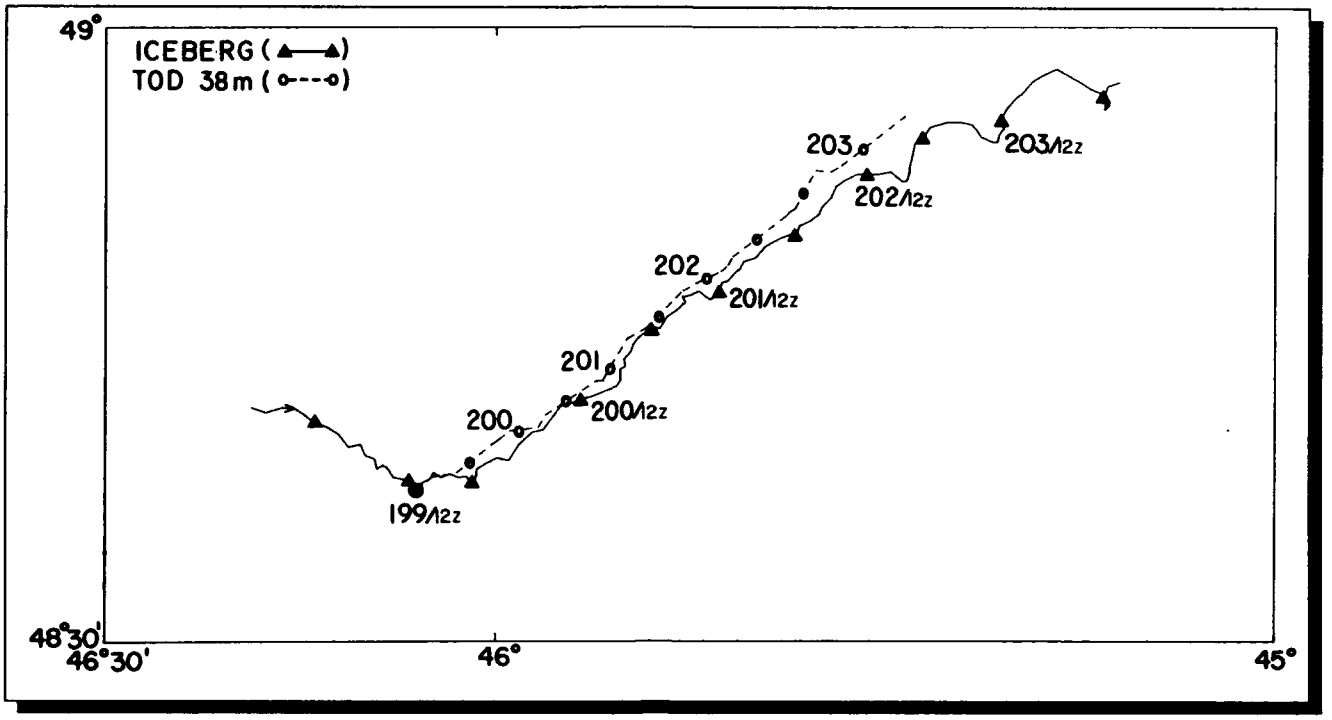

Figure D-3. Iceberg and TOD trajectories for Case II (1984)

Case II

This case is a 4.5-day segment of an iceberg track obtained in 1984 by USCGC HORNBEAM. The test period began 17 July (199) at 1300Z when HORNBEAM deployed a TOD drogued at 38m approximately 500m from a medium (120mx115mx37m) pinnacle iceberg in the region north of Flemish Cap. Although the iceberg was rapidly deteriorating, it was in the medium size range (>60m) for most of the drift period. Only in the last 24-30 hours of drift was it at or slightly below the medium/small border. Hourly iceberg positions were recorded using radar ranges and bearings and the HORNBEAM's LORAN C position (Figure D-3). Hourly wind speed and direction were measured using the shipboard anemometer (Figure D-4). The maximum separation between the iceberg and the TOD was less than 25km.

Case III

The third case is a 3.5-day [27 - 30 April 1985(117-120)] track of a medium (75mx56mx18m) drydock iceberg south of Flemish Pass obtained by USCGC EVERGREEN. Over the drift period, the target iceberg was deteriorating but only on the last day of drift did it fall into the upper part of the small range. Again, hourly iceberg position (Figure D-5) and wind data (Figure D-6) were collected using shipboard radar and anemometer, respectively.

Figure D-4. Hourly wind vectors for Case II

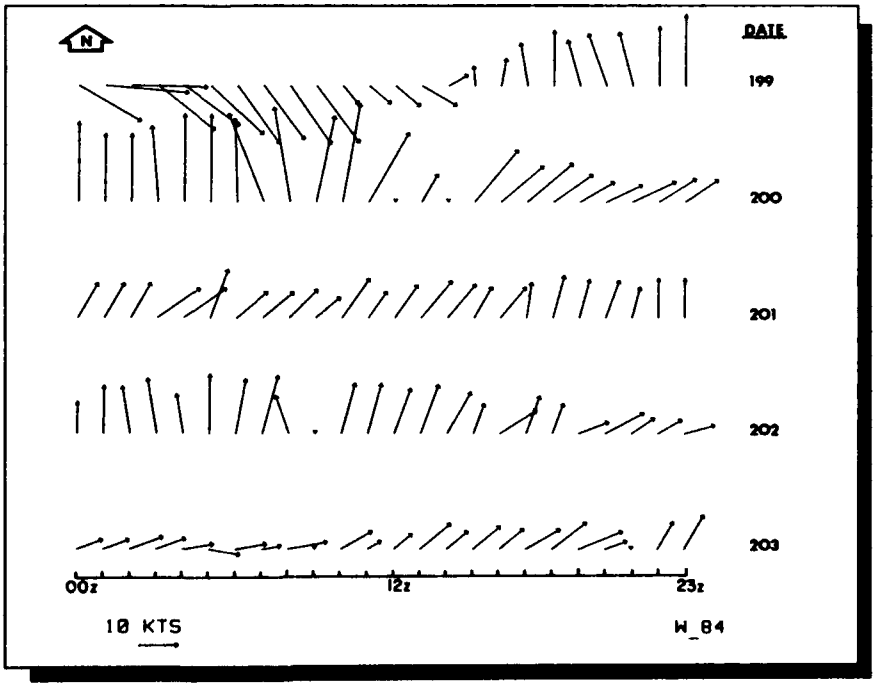

Two TOD's provided the current data. They were deployed, one drogued at 38m and the other at 58m, 300m from the iceberg on 27 April (117). Approximately halfway through the drift period, both buoys were retrieved and redeployed close to the iceberg to minimize the separation between the iceberg and the TOD's. Upon redeployment, the drogue at 38m was set to 8m. The maximum separation between the iceberg and the TOD's, which occurred during the first part of the drift period, was approximately 35km.

Case IV

A 4-day drift [1-5 May 1985(121-125)] of a small (60mx40mx10m) drydock iceberg provides the data for Case IV. As in Case III, the area of study was south of Flemish Pass, and EVERGREEN tracked the target (Figure D-7) and obtained the wind data (Figure D-8). Two TOD's, one drogued at 8m and the other at 58m, were deployed on 1 May (121); they were retrieved and redeployed at the iceberg on 4 May (124). The maximum separation between the iceberg and the TOD's was approximately 30km. On the last day of the experiment, there was a major calving event that left two small icebergs. At this time the parent (larger) iceberg had a maximum waterline length of 37m.

Test Runs

Table D-1 summarizes the runs made during the model tests. For each case, the first run used the mean surface geostrophic current field from the IIP data base and wind data from FNOC. This set of inputs is referred to as system currents and system winds. The remaining runs for each case differed from the first run only in that available on-scene environmental data (observed) were used to drive the model.

The observed currents were obtained from the TOD trajectories by linearly interpolating to positions at 0000Z and 1200Z each day, and then calculating the 12-hour averaged current. When wind data were available, 12-hour averages were computed for use in the model. When no observed wind data were available, FNOC data were employed.

For each run, the model computed a predicted iceberg position at 0000Z and 1200Z on each date. The range and bearing from the actual to the predicted iceberg position were computed for these times.

Table D-1. Model Test Runs Summary

Case	Size	Run Number	Inputs Winds	Currents	
I	Large	1	SYS	SYS	
I	Large	2	SYS	OBS	(38m)
II	Medium	1	SYS	SYS	
II	Medium	2	OBS	OBS	(38m)
III	Medium	1	SYS	SYS	
III	Medium	2	OBS	OBS	(38m/8m)
III	Medium	3	OBS	OBS	(58m)
IV	Small	1	SYS	SYS	*
IV	Small	2	OBS	OBS	(8m)
IV	Small	3	OBS	OBS	(58m)

Summary of the test runs. SYS=system, OBS=observed.The numbers in parentheses indicate the depth of the drogue center.

* Note: The observed currents for this case were a combination of data from buoys drogued at different depths: 38m for the first half of the period and 8m for the second half.

Results

Figures D-9 through D-12 show the magnitude of the drift errors as a function of elapsed time for each of the four cases. The IIP error estimate of 10nm for the first 24-hour period and an additional 5nm for each additional 24-hours of drift, up to a maximum error of 30nm, is also plotted.

In Case I (Figure D-9), the system inputs result in drift errors that increase rapidly and persistently; after approximately 2.5 days they exceed 40nm (~75km). The magnitude of this error is 52% of the total predicted drift. When observed currents drive the model, the errors are substantially reduced so that they are nearly consistent with the currently-used IIP error estimate. In Case I, both the iceberg and the buoy were in the southward-flowing Labrador Current with typical current speeds of 0.4-0.5 m/s.

In Case II (Figure D-10), the errors for the system/system run were less than 12nm (~22km) or 22% of the total predicted drift for the entire 104-hour drift period, well below the IIP error estimate. Using observed current and wind data improves the results; after 104 hours the error is 2.5nm (~4.6 km). The drift test was conducted north of Flemish Cap with typical current speeds of 0.2 m/s, approximately half that observed in Case I.

Figure D-5. Iceberg and TOD trajectories for Case III

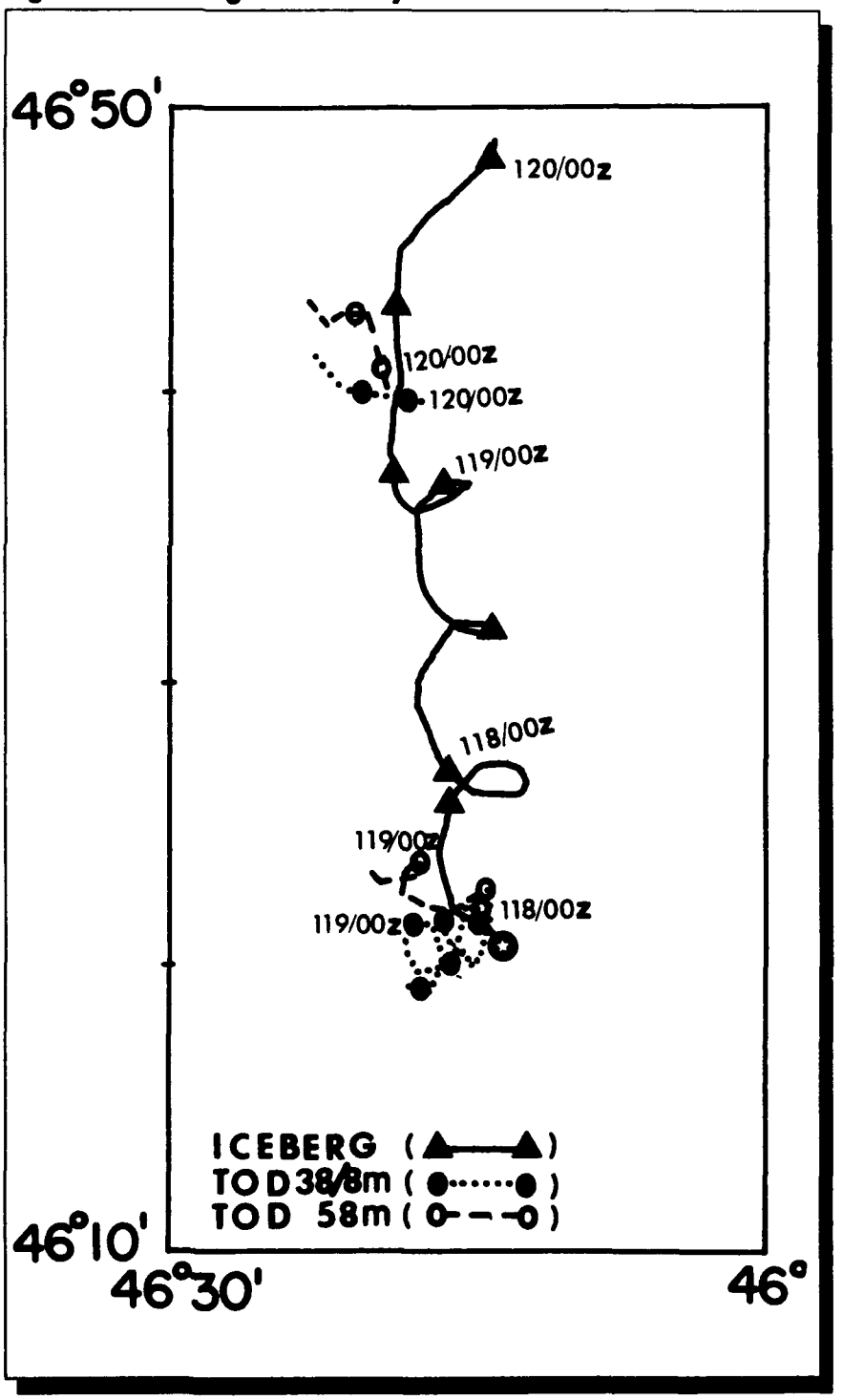

Figure D-6. Hourly wind vectors for Case III

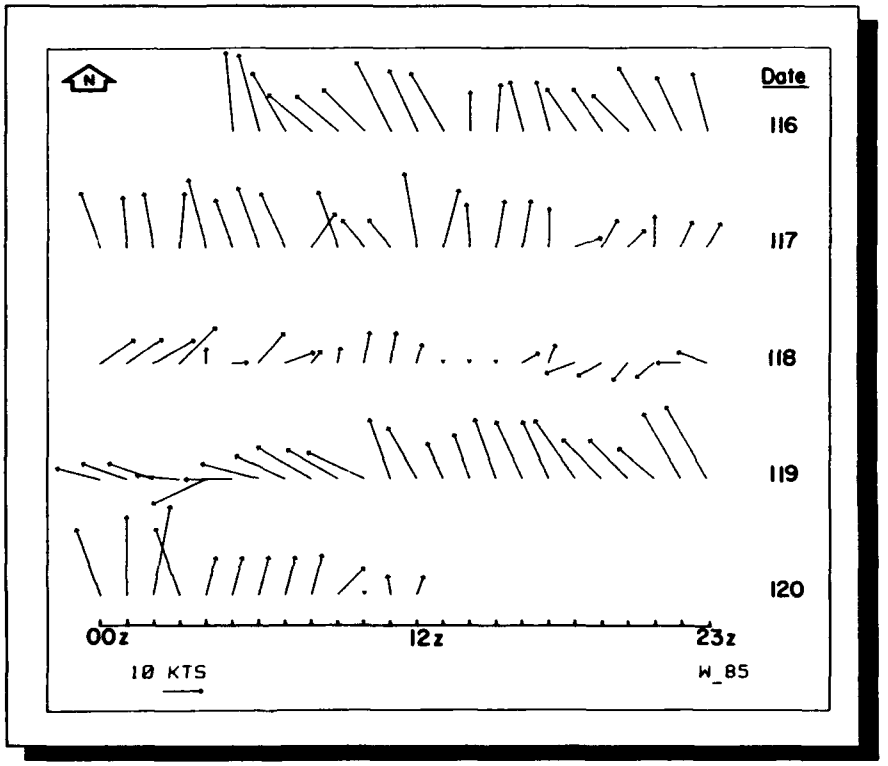

The Case III system/system run (Figure D-11) produced errors that increased persistently, exceeding the IIP error estimate after about 36 hours of drift. At the end of the drift period, the error was over 30nm (~56km), which is 73% of the total predicted drift. In the early part of the drift period (<48hrs.), the use of the observed current and wind data produced no improvement in the results; indeed, at one point, the results were less accurate than the system/system case. This result is not surprising because the iceberg moved rapidly to the north while both buoys remained close to the deployment area. When the buoys were retrieved and redeployed at the iceberg (~60 hrs.), the model results computed using observed data improved somewhat.

Using the observed data to drive the model in Case IV (Figure D-12) made an enormous improvement in the results. The system/system run produced errors between 30-45nm (~56-83km) while, for the observed data, the errors were approximately half those values. For most of the drift period, the currents measured at 58m provided more accurate model results than those measured at 8m. At 84 hours this situation reversed, and the 8m data produced better results. This is an expected result because as this small iceberg deteriorated, its motion should have been more consistent with the 8m currents than the 58m currents. However, the data are few and the difference between the results (8m vs. 58m) is small so there is no certainty that the reversal is meaningful.

Conclusions

No firm conclusions can be drawn from this small data set, but there is some consistency in the results that is worthy of note.

In all four cases, using on-scene measured data improved the model accuracy over the runs made using geostrophic currents and FNOC winds. The accuracy improvement was substantial in two cases: Case I and Case IV. Thus, the results of this study support the IIP practice of using TOD drift data to modify the geostrophic current. The more widespread the use of TOD's, the more we can rely on the model results. No attempt was made to separate the improvements due to on-scene current data and on-scene wind data because of the small amount of data. However, Case I, for which there were no on-scene wind data, showed considerable improvement when on-scene current data were used in the model predictions.

In three of the four cases (Case II excepted), the observed drift error was larger than the IIP estimated error when the system

Figure D-7. Iceberg and TOD trajectories for Case IV

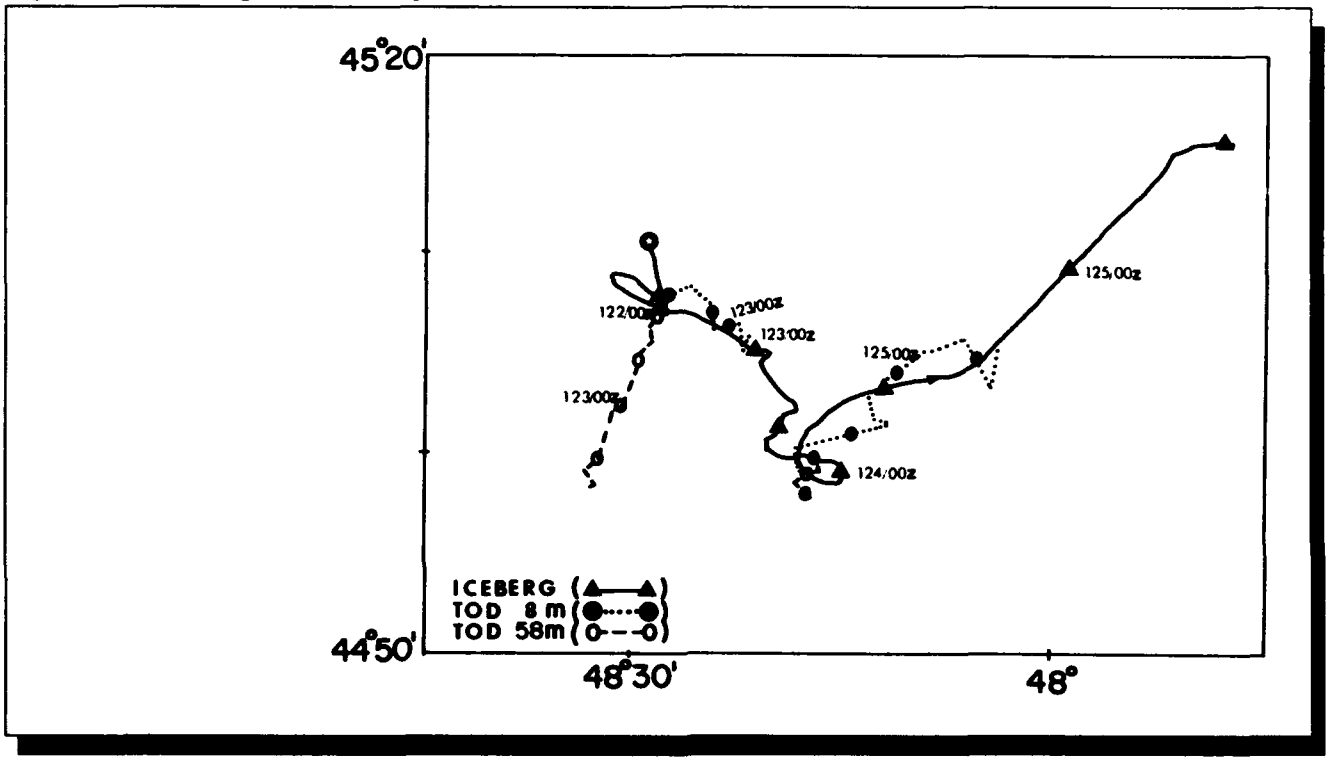

winds and currents were used. For these three cases, the drift errors were 52-73% of the total predicted drift; for Case II the drift error was 22% of the total predicted drift. While it is tempting to suggest that the estimated position error be linked to the total length of the predicted drift (distance along the predicted path), no clear guidance can be given based on these results. The limited data show that if there is a TOD providing current information in the vicinity of a drifting iceberg, the model will probably produce positions that are within the IIP error limits. If only geostrophic data are available, the errors can be substantially larger, even for drifts of short duration. This issue is particularly important when an iceberg is being used to set the limits of iceberg threat.

The importance of collecting current data as close as possible to the tracked iceberg cannot be overemphasized. Early in Case III, when the TOD's and the iceberg separated rapidly, there was no improvement in the model errors when observed inputs were entered. Later in the drift period (after the buoys were redeployed), the model errors were smaller when the observed data were used.

Finally, the results of this study provide some guidance on the deployment of IIP operational TOD's. Although TOD drift data directly north of Flemish Cap are useful, the results of Case II showed that the model performed within the error estimates using the geostrophic currents. The TOD's deployed in the Labrador Current (Case I) and south of Flemish Pass (Cases III and IV), on the other hand, provided bigger payoffs.

References

Anderson, I., 1983. *Oceanographic Conditions on the Grand Banks During the 1983 International Ice Patrol Season.* Appendix B of Report of the International Ice Patrol in the North Atlantic. Bulletin No. 69. CG-188-38. International Ice Patrol, Avery Point, Groton, CT 06340-6096, 73 pp.

Bessis, J.L., 1981, *Operational Data Collection and Platform Location by Satellite*, Remote Sensing of the Environment, Vol II

Mountain, D.G., 1980. *On Predicting Iceberg Drift*, Cold Regions Science and Technology, Vol 1 (3/4): 273-282.

Scobie, R.W., and R.H. Schultz, 1976. *Oceanography of the Grand Banks Region of Newfoundland March 1971 - December 1972.* Report No. 373-70. U. S. Coast Guard, Washington, DC, 298 pp.

Summy, A.D., and I. Anderson, 1983. *Operational Use of TIROS Oceanographic Drifters by International Ice Patrol (1978-1982).* Proc. 1983 Symposium on Buoy Technology. Marine Technology Society, Gulf Coast Section, Bldg. 2204, NSTL, MS 39529, p. 246-250.

Figure D-8. Hourly wind vectors for Case IV

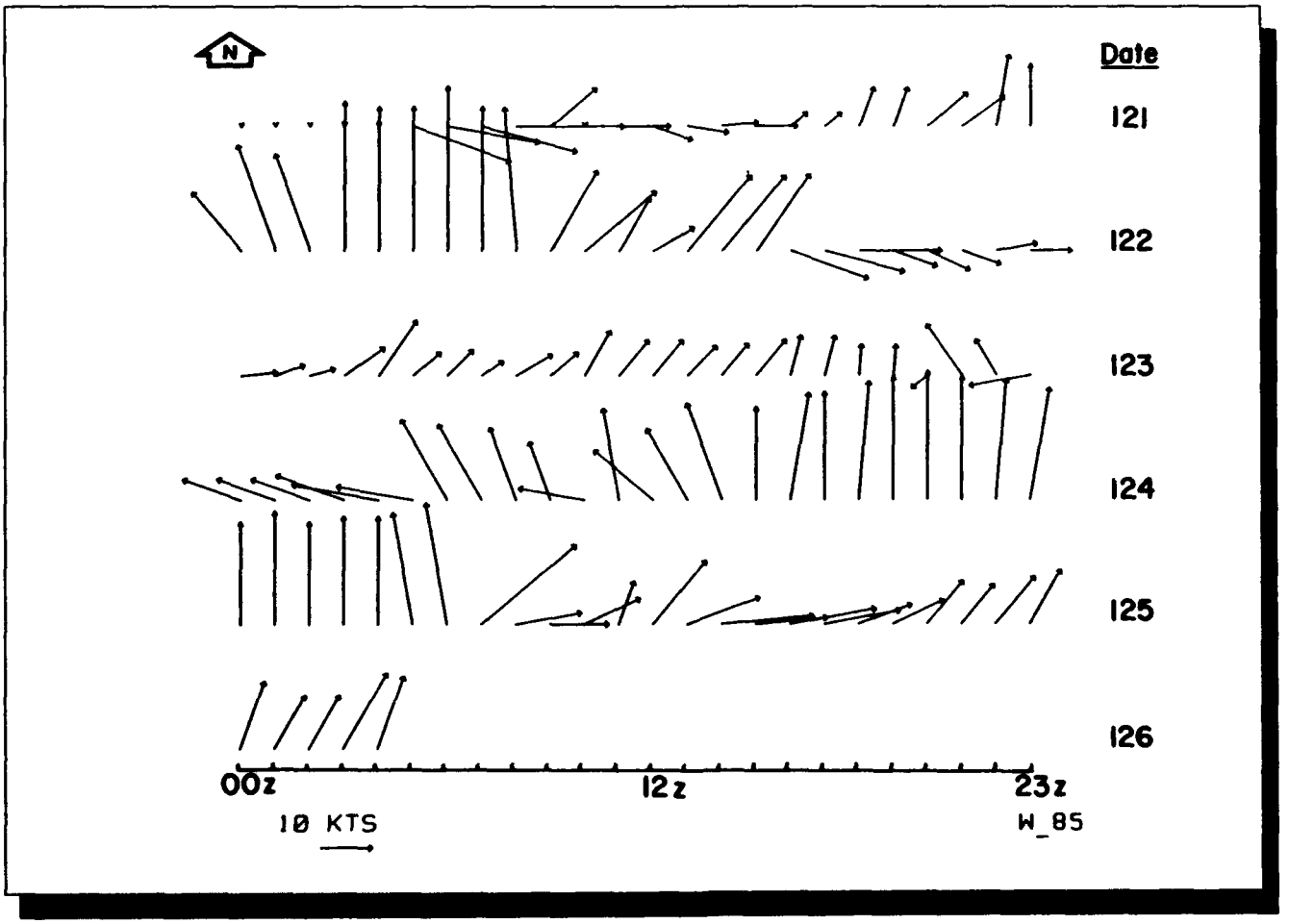

Figure D-9. Case I model errors

Figure D-10. Case II model errors

Figure D-11. Case III model errors

Figure D-12. Case IV model errors

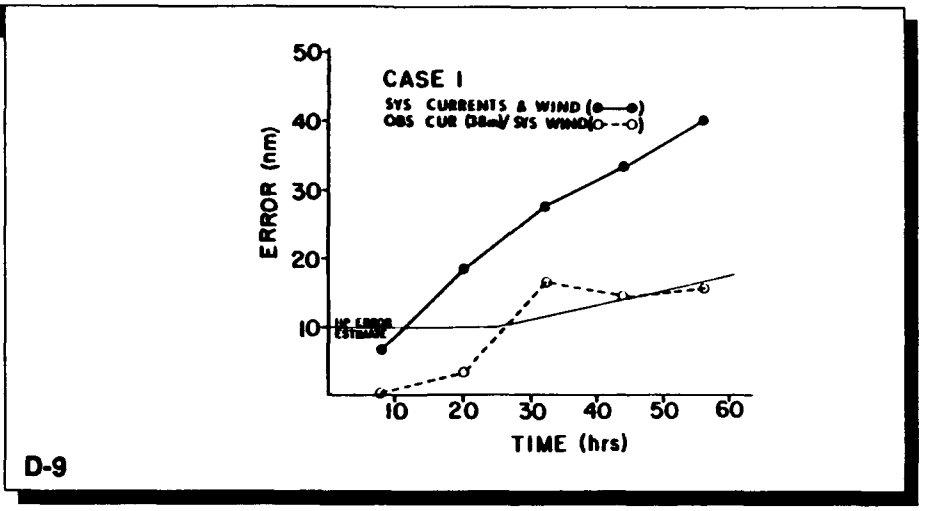

D-9

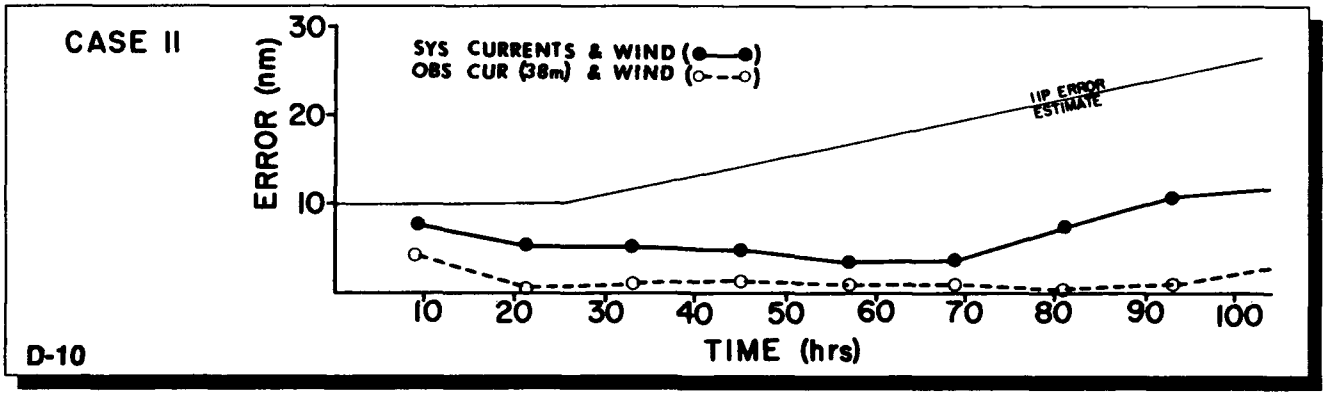

D-10

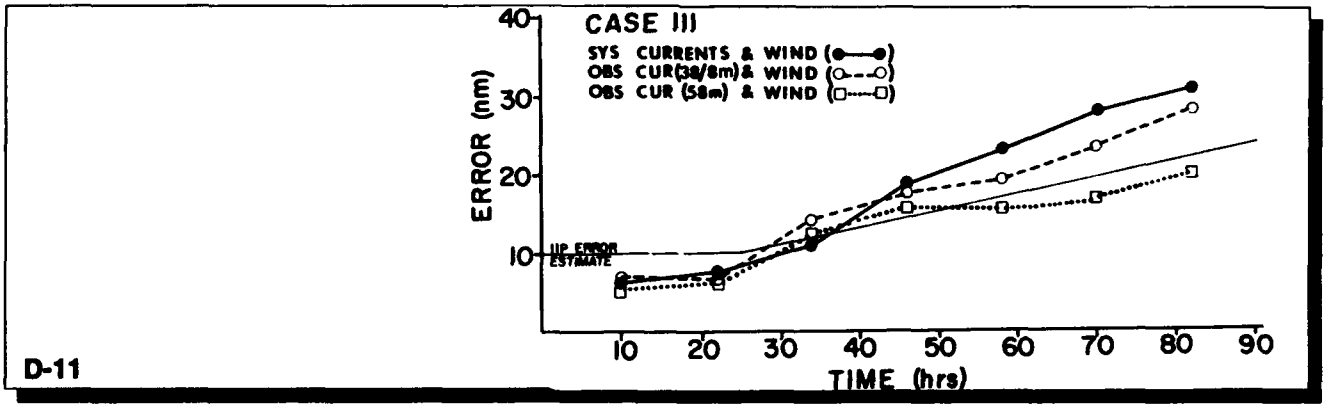

D-11

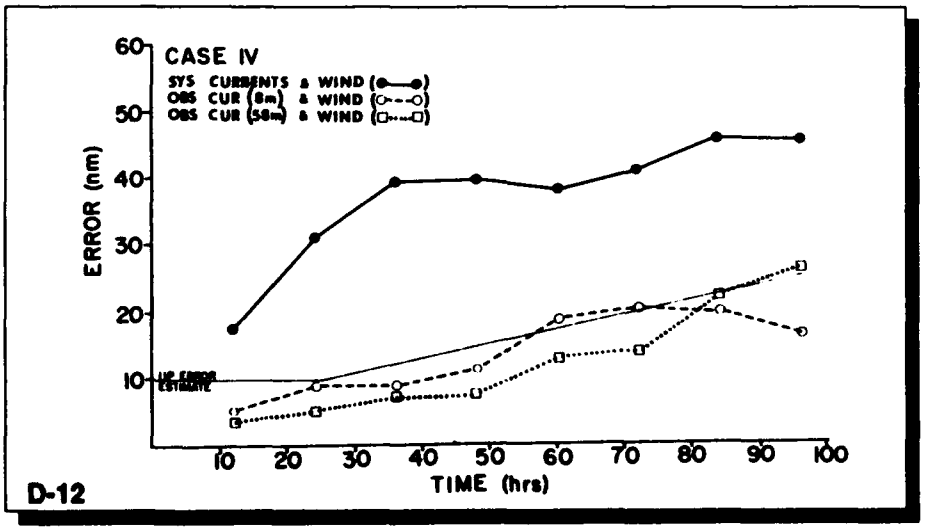

D-12

Appendix E

An Analysis of Eddy Formation in the Vicinity of the Grand Banks of Newfoundland

LT F. J. Williams, USCG
D. L. Murphy

Introduction

The International Ice Patrol conducted a study of the eddy population in the Newfoundland Basin region based on data from the period from November 1981 to December 1984 to investigate the importance and basic character of eddy motion in the southern portion (40°N - 45°N and 40°W - 55°W) of our patrol area. This area (Figure E-1) contains the confluence of three surface currents and is bathymetrically dominated by the Grand Banks of Newfoundland, the Newfoundland Seamount Range and the Newfoundland Ridge.

A similar study was conducted by Voorheis, Aagaard and Coachman in 1973. They researched hydrographic data collected during IIP cruises in an attempt to establish an eddy population. The present study encompasses a larger geographic area and also introduces infrared (IR) imagery. Voorheis, *et al.* looked for eddies in hydrographic data along standard IIP transects. The present study uses data collection specifically designed to locate eddies.

Ocean frontal analysis charts maintained by National Weather Service (NWS) and Naval Eastern Oceanographic Center (NEOC), and Canadian Forces METOC Center sea surface temperature data formed the data base for the investigation. Analysts produce these charts from satellite IR imagery gathered predominantly from the GOES and NOAA 6 and 9 satellites. The research area is dominated by cloud and fog cover and so does not always present ideal conditions for use of IR imagery, but these charts represent the only complete data set displaying eddies. An explanation of the methodology is given in Williams (1985). Data analyzed include the number of eddies in the area, their average life span and size, the area of formation, generation and deterioration patterns, and their movement through the area. Eddies included in the study are only those in the southern portion of the area that had an IR signature. Other eddies may affect the operations area, but are not included.

Eddy Population

Eighty-five percent of the time at least one eddy was active in the research area, and on several occasions two or more were present. During the 38 months of the experiment the NWS and NEOC charts indicated 46 eddies in the area. The life of the eddies ranged from two to 218 days with an average life span of 42 days. Voorheis, *et al.* (1973), indicates an average life span of 30 to 120 days.

Areas of Formation

The positions of formation of the eddies as shown in Figure E-2 indicate that they formed in two major areas: over the Newfoundland Ridge and over the Newfoundland Seamount Range. Of the 46 observed eddies, 12 (26%) were first sighted directly over the Newfoundland Seamount Range and 34 (74%) were first sighted west of the Newfoundland Ridge. These areas are both dominated by large, relatively shallow bathymetric features. Huppert and Bryan (1976) have demonstrated that the Atlantis II Seamounts are instrumental to eddy

Figure E-1. The research area, showing major ocean currents and bathymetry

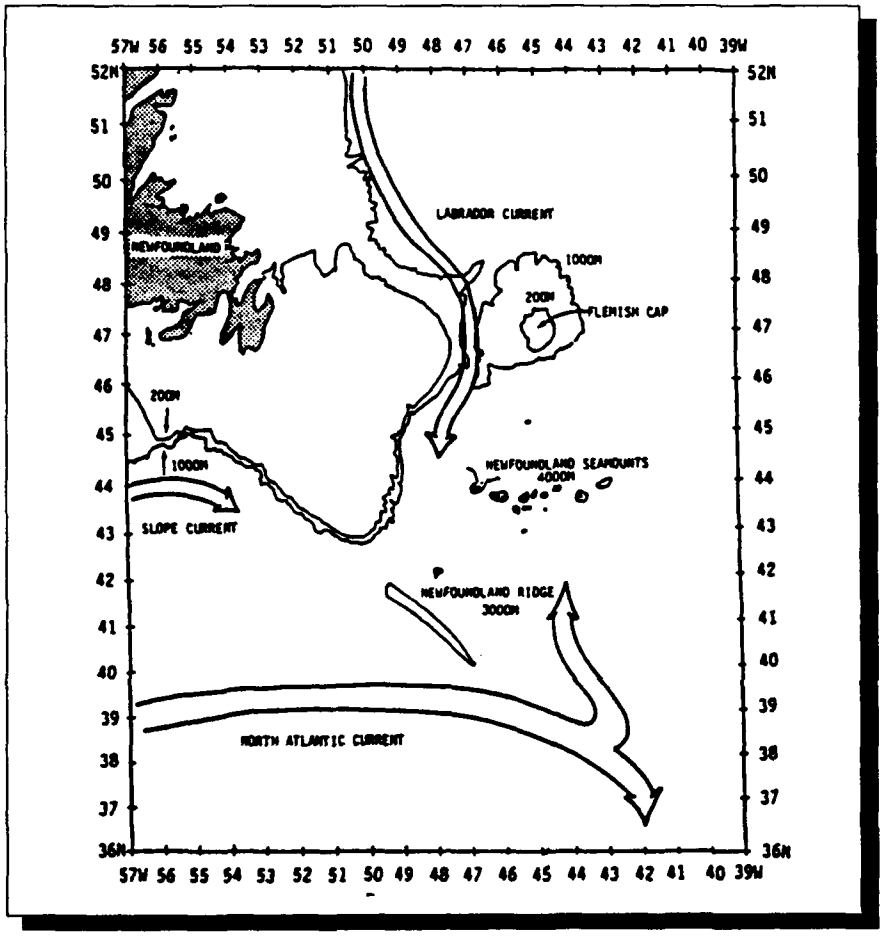

formation. Voorheis *et al.* (1973) suggest eddies in the Newfoundland Basin are bathymetrically generated. The formation of eddies in this study near the bathymetric features support the theory that interaction of the ocean currents with the topography of the Seamounts or the Ridge is important to eddy generation. Figure E-2 indicates that except for these two regions the remainder of the area appears to be relatively eddy free.

Generation and Deterioration

IR signatures indicate that twenty-one of the eddies (46%) formed from pinched-off meanders, eight (17%) from interactions between currents. Seventeen eddies (37%) had no identifiable source. It is possible that the cloud cover hid the meander from which the eddy formed and that by the time visibility improved, the eddy was in place and the generative process was unobserved. Seven of these eddies were in the Seamount area and ten were near the Ridge.

Translation Through the Area

Twenty-one eddies showed a net westward drift throughout their lives. Only three displayed a net eastward drift. The remaining 22 showed no net drift.

Of the 22 showing no net drift, 18 had a fully-observed life span of fifteen days or less and so may not have had the opportunity to drift at all. Three were seen in periods of heavy clouds and so were carried in the original reported position for a month and deleted from the NWS charts. The other four showing no net drift display an oscillatory drift, both east and west alternately. This motion is also displayed by many of the longer-lived eddies that show definite westward net drift. The motion may be explained by positioning errors due to the analysis of the satellite data.

These same factors may have influenced the three eddies that displayed a net eastward drift. Joyce (1984), working in an area bounded by 40°N - 45°N and 55°W - 75°W (immediately to the west of this study area), demonstrated that eddies interacting with the Gulf Stream display a predominantly westward drift. The present study shows similar results because of the 21 eddies showing westward drift, 12 interacted with the North Atlantic Current (NAC) during their life spans. Of the three that drifted east, one showed no interaction with the parent current. Interactions with the NAC then could not have caused the net eastward drift of the eddies.

Figure E-2. Initial reported positions of eddies in this study. *Symbols indicate the source(s) of each eddy report, numbers indicate sequence of formation.*

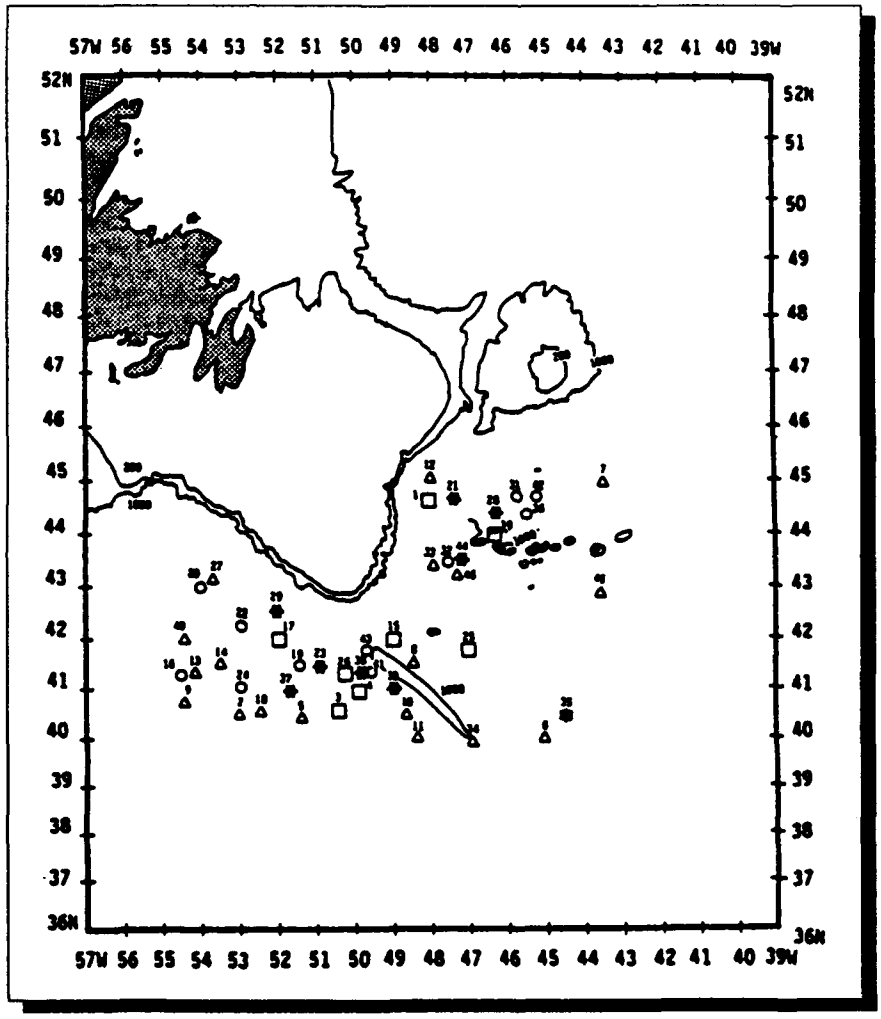

predominantly westward drift. The present study shows similar results because of the 21 eddies showing westward drift, 12 interacted with the North Atlantic Current (NAC) during their life spans. Of the three that drifted east, one showed no interaction with the parent current. Interactions with the NAC then could not have caused the net eastward drift of the eddies.

Eddy Size

The eddies varied in shape from roughly circular to elongated ellipses and many had irregular circumferences. To estimate the average size, all eddies were assumed to be of circular form of diameter equal to the average of the major and minor axes. The mean characteristics are shown in Table E-1.

Comparison of Eddy Characteristics in Two Areas

The following discussion centers on whether or not the area of formation had any effect on eddy characteristics.

The duration of eddies over the Seamounts ranged from six to 115 days with an average duration of 46 days. The same statistics for the 34 eddies formed near the Ridge show a range of two to 218 days with an average of 41 days. These figures indicate that the area of formation has no significant effect on the life span of the eddy. In general, eddies in this area have a shorter life span than the two to three year spans reported by Joyce (1984), Richardson (1980) and Richardson (1983) in other areas of the Gulf Stream system.

The area of the Seamounts showed eddy activity 63% of the time; the Ridge, 69% of the time. Both areas have equal potential for eddy activity.

The areas of formation shows no apparent affect on the migration of the eddy through the area. The eddies that formed over the Seamounts showed a westward migration in six of twelve eddies while five showed no significant migration. The remaining eddy showed eastward migration. Those formed in conjunction with the Ridge topography showed westward migration in 16 of 34 eddies and

was cold core. Eight cold core eddies formed in the area of the Ridge. There are two possible explanations for this: either the cold-core eddies form more as an interaction with the NAC in the Newfoundland Ridge/Tail of the Bank area, or they drifted southeast out of the Seamount area hidden by cloud cover before they were reported.

A much higher percentage of Seamount eddies had an unidentified generation mechanism. Seven out of twelve or 58% had an unknown source of origin as compared with ten out of 34 or 23% of the Ridge eddies.

Labrador Current Eddies

Perhaps one of the most interesting results of this study is the location of five cold-core eddies in the area north of the Gulf Stream in the normal domain of warm-core NAC eddies. A possible explanation for the presence of these eddies is the Labrador Current. No studies have been conducted on the generation of eddies by this current, but Hayes and Robe (1978) showed that the Labrador Current extends to the bottom and that the flow is variable and quite often influenced by the position of the NAC. If we make the assumption that the bottom features may cause the bifurcation noted in the current's flow, it is reasonable to assume the varied bathymetry can also cause meander and eddy generation in much the same way as it does in the NAC. Research dedicated to the generation of eddies by the Labrador Current is necessary.

Conclusions

For the three-year period, this study evaluated data from several different sources and identified a total of 46 eddies in the research area. The research area was eddy free only 15% of the study period. This clearly indicates that eddies are frequently in the area and that they are important to the dynamics of the area. The eddies were concentrated near the Newfoundland Seamount Range and the Newfoundland Ridge. Except for these two areas, the research area showed no sign of eddy activity. This distribution suggests that the topography features had an influence on the formation of the eddies. This indicates that, at least in some areas, the NAC is influenced by the bottom in the Newfoundland Basin area.

The study also suggests that the Labrador Current is capable of generating eddies. Five cold-core eddies were found in an area where they could not have been generated by the NAC. Kollmeyer, *et al.* (1965) documented the existence of a cold-core eddy spawned by the Labrador Current and recognized its importance as a cold trap for icebergs. However, no systematic study of Labrador Current cold-core eddies has yet been conducted. This is a subject that requires further investigation.

In their movement, the eddies followed the pattern predicted by Joyce (1984) and drifted predominantly to the west. This was true even for those eddies that showed a considerable interaction with the eastward-flowing NAC. The most common method of formation was pinched-off meanders. Absorption back into the parent current by similar meanders was the most common method of deterioration.

The area of formation had no apparent effect on the characteristics of the eddies. Those formed over the Seamounts displayed features similar to those formed over the Ridge. All were of equivalent size and duration.

The study indicates that the average eddy in the southern IIP operations area will be a warm core eddy approximately 116 km in diameter. It will form over the Seamounts or over the Ridge, normally from a pinched-off meander, and will migrate to the west after formation. It will remain on plot for about 42 days and will normally be absorbed back into the parent current. We can expect to see an eddy similar to the one described here in the southern IIP operations area about 80% of the time.

Table E-1. Average Characteristics of Eddies in study area

Eddy Type	Number of Observations	Average Size	Average Life (days)
Warm Core	38	117	49
Cold Core	8	94	21

Table E-2. A Comparison of Characteristics of the Eddies near the Newfoundland Ridge and the Newfoundland Seamounts

Warm Core			
Newfoundland Ridge	26	127	47
Newfoundland Seamounts	11	105	55
Cold Core			
Newfoundland Ridge	8	100	23
Newfoundland Seamounts	1	55	6

These figures are in general agreement with Voorheis *et al.* (1973). The only difference in the conclusions is the rotation of the eddies. Their data indicated cold core eddies are more numerous. The present study indicates warm core eddies dominate. It is difficult to address this difference, but IR positively indicates the temperature differences in water masses. Additional long term analyses may resolve this discrepancy.

References

Hayes, R.M. and R.Q. Robe, 1978. *Oceanography of the Grand Banks Region of Newfoundland, 1973.* U.S. Coast Guard Oceanographic Report No. 13, CG-373-13, United States Coast Guard, Washington, DC 20593.

Huppert, H.E. and K. Bryan, 1976. "Topographically Generated Eddies". *Deep-Sea Research*, 23, 655-679.

Joyce, T.M., 1984. "Velocity and Hydrographic Structure of a Gulf Stream Warm-Core Ring". *Journal of Physical Oceanography*, 14(5), 936-941.

Kollmeyer, R.C., R.M. O'Hagan, R.M. Morse, D.A.McGill, and N. Corwin, 1965. *Oceanography of the Grand Banks Region and the Labrador Sea in 1964.* U.S. Coast Guard Oceanographic Report 10, CG 373-10. United States Coast Guard, Washington, DC 20593.

Lai, D.Y. and P.L. Richardson, 1977. "Distribution and Movement of Gulf Stream Rings". *Journal of Physical Oceanography*, 7(9), 670-683.

Richardson, P.L., 1980. "Gulf Stream Ring Trajectories". *Journal of Physical Oceanography*, 10(1), 90-104.

Richardson, P.L., 1983. "Eddy Kinetic Energy in the North Atlantic Ocean from Surface Drifters". *Journal of Geophysical Research*, 88(C7), 4355-4367.

Voorheis, G. M., K. Aagaard and L. K. Coachman, 1973. "Circulation Patterns Near the Tail of the Banks". *Journal of Geophysical Research*, 3(10), 397-405.

Williams, F.J., 1985. *Investigation into the Population and Motion of Eddies in the Southern International Ice Patrol Operations Area.* Master of Science Thesis. Old Dominion University, Norfolk, Virginia.

Appendix F

Detection of Ocean Fronts in the Gulf Stream / Labrador Current System by Side-Looking Airborne Radar

LTJG N. B. Thayer, USCGR
D. L. Murphy

Introduction

The Gulf Stream probably reaches its greatest complexity in the region south and southeast of Newfoundland where it interacts with complex bathymetry and the southward-flowing Labrador Current to produce an ever-changing system of fronts, eddies and associated features. This complex current system is responsible, in large part, for the distribution of icebergs in much of the International Ice Patrol's (IIP) operating area.

The IIP iceberg drift model, an integral part of the IIP operations, relies primarily on historically time-averaged currents. Using these currents can lead to substantial drift errors, particularly in regions with large current fluctuations. To address this problem, IIP uses the drift of satellite-tracked drift buoys, deployed by IIP aircraft, to provide near real-time current data to the model. Although this program is successful, the updates to the current field are limited temporally and spatially to the period for which a buoy is drifting through a specific region.

Remote sensing techniques hold the most promise for providing current data for future IIP operations. For example, satellite infrared imagery is used successfully under certain conditions to define ocean frontal boundaries and, thus, infer circulation patterns for several ocean areas. Unfortunately, infrared imagery is of limited operational use in the IIP area due to persistent fog and cloud cover. However, active microwave systems (radars) are capable of penetrating clouds and, under the right circumstances, detecting frontal features.

In 1985 IIP began investigating the feasibility of using imagery from a side-looking airborne radar (SLAR) to map ocean fronts in the IIP area. This report describes some of the preliminary results of that investigation.

Background

The International Ice Patrol deploys one week out of two to Gander, Newfoundland, during the icebergs season, typically March through August. Using U.S. Coast Guard HC-130 aircraft, IIP conducts iceberg reconnaissance flights within the area bounded by 40°-52°North and 39°-57°West. Reconnaissance flights are made each day during the deployments, each flight approximately 3,150 km long (1,700 nm), covering approximately 65,000 square km.

Since the spring of 1983, IIP has used SLAR as the main method of iceberg reconnaissance, replacing visual reconnaissance. SLAR is an X-band radar that scans the sea surface in a plane normal to the flight path. The radar image is displayed on a narrow CRT that produces a negative image on photographic film (Figure F-1). The standard altitude for IIP reconnaissance is 8,000 feet, with a SLAR swath width of 100 km, 50 km to each side of the aircraft with an unimaged swath directly below the aircraft of about 5 km. SLAR is largely unaffected by weather, with only heavy precipitation obscuring the view of the surface.

Review of IIP SLAR films for 1983-1985, representing some 200 flights, has revealed that SLAR is capable of detecting the fronts of the Gulf Stream and Labrador Current, with the water masses of different temperatures showing up as different shades on the SLAR film's negative image, warm water appearing dark and cooler water appearing light. These correspond to high radar backscatter and low radar

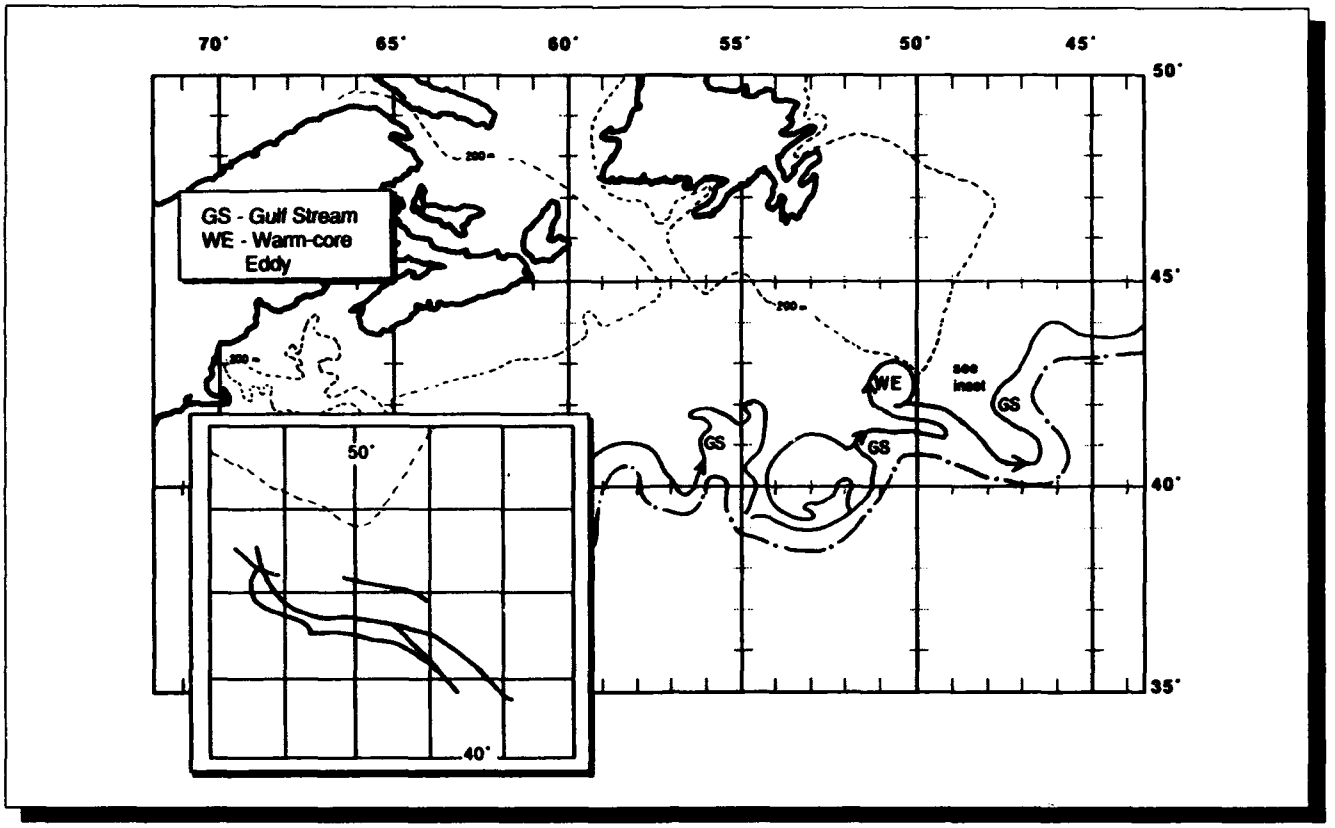

Figure F-1. Reproduced National Earth Satellite Service (NESDIS) product from April 26, 1985. Inset — NESDIS worksheet from 25-26 April 1985.

Figure F-2. A segment of SLAR film from the International Ice Patrol reconnaissance flight of April 28, 1985, with a photo mosaic of the same piece of film. Warm (rough) water appears dark.

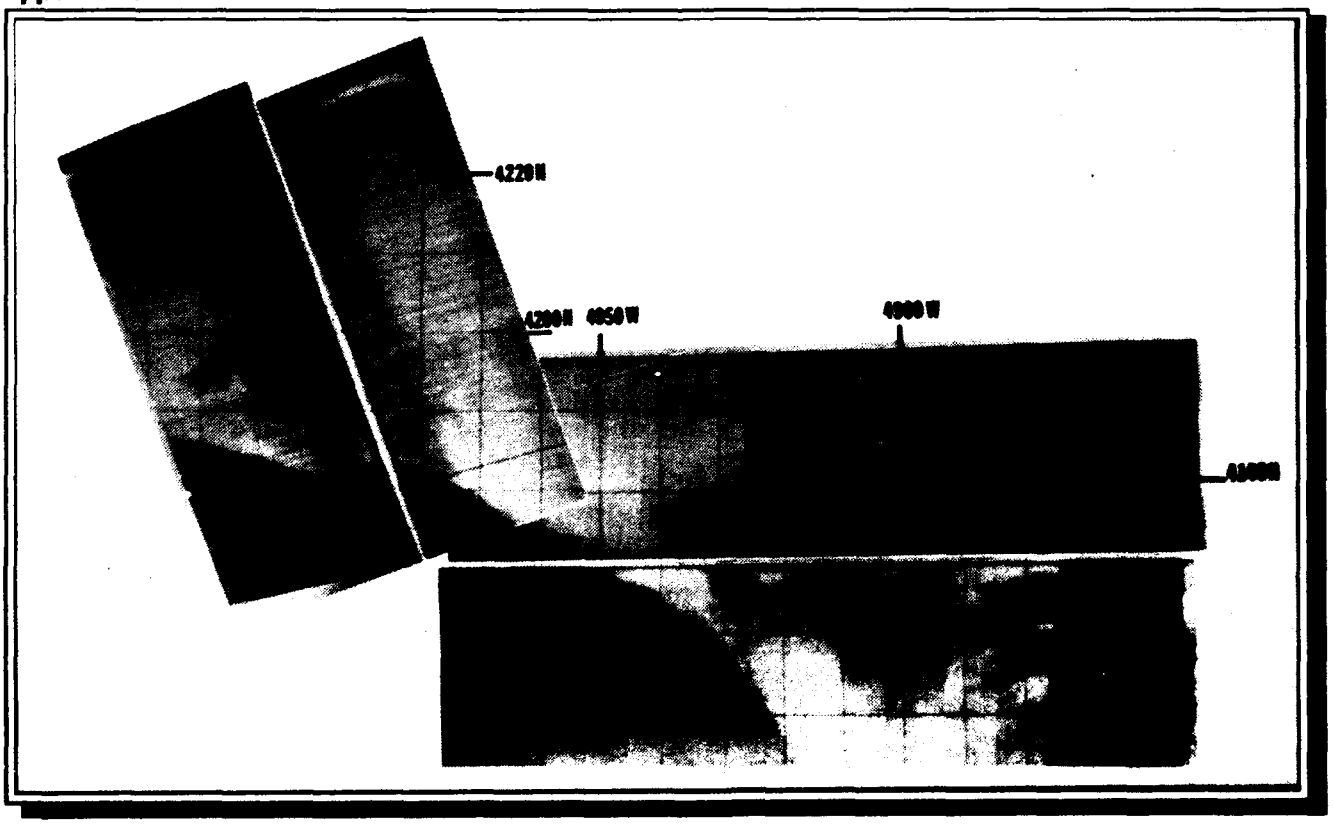

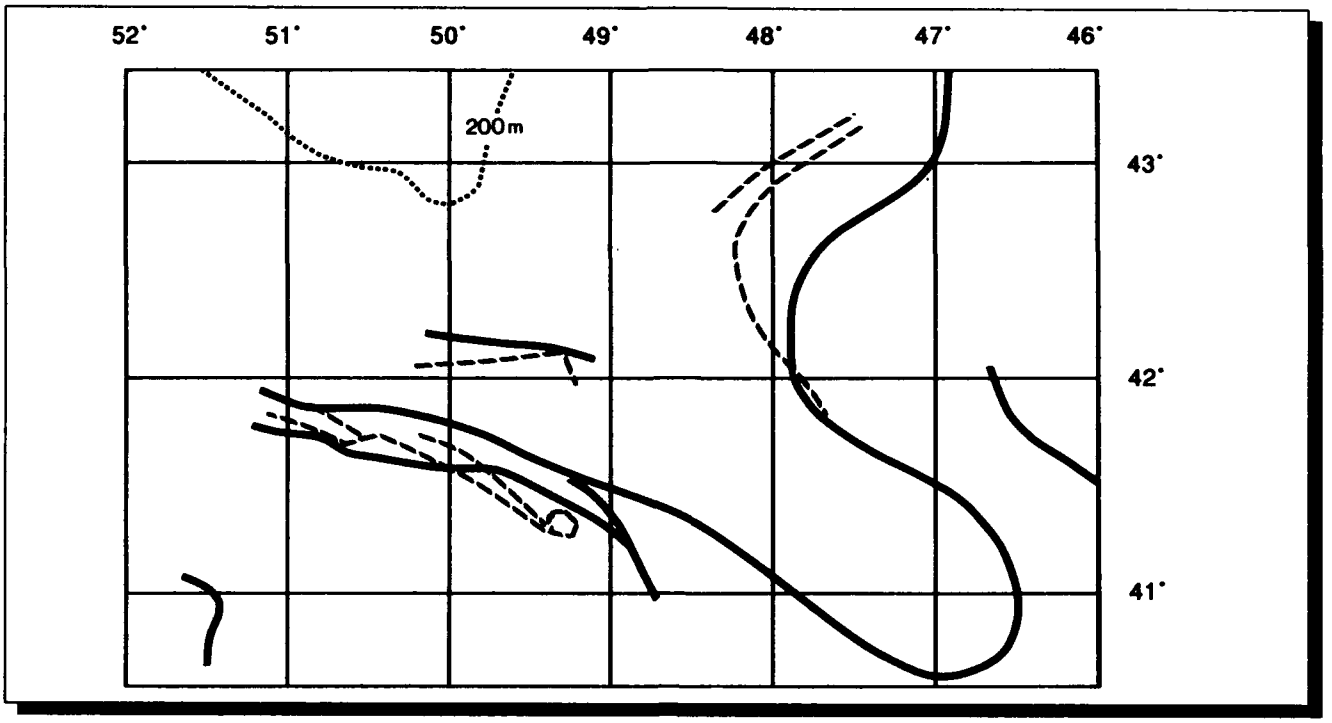

Figure F-3. Superimposition of the ocean features detected by NESDIS (solid line) on 25-26 April 1985 (see inset, Figure F-1) and features detected by IIP SLAR (dashed line) on 28 April 1985, some of which are visible in Figure F-2.

backscatter respectively. The imagery frequently shows very sharply delineated fronts in great detail.

Previous work using SLAR and satellite infrared in the Grand Banks area was done by LaViolette (1983), using an earlier Coast Guard SLAR and a NASA SLAR. The earlier SLAR's had lower power outputs and the images reproduced by LaViolette are apparently less sharp and less detailed than the ones produced by the present model, a Motorola AN/APS-135 Side-Looking Airborne Multi-Mission Radar (SLAMMR).

The most extensive body of work involving detection of ocean features with an active microwave system has been done with SEASAT synthetic aperture radar (SAR) (Beal, *et al.*, 1981). Some of the work done with SEASAT imagery has included comparison with satellite infrared imagery (Fu and Holt, 1982, 1983; Hayes, 1981).

Although the precise mechanism is uncertain, it is clear that the difference in backscatter is due to a difference in surface roughness. Visual inspection of the sea surface during IIP flights has shown that the dark and light areas on the SLAR film correspond closely to rough and smooth areas visible under conditions of light wind. Also, the SLAR films contain many images of internal wave trains, many of them closely linked to the bathymetry of the edge of the continental shelf. The alternate rough and smooth bands of internal waves detected by SEASAT SAR have been described in Alpers and Salusti (1983) and Hughes and Gower (1983), among others.

Discussions of the mechanism of detecting ocean features in radar imagery usually invoke Bragg scattering (Valenzuela, 1978; Brown, Elachi and Thompson, 1976), which defines a critical surface wavelength for maximum backscatter. For the X-band SLAR and the range of incidence angles encountered in IIP operations, the range of ocean wavelengths causing Bragg scattering is approximatley 2-30 cm. The relationship between the rough and smooth patches seen visually and the SLAR imagery reflects the relative spectral energy density in those patches, (i.e., the wave height at the Bragg wavelength).

Results

IIP SLAR imagery of ocean fronts has frequently been confirmed by the interpretations of Advanced Very High Resolution Radiometry (AVHRR) imagery by NOAA's National Environmental Satellite, Data and Information Service (NESDIS). A simplified reproduction of the NESDIS chart for 26 April 1985 is seen in Figure F-1, with an inset showing the interpreter's worksheet for the area outlined on the main chart. Figure F-2 is a SLAR image from 28 April, from the area outlined in Figures F-1

and F-3, showing a complex set of frontal features. The NESDIS worksheet and a SLAR interpretation are superimposed in Figure F-3, showing a very close match of the features.

In comparing the two images in Figure F-3, the similarities are apparent. The two fronts that converge to the east, the transverse north-south feature to the west and the area of sharp curvature on the western part of the southern front are present in both images, but differ somewhat in spatial orientation. The SLAR fails to detect the warm-core eddy shown on the final NESDIS chart (probably off the edge of the film), but SLAR shows an additional small-scale (10 km) eddy along the front. The differences between the SLAR interpretation and the NESDIS worksheet do not appear to be due to navigational displacement or rotation between the two, and are probably due to movement of the feature during the two day span between images.

Discussion

It is significant that by using the apparent SLAR temperature/backscatter relationship, the gradation of temperature from south to north is the same for both SLAR and AVHRR, i.e., a large area of warm water to the south (the Gulf Stream), a narrow band of cool water, a band of warm water and finally a band of cool water. Perhaps more important is that, giving the good match of location, shape and apparent temperature gradients across fronts, both SLAR and AVHRR appear to be detecting the same features.

The SLAR and satellite infrared imagery from 28 April and 26 April, respectively, show a good match of the features detected, both in location and overall shape. The particular SLAR image is a good illustration of how well the two sources can agree. Over the three years of SLAR operation at IIP, a large number of SLAR images of fronts have been collected. Of these, there have been a number of cases in which SLAR and AVHRR do not seem to agree both in location and shape of features. Williams (1985) examines the match and mismatch of SLAR and AVHRR images in eddies and associated features in the IIP region. Most frequently the difference seems to be one of placement rather than shape, reflecting a navigational discrepancy between the two sources.

Of the two, SLAR offers the greater positional accuracy. It makes use of the aircraft's Inertial Navigation System (INS), yielding an accuracy of ±5 km (Thayer SLAR/LORAN, unpub.). Positioning on the NESDIS chart is done using visible known land forms on the image, which may be obscured by cloud cover, making it less accurate, with errors possibly as much as 15-20 kilometers (personal communication, Jennifer Clark, NESDIS). Given the nature of the NESDIS product, i.e., the large area covered, more accurate positioning is unnecessary.

There are other cases in which there is considerable difference in overall shape between SLAR and the NESDIS product. This usually occurs when the area is obscured by clouds and NESDIS is estimating the location and shape of features based on information that is up to several days old.

In working with the original satellite imagery, the worksheets produced from it, and the final NESDIS product, it becomes apparent that NESDIS is able to take very complex, detailed imagery and produce from it remarkably accurate, coherent information. The imagery compared in Figure F-3 occupies approximately 1 square centimeter on the satellite image, from which the NESDIS interpreter was able to extract and correctly interpret several features.

Conclusions

Each system has its own application, capabilities and limitations. Satellite imagery is able to cover very large areas with a reasonable amount of detail. It is limited by cloud cover and offers limited navigational accuracy. SLAR, on the other hand, offers a very detailed look at an area, even through cloud cover, with good positioning. It can only cover small areas compared to a satellite and is limited by the operational constraints of IIP, with oceanographic applications of secondary importance to iceberg reconnaissance.

Although the mechanism involved in SLAR detection of temperature differences is not yet clear, both systems are able to detect the temperature gradients across the same fronts.

For the immediate future, SLAR will play an important role in IIP operations, locating frontal features for hydrographic research and for planning TOD deployments. Future research with SLAR should be directed toward providing real-time quantitative input for the IIP iceberg drift model. Another possible application of this technology is real-time mapping of current systems for other Coast Guard missions such as search and rescue and pollution response.

Acknowledgements

We wish to thank Jennifer Clark and her staff at NESDIS for providing satellite images and NESDIS worksheets.

References

Alpers, W., and E. Salusti, 1983. "Scylla and Charybdis Observed from Space". *Journal of Geophysical Research 88(C3)*: 1800-1808.

Beal, R. C., P. S. DeLeonibus and I. Katz, 1981. *Spaceborne Synthetic Aperture Radar for Oceanography.* Johns Hopkins University Press, Baltimore, MD.

Brown, W. E., Jr., C. Elachi and T. W. Thompson, 1976. "Radar Imaging of Ocean Surface Patterns". *Journal of Geophysical Research 81(15)*: 2657-2667.

Fu., L., and B. Holt, 1982. *SEASAT Views Oceans and Sea Ice With Synthetic Aperture Radar.* JPL Publication 81-120. Jet Propulsion Laboratory, Pasadena, CA.

Fu., L., and B. Holt, 1983. "Some Examples of Detection of Oceanic Mesoscale Eddies by the SEASAT Synthetic Aperture Radar". *Journal of Geophysical Research 88(C3)*: 1844-1852.

Hayes, R. M., 1981. "Detection of the Gulf Stream." In: *Spaceborne Synthetic Aperture Radar for Oceanography.* Johns Hopkins University Press, Baltimore, MD.

Hughes, B. A. and J. F. R. Gower, 1983. "SAR Imagery and Surface Truth Comparisons of Internal Waves in Georgia Strait, British Columbia, Canada." *Journal of Geophysical Research 88(C3)*: 1809-1824.

LaViolette, P. E., 1983. *The Grand Banks Experiment: A Satellite/Aircraft/Ship Experiment to Explore the Ability of Specialized Radars to Define Ocean Fronts.* NORDA Report #49, U. S. Naval Oceanographic Research and Development Activity, U. S. Navy, Washington, DC.

Sabins, F. F., Jr., 1978. *Remote Sensing: Principles and Interpretation.* pp 195-202. W. H. Freeman and Company, San Francisco, CA.

Valenzuela, G. R., 1978. *Theories for the Interaction of Electromagnetic and Oceanic Waves - A Review.* Boundary-Layer Meteor. 13: 61-85

Williams, F. J., 1985. "Investigation into the Population and Motion of Eddies in the Southern International Ice Patrol Operations Area." Master of Science Thesis, Old Dominion University, Norfolk, VA.

☆ U. S. GOVERNMENT PRINTING OFFICE; 1987--701-823--60028